A genetic and linguistic analysis of the admixture histories of the islands of Cabo Verde

Authors:
Romain Laurent[1], Zachary A. Szpiech[2,3], Sergio S. da Costa[1], Valentin Thouzeau[4,5], Cesar A. Fortes-Lima[6], Françoise Dessarps-Freichey[1], Laure Lémée[7], José Utgé[1], Noah A. Rosenberg[8], Marlyse Baptista[9,10], and Paul Verdu[1,*].

Authors' affiliations :
1. UMR7206 Eco-anthropologie, CNRS-MNHN-Université Paris Cité, Paris, France
2. Department of Biology, Pennsylvania State University, University Park, PA 16802, USA
3. Institute for Computational and Data Sciences, Pennsylvania State University, University Park, PA 16802, USA
4. UMR 7534 Centre de Recherche en Mathématiques de la Décision, CNRS-Université Paris-Dauphine-PSL University, Paris, France
5. Département d'Etudes Cognitives, Laboratoire de Sciences Cognitives et Psycholinguistique, ENS-PSL University-EHESS-CNRS, Paris, France
6. Department of Organismal Biology, Sub-department of Human Evolution, Evolutionary Biology Centre, Uppsala University, Uppsala, Sweden
7. Plate-forme Technologique Biomics–Centre de Ressources et Recherches Technologiques (C2RT), Institut Pasteur, Paris, France.
8. Department of Biology, Stanford University, Stanford, CA, USA
9. Department of Linguistics, University of Michigan, Ann Arbor, MI, USA
10. Department of Afroamerican and African Studies, University of Michigan, Ann Arbor, MI, USA

***Corresponding author:**
Paul Verdu, UMR7206 Eco-anthropologie, CNRS-MNHN-Université Paris Cité, Musée de l'Homme, 17, place du Trocadéro, 75016 Paris, France. Email : paul.verdu@mnhn.fr. Tel : +33 144057317

Ethics statement
Research sampling protocols followed the Declaration of Helsinki guidelines and the French laws of scientific research deontology (Loi n° 2016-483 du 20 avril 2016). Research and ethics authorizations were provided by the Ministério da Saúde de Cabo Verde (228/DGS/11), Stanford University IRB (Protocol ID n°23194–IRB n°349), University of Michigan IRB (n°HUM00079335), and the French ethics committees and CNIL (Declaration n°1972648). All volunteer participants provided written and video-recorded informed consent.

Data availability
The novel genome-wide genotype data, the linguistic utterance counts, and the self-reported anthropological data presented here can be accessed and downloaded via the European Genome-Phenome Archive (EGA) database accession numbers EGAD00001008976, EGAD00001008977, EGAD00001008978, and EGAD00001008979. All datasets can be shared provided that future envisioned studies comply with the informed consents provided by the participants, and in agreement with institutional ethics committee's recommendations applying to this data.

Software availability
MetHis is an open source C software available with user manual on GitHub at https://github.com/romain-laurent/MetHis (Fortes-Lima et al. 2021).

Keywords
Admixture; population genetics; historical inference; machine-learning; approximate Bayesian computations; genetic diversity; linguistic diversity; anthropology; slave-trade

ABSTRACT

From the 15th to the 19th century, the Trans-Atlantic Slave-Trade (TAST) influenced the genetic and cultural diversity of numerous populations. We explore genomic and linguistic data from the nine islands of Cabo Verde, the earliest European colony of the era in Africa, a major Slave-Trade platform between the 16th and 19th centuries, and a previously uninhabited location ideal for investigating early admixture events between Europeans and Africans. Using local-ancestry inference approaches, we find that genetic admixture in Cabo Verde occurred primarily between Iberian and certain Senegambian populations, although forced and voluntary migrations to the archipelago involved numerous other populations. Inter-individual genetic and linguistic variation recapitulates the geographic distribution of individuals' birth-places across Cabo Verdean islands, following an isolation-by-distance model with reduced genetic and linguistic effective dispersals within the archipelago, and suggesting that Kriolu language variants have developed together with genetic divergences at very reduced geographical scales. Furthermore, based on approximate bayesian computation inferences of highly complex admixture histories, we find that admixture occurred early on each island, long before the 18th-century massive TAST deportations triggered by the expansion of the plantation economy in Africa and the Americas, and after this era mostly during the abolition of the TAST and of slavery in European colonial empires. Our results illustrate how shifting socio-cultural relationships between enslaved and non-enslaved communities during and after the TAST, shaped enslaved-African descendants' genomic diversity and structure on both sides of the Atlantic.

INTRODUCTION

Between the 15th and 19th centuries, European colonization and the Trans-Atlantic Slave-Trade (TAST) put into contact groups of individuals previously isolated genetically and culturally. These forced and voluntary migrations profoundly influenced the descent of numerous European, African, and American populations, creating new cultures, languages, and genetic patterns (1,2).

Population geneticists have extensively described genetic admixture patterns in enslaved-African descendants in the Americas, and mapped their genomes for regions of ancestry recently shared with continental Africa and Europe (3,4). This allowed for reconstructing their detailed possible origins, as this knowledge is often intractable with genealogical records alone (1). Furthermore, genetic admixture-mapping methods have been used to identify genetic variation underlying phenotypic variation (5,6), and to identify post-admixture natural selection signatures (7), thus revealing how admixture shaped human populations' recent evolution. Maximum-likelihood approaches based on linkage-disequilibrium (LD) patterns of admixed individuals (8,9) have repeatedly highlighted the diversity of admixture processes experienced by populations historically related to the TAST. In particular, they identified different European, African, and American populations, respectively, at the source of genetic admixture patterns, sometimes consistent with the preferred commercial routes of each European empire (8,10). Furthermore, they identified variable timing of admixture events during and after the TAST, sometimes consistent with major socio-historical events such as the expansion of the plantation economic system or the abolition of slavery (11,12). From a cultural perspective, linguists have shown that novel contact-languages, such as creole languages (13,14), emerged from recurring interactions between socio-economically dominant Europeans with Africans and Americans. Furthermore, they identified the languages of origin of numerous linguistic traits in several creole languages (15–17), and emphasized the complex histories of contacts that shaped language diversity on both sides of the Atlantic.

Numerous questions remain unsolved and novel interrogations have emerged concerning the history of admixture during and after the TAST. *i)* While the genetic history of enslaved-African descendants in the Americas has been extensively studied, the influence of the TAST on genetic admixture in Africa remains under-investigated. Studying these questions in Africa would provide invaluable information about the influence of the onset and early stages of the TAST and the subsequent expansion of European empires on genetic admixture patterns on both sides of the Atlantic. *ii)* While admixture-LD inference methods have repeatedly brought novel insights into the admixture processes experienced by enslaved-African descendant populations, they could only explore historical models with one or two pulses of admixture, a methodological limitation (8,9). Complex admixture histories may be expected as a result of the recurring flows of enslaved-Africans forcibly displaced between and within continents, changes of social relationships among enslaved and non-enslaved communities, and variable assimilation of new migrants in pre-existing communities, during and after the TAST (18,19). *iii)* Finally, while the comparison of genetic and linguistic diversities has been the focus of numerous evolutionary anthropology studies at large geographical scales (20,21), it has rarely been endeavored for creole-speaking populations at a local scale in the historical context of the TAST (22–24).

Here, we propose to reconstruct the detailed genetic and linguistic admixture histories of Cabo Verde, as this archipelago represents an ideal case to address these three understudied aspects of TAST history. First, Cabo Verde is the first European settlement-colony in Sub-Saharan Africa, located 500 kms West of Senegal in Western Africa (**Figure 1**), and settled in the 1460s by Portuguese immigrants and enslaved-Africans forcibly removed from the continental mainland. After 1492, and in particular after the 17th century expansion of the plantation economy in the Americas, Cabo Verde served as a major slave-trade platform between continents (25). Second, Cabo Verde forms an archipelago of nine inhabited islands that were settled over the course of three centuries due to the changing political, commercial, and migratory contexts (26–28). Therefore,

studying the admixture history of Cabo Verde will provide unique insights into the onset of the TAST before 1492, and into the history of slavery thereafter. This setting further promises to illustrate, at a micro-geographical scale, island-per-island, the fundamental socio-historical and serial founding migrations mechanisms having influenced genomic patterns in admixed populations throughout the TAST. Finally, Cabo Verdean Kriolu is the first creole language of the TAST, born from contacts between the Portuguese language and a variety of African languages (15,17,29,30). The archipelago thus represents a unique opportunity to investigate, jointly, genetic and linguistic admixture histories and their interactions since the mid-15th century.

Previous genetic studies exploring, first, sex-specific genetic diversity, and, then, genome-wide markers from several islands of the archipelago (31–34), attested to the dual, sex-biased, origins of the Cabo Verdean gene-pool, resulting mainly from admixture between African females and European males. Furthermore, these studies described variable admixture patterns between mainland Africa and Europe across islands without distinguishing source populations from different sub-regions within continents. Another, more recent, study investigated which continental mainland European and African populations may have contributed to the Cabo Verde gene-pool without focusing on possible variation across islands (3). Interestingly, adaptive-introgression signals for malaria resistance in Santiago island were recently identified as a result of migrations and genetic admixture during the TAST (35). Finally, while joint analyses of genetic and linguistic diversities from the island of Santiago showed that genetic and linguistic admixture histories possibly occurred in parallel (23), these previous studies did not attempt to formally reconstruct the admixture processes and detailed demographic histories that influenced the observed patterns of genetic or linguistic diversity on the islands of Cabo Verde.

Based on these previous studies, we propose to first determine which continental African and European populations in fact contributed to the genetic landscape of each Cabo Verdean island today. Indeed, which enslaved-African populations only briefly transited through the archipelago, and which remained for longer periods is largely debated by historians (25–27); and, while Portuguese influence is clear, further details about which European migrations genetically influenced Cabo Verde remain to be assessed (36). These aspects are often crucial for understanding the genetic history of enslaved-African descendant populations on either side of the Atlantic (1,12,37,38). Second, we propose to further evaluate the possible parallels between genetic and linguistic admixture histories at a micro-geographical scale within each island. We aim at better understanding how contacts shaped cultural variation during the TAST by deciphering the parent-offspring dispersal behaviors within and across islands which shaped the biological and cultural diversity in the archipelago (23). This can be achieved indirectly by exploring the influence of isolation-by-distance mechanisms on the distribution of genetic and linguistic diversity at very reduced geographical scale (~50 km) within a population (39–44). Finally, we reconstruct the detailed history of admixture dynamics in each island since the 15th century, using statistical inference of possible complex admixture histories with Approximate Bayesian Computation (45). Altogether, this highlights the socio-historical mechanisms that shaped the genetic and linguistic diversity of the Cabo Verde population, the first to be born from the TAST.

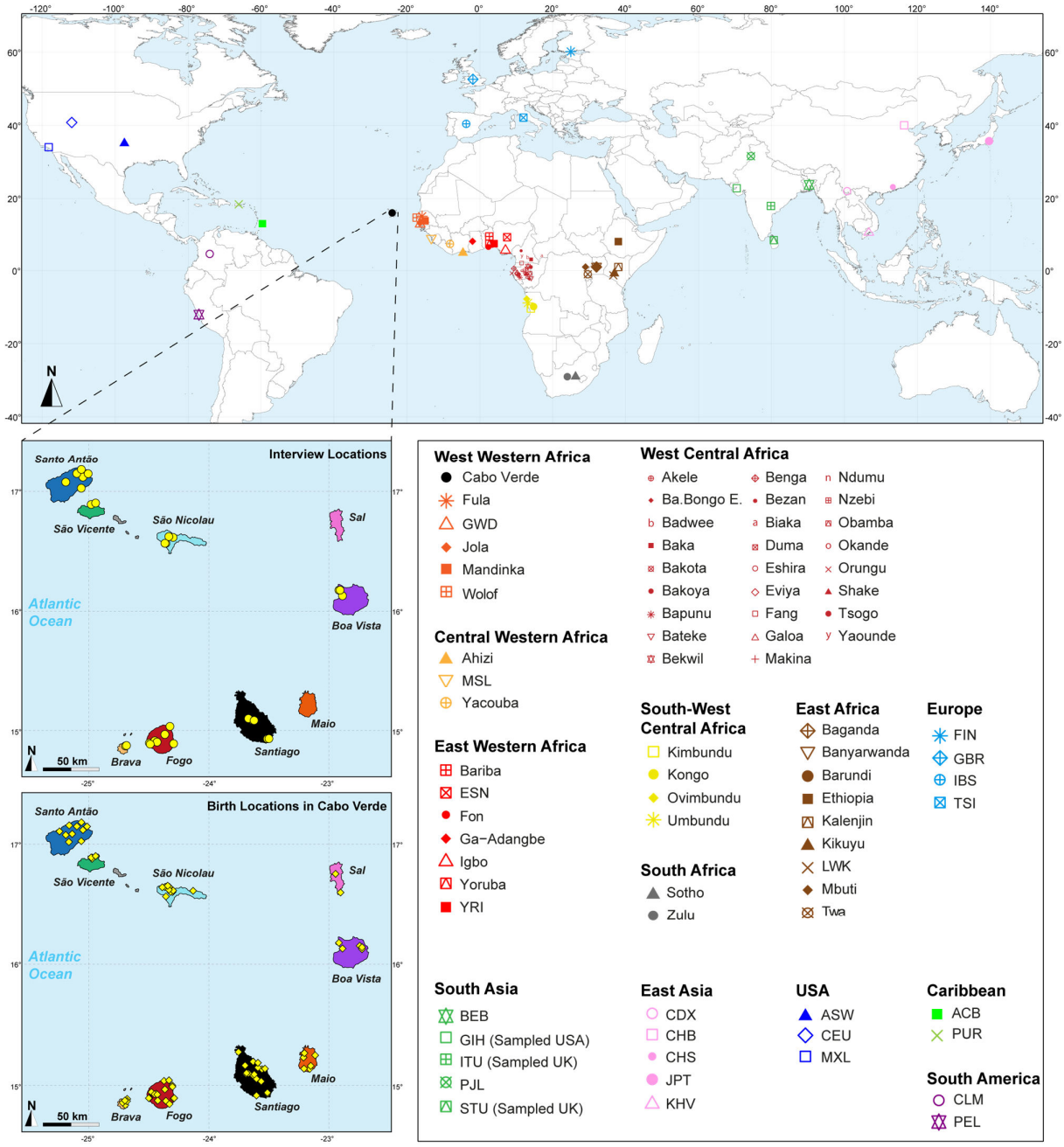

Figure 1:

Sampling location of 233 unrelated Cabo Verdean individuals, merged with data on 4924 individuals from 77 worldwide populations.

Birth-location of 225 individuals within Cabo Verde are indicated in the bottom map-panel, and birth locations outside Cabo Verde for 6 individuals are indicated in **Figure 1-source data 1**. Linguistic and familial anthropology interview, and genetic sampling for Cabo Verde participants were conducted during six separate interdisciplinary fieldworks between 2010 and 2018. Further details about populations are provided in **Figure 1-source data 1**.

Figure 1-source data 1: ***provided in .xls format***

Population table corresponding to the map in Figure 1 and sample inclusion in all analysis.

RESULTS

We investigate genetic and linguistic variation in 233 family unrelated Kriolu speakers from the nine Cabo Verdean islands (Brava, Fogo, Santiago, Maio, Sal, Boa Vista, São Nicolau, São Vicente, Santo Antão, **Figure 1**, **Figure 1-source data 1**). With novel genome-wide genotyping autosomal data (**Appendix 1-figure 1**), we first describe genetic differentiation patterns in Cabo Verde and other enslaved-African descendants in the Americas from previous datasets, in particular with respect to continental Africa and Europe. Next, we deploy local-ancestry inferences and determine the best proxy source-populations for admixture patterns in each Cabo Verde island. We then describe runs of homozygosity and genetic isolation-by-distance patterns at reduced geographical scale within Cabo Verde. We also investigate Kriolu linguistic diversity with respect to geography and socio-cultural co-variates and, then, investigate jointly genetic and linguistic admixture patterns throughout the archipelago. Finally, we infer the detailed genetic admixture history of each island using the machine-learning *MetHis*-Approximate Bayesian Computation (ABC) approach (45).

1. Cabo Verde and other TAST-related admixed populations in the worldwide genetic context

We explored genetic diversity patterns captured along the first three axes of the multi-dimensional scaling (MDS) projection of individual pairwise allele sharing dissimilarities (ASD (46)), computed from different individual subsets (**Figure 1-source data 1**). This ASD-MDS approach is mathematically analogous to PCA based on individual genotypes and therefore captures similar information about individual pairwise genetic differentiation (47)[Chap.-18.5.2]. However, ASD-MDS allows to explore pairwise genetic differentiation for successive individual subsets much more efficiently computationally than classical PCA. Indeed, the individual pairwise ASD matrix only needs to be computed once and then simply subsampled before being projected, and successive subset of individual-pairwise ASD matrices are thus always several orders of magnitude smaller in dimensions than the genotype table to be projected with PCA which comprises, here, 455,705 SNPs in all cases. Detailed ASD-MDS decompositions are provided in **Appendix 2** and **Appendix 2-figure 1-4**. Note that we considered seven geographical regions in Africa shown in **Figure 1**.

Figure 2 shows that the second ASD-MDS axis distinguishes West Western African Senegambian populations from East Western Africans, while Central Western Africans are at intermediate distances between these two clusters. Moreover, the third MDS axis separates Northern and Southern European populations; the British-GBR and USA-CEU individuals clustering at intermediate distances between the Finnish-FIN, and a cluster represented by Iberian-IBS and Tuscan-TSI Western Mediterranean individuals. Consistently with previous results (3,23), on the first three MDS axes, Cabo Verdean individuals cluster almost exclusively along a trajectory from the Southern European cluster to Senegambia (**Figure 2A-C**), with little traces of affinity with other African or European populations. Instead, the USA African-American ASW (**Figure 2-figure supplement 1-A-C**) and Barbadian-ACB (**Figure 2-figure supplement 1-D-F**) cluster along a trajectory going from the GBR and CEU cluster to Central and East Western Africa; and Puerto Ricans-PUR cluster along a trajectory going from the Southern European cluster to the Central Western African cluster (**Figure 2-figure supplement 1-G-I**).

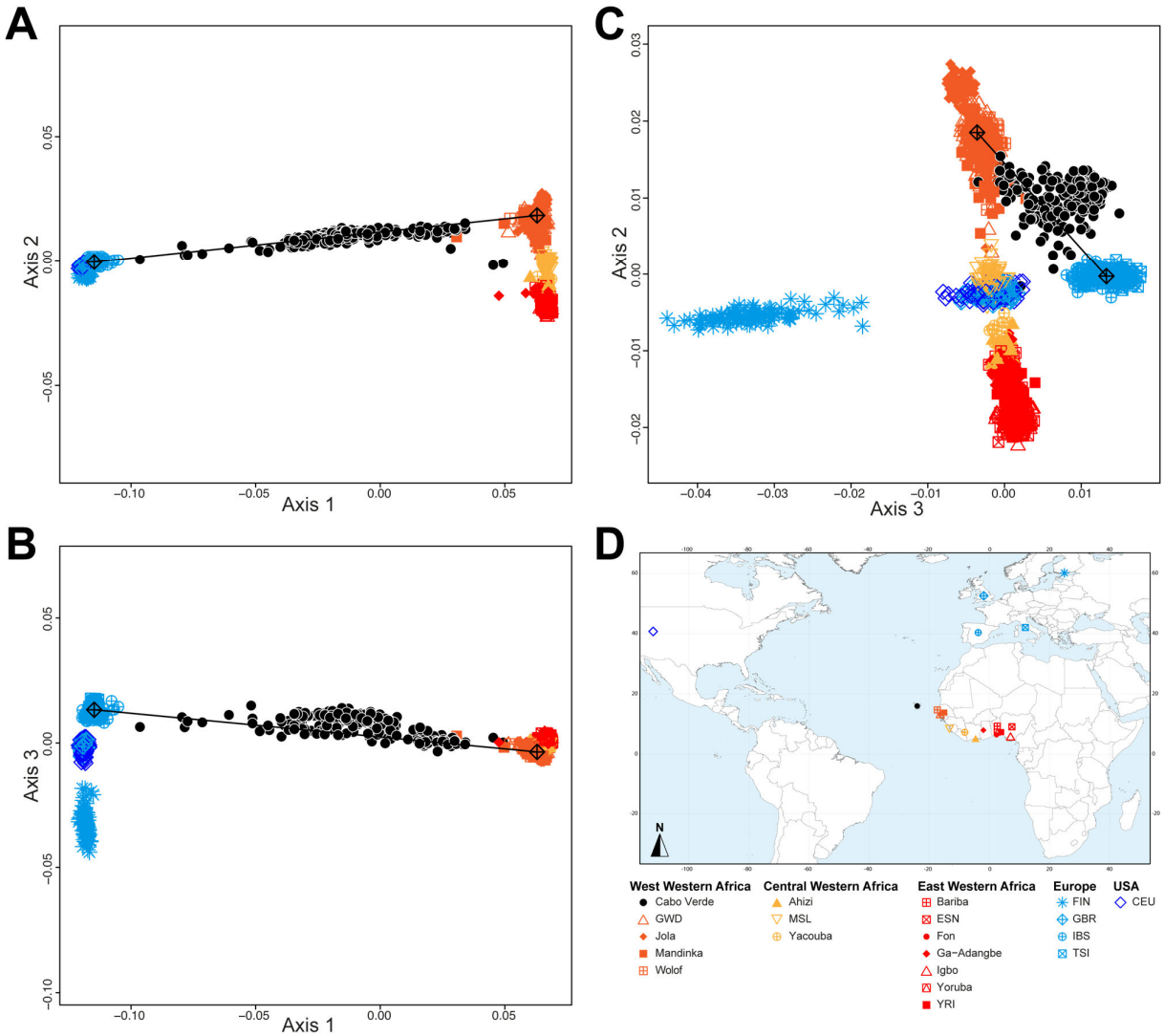

Figure 2:

Multidimensional scaling projections of pairwise allele sharing dissimilarities in Cabo Verdeans and continental African and European populations.

A-C) Three-dimensional MDS projection of ASD computed among 233 unrelated Cabo Verdeans and other continental African and European populations using 445,705 autosomal SNPs. Cabo Verdean patterns in panels **A-C** can be compared to results obtained considering instead the USA African-Americans ASW, the Barbadians-ACB, and the Puerto Ricans-PUR in the same African and European contexts and presented in **Figure 2-figure supplement 1**. We computed the Spearman correlation between the matrix of inter-individual three-dimensional Euclidean distances computed from the first three axes of the MDS projection and the original ASD matrix, to evaluate the precision of the dimensionality reduction. We find significant ($p<2.2\text{x}10^{-16}$) Spearman $\rho=0.9635$ for the Cabo Verde analysis (**A-C**). See **Figure 1-source data 1** for the populations used in these analyses. Sample locations and symbols are provided in panel **D**.

Figure 2-figure supplement 1:

Multidimensional scaling three-dimensional projection of allele sharing pairwise dissimilarities, for the closest subsets of West African and European populations to the African American ASW, Barbadian ACB, and Puerto Rican PUR populations, separately.

228 **Figure 2-figure supplement 1:**

229 **Multidimensional scaling three-dimensional projection of allele sharing pairwise dissimilarities, for the closest subsets of West**
230 **African and European populations to the African American ASW, Barbadian ACB, and Puerto Rican PUR populations, sep-**
231 **arately.**

232 Three-dimensional MDS projection of ASD computed using 445,705 autosomal SNPs among continental African and European
233 populations and, respectively, the USA African-American ASW (panels **A-C**), the Barbadians-ACB (panels **D-F**), or the Puerto Ricans-
234 PUR (panels **G-I**), in the same European and African contexts as explored in **Figure 2** for Cabo Verdeans in the main text. We computed
235 the Spearman correlation between Euclidean distances on the 3D-MDS projections and the original ASD matrix to evaluate the
236 precision of the dimensionality reduction. We find Spearman ρ=0.9383 (p<2.2x10^{-16}) for the ASW (A-C); 0.9306 (p<2.2x10^{-16}) for the
237 ACB (D-F); and 0.9437 (p<2.2x10^{-16}) for the PUR (G--I). Each individual is represented by a single point. Sample locations and
238 symbols are given in **panel J** (**Figure 1-source data 1**).
239

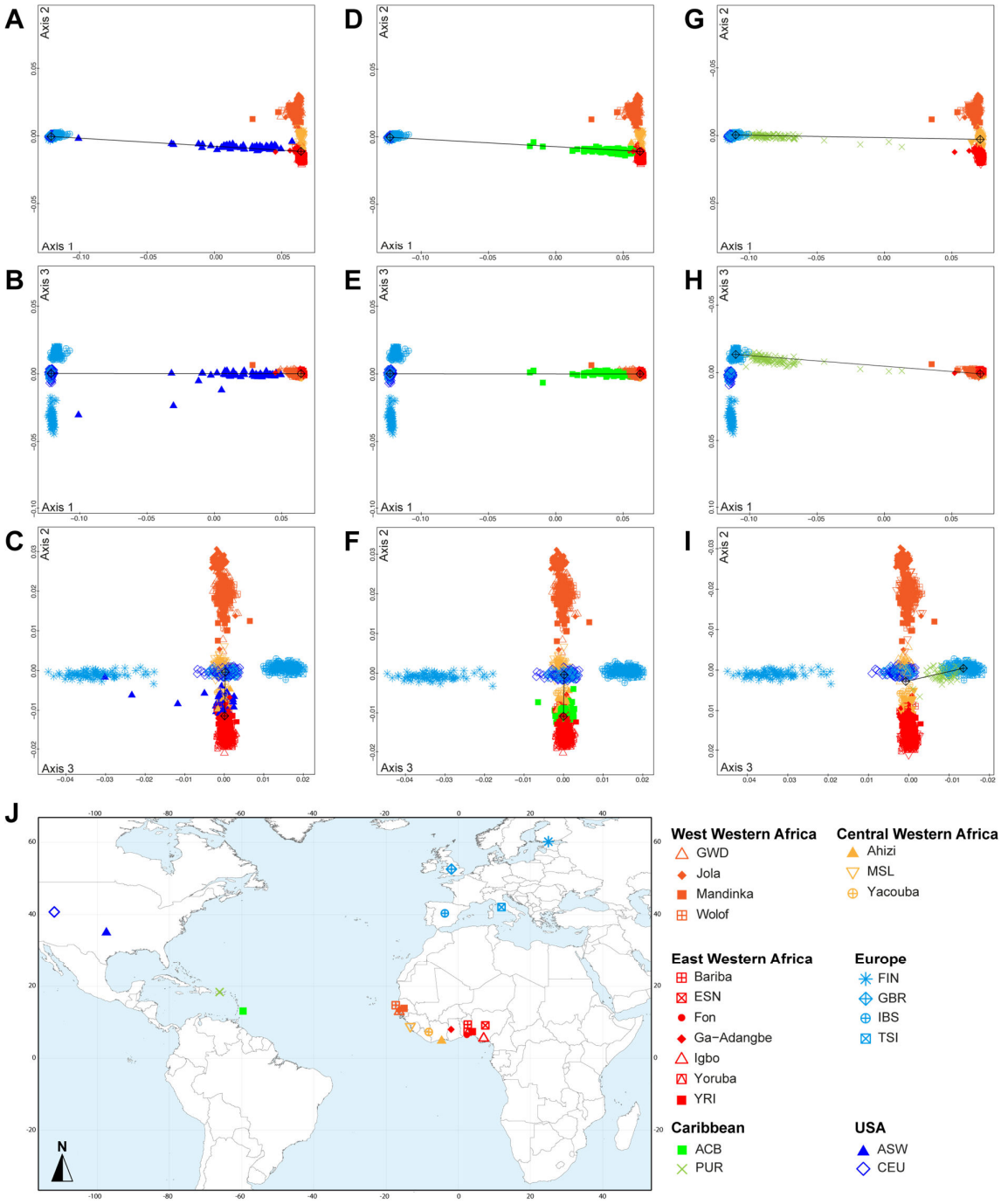

240
241

242 **2. Genetic structure in Cabo Verde and other TAST-related admixed populations**

243 Based on these results, we further investigated patterns of individual genetic structure among Cabo Verde-
244 born individuals, ASW, and ACB populations with respect to European and Western, Central, South-Western,
245 and Southern African populations (**Figure 1-source data 1**), using ADMIXTURE (48). Indeed, ASD-MDS
246 decompositions allow to efficiently identify major genetic pairwise dissimilarities among numerous samples,
247 but exploring multiple combinations of higher order axes remains extremely difficult with this multivariate
248 method. Instead, ADMIXTURE results recapitulate the major axes of genetic variation with increasing values
249 of the number of clusters *K*, which allows to explore individual pairwise genetic resemblances for numerous
250 major axes of variation at once. Extended descriptions of the results are presented in **Appendix 3**.

251 At *K*=2, the orange genetic-cluster in **Figure 3A** is maximized in African individuals while the blue al-
252 ternative cluster is maximized in Europeans. Cabo Verdean, ASW and ACB individuals exhibit intermediate
253 genotype-membership proportions between the two clusters, consistently with patterns expected for European-
254 African admixed individuals. Among the Cabo Verdean, ASW, and ACB populations, ACB individuals show,
255 on average, the highest membership to the orange "African" cluster (88.23%, SD=7.33%), followed by the
256 ASW (78.00%, SD=10.88%), and Cabo Verdeans (59.01%, SD=11.97%). Membership proportions for this
257 cluster are highly variable across Cabo Verdean islands, with highest average memberships for Santiago-born
258 individuals (71.45%, SD=10.39%) and Maio (70.39%, SD=5.26%), and lowest for Fogo (48.10%, SD=6.89%)
259 and Brava (50.61%, SD=5.80%). Inter-individual membership variation within Cabo Verde islands, captured
260 as F_{ST}/F_{ST}^{max} values (49), are significantly different across pairs of islands for 32 out of 36 comparisons (Wil-
261 coxon rank-sum test $p<3.96\text{x}10^{-8}$), with variability across islands ranging from a lowest value of 0.010 in
262 individuals from Santo Antão to a highest value of 0.0519 in Santiago (**Figure 3-figure supplement 1**).

263 At *K*=5, the new red cluster is maximized in the YRI, Igbo and ESN populations, distinct from Western
264 and Southern African orange and grey clusters, respectively. Note that the former orange cluster is almost
265 completely replaced with red membership in the ACB and ASW populations, while it remains large for all
266 Cabo Verdean-born individuals. Moreover, Cabo Verde-born individuals' patterns of membership proportions
267 to the orange, red or grey "African" clusters differ here between individuals born on Santiago, Fogo, Brava,
268 and Maio, and individuals born on Sal, Boa Vista, São Nicolau, São Vicente, and Santo Antão, respectively.
269 The former group of islands exhibit an "African" component resembling patterns of membership proportions
270 found in West Western African individuals, with a majority of membership to the orange cluster and a minority
271 to the red cluster. Instead, the "African" component in individuals born in the latter islands is almost exclu-
272 sively orange. This potentially indicates differences in shared ancestries with different continental African
273 populations across islands in Cabo Verde, which remains to be formally tested (see **Result 3**).

274 At *K*=6, these two groups of islands are now clearly differentiated, as the novel green cluster is maximized
275 in numerous individuals born on Sal, Boa Vista, São Nicolau, São Vicente, and Santo Antão, but represented
276 to a much lesser extent in Santiago, Fogo, and Brava. Instead, individuals in these latter islands retain a ma-
277 jority of membership to the orange "West Western African" cluster, and Maio-born individuals are now found
278 intermediately between the two groups with relatively even memberships to the orange and green clusters
279 respectively. Interestingly, this new green cluster appears to be specific to Cabo Verdean genetic variation, as
280 it is virtually absent from other populations in our dataset except for a small proportion in certain Wolof indi-
281 viduals from West Western Africa.

282 At *K*=10, the light-green cluster is maximized in Cabo Verdean individuals born on Maio, Boa Vista, Sal,
283 and São Nicolau, distinct form the dark green cluster maximized in individuals born on Santo Antão and São
284 Vicente, and hence producing three distinct ADMIXTURE patterns among Cabo Verdean birth-islands. Fur-
285 thermore, an alternative mode at *K*=10 shows (**Appendix 3-figure 1**) that Cabo Verde-born individuals resem-
286 ble more IBS and TSI patterns for their European-like membership than ASW and ACB individuals who,

instead, resemble more CEU and GBR patterns, consistently with ASD-MDS results (**Figure 2** and **Figure 2-figure supplement 1**).

While the modal results comprising the most ADMIXTURE runs for increasing values of *K* from 11 to 13 differentiate novel clustering patterns among continental African and/or European populations (**Figure 3**), alternative, minority, modes here highlight novel possible clustering solutions in turn maximized in different groups of Cabo Verdean islands (**Appendix 3-figure 1**). Ultimately, these alternative ADMIXTURE results are resolved at *K*=14 (**Figure 3**), with the emergence of the new bright yellow cluster maximized in individuals from Boa Vista, and in part in individuals from Maio, while virtually absent from the rest of our data set.

Finally, at *K*=15, the novel dark green cluster is maximized in individuals born on Fogo and substantially present in Brava-born individuals' membership proportions, while virtually absent from all other populations in our data set. Note that alternative clustering solutions at *K*=15 disentangle resemblances across other West Central and South-West Central African populations, but do not further propose additional clusters specifically represented by Cabo Verdean variation (**Appendix 3-figure 1**).

Therefore, altogether, we identified at least five clustering patterns across Cabo Verdean islands of births nested in increasing values of *K*, where, respectively, individuals from Fogo and Brava, from Santiago, from Boa Vista, from Sal and São Nicolau, and from Santo Antão and São Vicente resembled more one another than other individuals from elsewhere in Cabo Verde. In this context, note that Maio individuals cluster intermediately between the Santiago, Boa Vista and São Vicente clusters.

Finally, we aim at describing potential genetic resemblances between the East Asian gene-pool, represented here by the Chinese CHB population, and the Cabo Verdean gene-pool, as a community from China is established in the archipelago since at least the 1950's. Note that for every value of *K* above 3, the light-pink cluster mainly represented by Chinese CHB individuals is found in three ASW and one ACB individuals, as previously identified (10), but is virtually absent in the Cabo Verdean individuals that were included in our study without criteria of geographic origins nor community belonging (see also **Appendix 3**).

Altogether, these ADMIXTURE results, differentiating patterns of genetic resemblance across Cabo Verde and with respect to varied continental African and European populations, have been possible to uncover due to inclusion of varied reference populations from continental Atlantic Africa and Europe, treating all Cabo Verdean islands of birth as differentiated in the analyses (3,23,34).

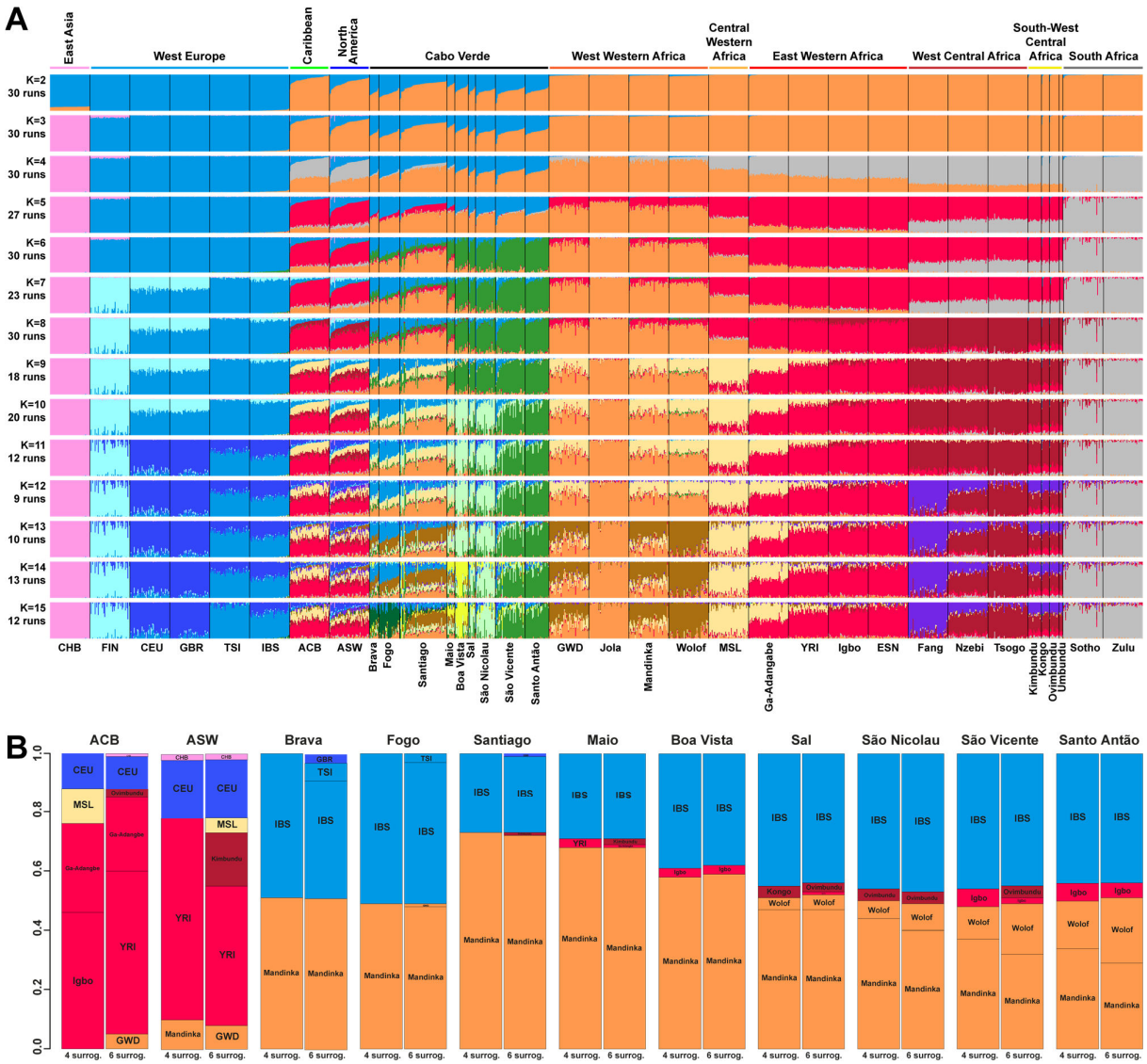

Figure 3:

Individual genetic structure and haplotypic local ancestry inference among Cabo Verdean, Barbadian-ACB and African-American ASW populations.

A) Unsupervised ADMIXTURE analyses using randomly resampled individual sets for populations originally containing more than 50 individuals (**Figure 1-source data 1**). 225 unrelated Cabo Verdean-born individuals in the analysis are grouped by birth island. Numbers of runs highly resembling one another using CLUMPP are indicated below each *K*-value. All other modes are presented in **Appendix 3-figure 1**. **B)** SOURCEFIND results for each eleven target admixed populations (ASW, ACB, each of the nine Cabo Verde birth islands), considering respectively 4 or 6 possible source surrogate populations (abbreviated "surrog.") among the 24 possible European, African, and East Asian populations considered in the ADMIXTURE analyses. The cumulated average African admixture levels in each admixed population was highly consistent between SOURCEFIND estimates and ADMIXTURE results at K=2 (Spearman ρ=0.98861, $p<2\text{x}10^{-8}$ and 0.99772, $p<8\text{x}10^{-12}$, for 4 or 6 surrogates, respectively). Furthermore, individual admixture levels estimated using an ASD-MDS based approach (**Material and Methods 2** and **Appendix 1-figure 2**), were highly consistent with individual admixture estimates based on ADMIXTURE results at K=2 (ρ=0.99725; $p<2.2\text{x}10^{-16}$ for Cabo Verde; ρ=0.99568; $p<2.2\text{x}10^{-16}$ for ASW; ρ =0.99366; $p<2.2\text{x}10^{-16}$ for ACB).

Figure 3-figure supplement 1:

Population F_{ST}/F_{ST}^{max} values for the ASW, ACB, and each Cabo Verdean birth-island separately considering the ADMIXTURE mode result at K=2 in Figure 3A.

338 **Figure 3-figure supplement 2:**
339 ***f_3*-admixture tests of admixture for each Cabo Verdean birth-island, the Barbadian-ACB, and the African-American ASW**
340 **populations related to the TAST.**
341
342

Figure 3-figure supplement 1:

Population F_{ST}/F_{ST}^{max} values for the ASW, ACB, and each Cabo Verdean birth-island separately considering the ADMIXTURE mode result at *K*=2 in Figure 3A.

FST/FST^{max} values were computed using FSTruct (49) with 1000 bootstrap replicates per population. All population pairwise distributions of bootstrap F_{ST}/F_{ST}^{max} values were significantly different from one another after Bonferroni correction (Wilcoxon two-sided rank sum test $p<3.96\text{x}10^{-8}$), except the following pairwise comparisons: ACB-Santiago, Brava-Maio, Fogo-Sal, and Maio-Santo Antão.

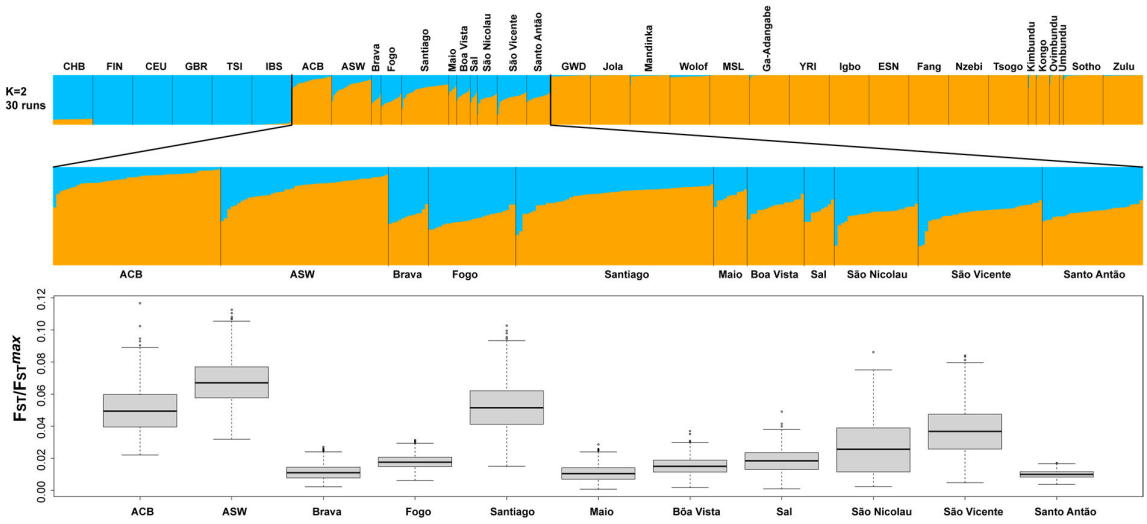

Figure 3-figure supplement 2:

***f_3*-admixture tests of admixture for each Cabo Verdean birth-island, the Barbadian-ACB, and the African-American ASW populations related to the TAST.**

As mentioned in the main text of the article, we calculated f_3-admixture (50) considering as admixture targets each Cabo Verdean birth-island (**panel A**), the ASW (**panel B**), and the ACB (**panel B**) separately, with, as admixture sources, all 108 possible pairs of one continental European population (Source 1) and one continental African population (Source 2), or the East Asian CHB (Source 1) and one continental African population (Source2), using the same individuals, population groupings, and genotyping dataset as in the previous ADMIXTURE analyses (**Figure 1-source data 1**). Results for each pair of possible sources are plotted in diminishing values of f_3-admixture obtained specifically with Cabo Verde individuals born on Santiago as targets. Target population symbols are indicated in the legend at the bottom-right of each panel.

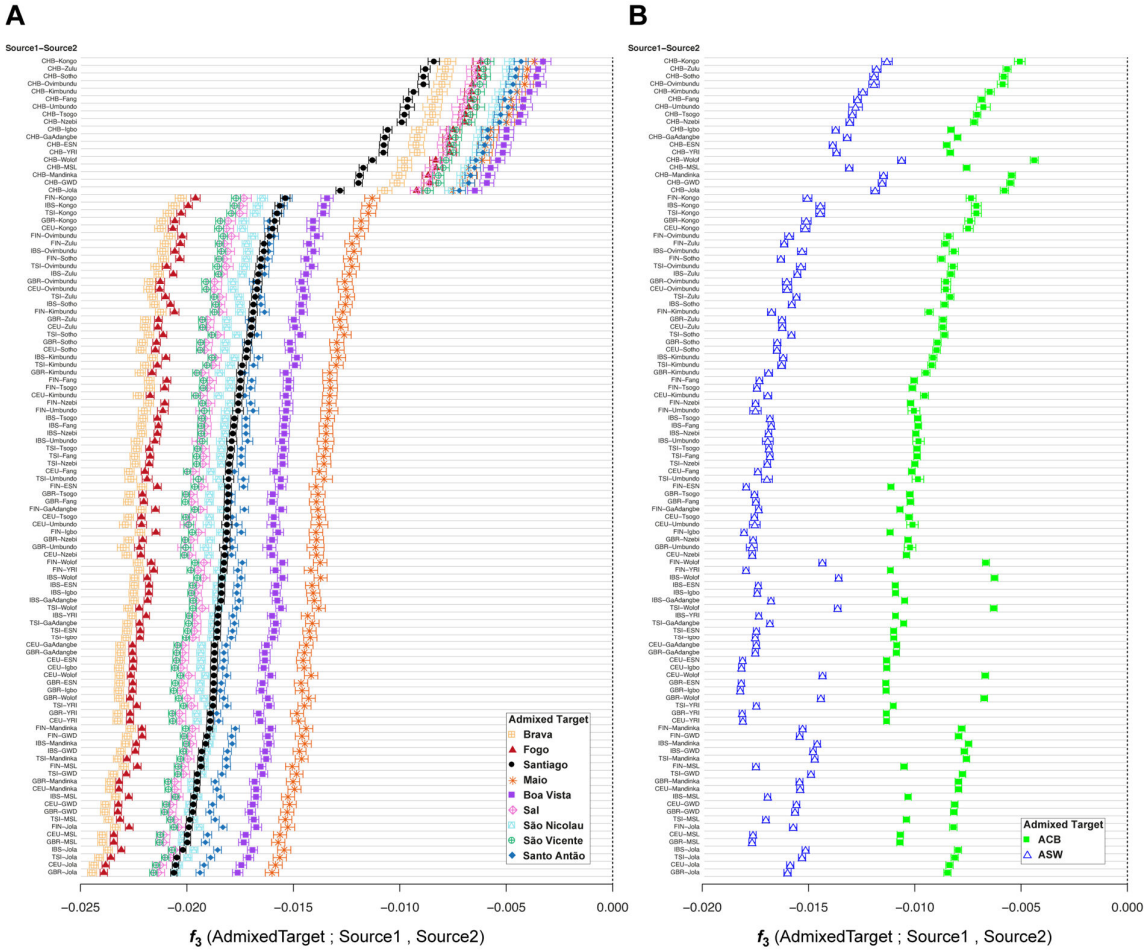

366 **3. Local-ancestry in Cabo Verde and other TAST-related admixed populations**
367 ASD-MDS and ADMIXTURE descriptive analyses do not formally test admixture and putative source popu-
368 lations of origins, they rather disentangle genetic resemblances among groups of individuals. The resulting
369 ADMIXTURE patterns could be due either to admixture from populations represented in our dataset, to ad-
370 mixture from populations un-represented in our dataset, or to common origins and drift (48,51–54). We further
371 analyzed the observed ADMIXTURE results by computing f_3-admixture tests (50). We considered as admix-
372 ture targets each Cabo Verdean birth-island, the ASW, and the ACB separately, with, as admixture sources, in
373 turn all 108 possible pairs of one continental African population and one continental European population, or
374 one continental African population and the East Asian CHB, using the same individuals, population groupings,
375 and genotyping dataset as in the previous ADMIXTURE analyses.
376 For each Cabo Verdean birth island as a separate target population and for all pairs of possible sources
377 tested, we obtain negative values of f_3-admixture (**Figure 3-figure supplement 2**), indicative of possible ad-
378 mixture signals (50). Altogether for the admixture of each Cabo Verdean birth-island, f_3-admixture tests do not
379 allow us to clearly discriminate among possible African sources, nor among possible European sources, due
380 to largely overlapping f_3-admixture values across tests (**Figure 3-figure supplement 2**). Note that f_3 and f_4
381 statistics have been recently shown to be strongly geometrically related to MDS/PCA and that its results need
382 not be due to admixture only (55), similarly to MDS/PCA or ADMIXTURE results (48,51–54). Therefore, we
383 conducted admixture-LD haplotypic local-ancestry inferences with the SHAPEIT2-CHROMOPAINTER-
384 SOURCEFIND pipeline (56–58), to more precisely identify the possible European and African populations at
385 the sources of genetic patterns observed in enslaved-African descendant populations and Cabo Verdeans in
386 particular.
387 **Figure 3B** shows striking differences concerning both the European and the African source populations
388 involved in the admixture history of ACB, ASW, and individuals born on different Cabo Verdean islands. We
389 find that individuals from all Cabo Verdean islands share almost all their European haplotypic ancestry with
390 the Iberian-IBS population rather than other European populations. Santiago-born individuals present the
391 smallest (27%) average haplotypic ancestry shared with IBS, and Fogo-born the highest (51%). Conversely,
392 the ASW and ACB both share haplotypic ancestries only with the USA-CEU of North-Western European
393 origin (20% and 12% respectively).
394 Furthermore, we find that all Cabo Verdeans almost exclusively share African haplotypic ancestries with
395 two Senegambian populations (Mandinka and Wolof) and very reduced to no shared ancestries with other
396 regions of Africa. More specifically, we find that the Mandinka from Senegal are virtually the sole African
397 population to share haplotypic ancestry with Cabo Verdeans born on Brava, Fogo, Santiago, Maio, and Boa
398 Vista, and the majority of the African shared ancestry for Sal, São Nicolau, São Vicente, and Santo Antão. In
399 individuals from these four latter islands, we find shared haplotypic ancestry with the Wolof population rang-
400 ing from 4%-5% for individuals born on Sal (considering four or six possible sources, respectively), up to
401 16%-22% for Santo Antão. Finally, we find limited (1%-6%) shared haplotypic ancestry with East Western
402 (Igbo, YRI, or Ga-Adangbe) or South-West Central (Kimbundu, Kongo, or Ovimbundu) African populations
403 in all Cabo Verdean islands, except Fogo and Brava, and the specific populations identified and their relative
404 proportions of shared haplotypic ancestries vary across analyses. Conversely, we find that the ASW and ACB
405 populations share African haplotypic ancestries in majority with East Western African populations (YRI, Ga-
406 Adangbe, and Igbo), and substantial shared ancestries with Senegambian populations (5-10%), the MSL from
407 Sierra Leone in Central Western Africa (5-12%), and South-West Central African populations (3-18%), albeit
408 variable depending on the number of putative sources considered.
409

410 **4. Runs of homozygosity (ROH) and admixture patterns within Cabo Verde**

411 Runs of homozygosity (ROH) are Identical-By-Descent haplotypes resulting from recent parental
412 relatedness and present in individuals as long stretches of homozygous genotypes. Their length and abundance
413 can reflect demographic events, such as population bottlenecks and founder events, natural selection, and
414 cultural preferences for endogamy (59–61); and ROH have not been seen to depend strongly on recombination
415 or mutation rate variation across the genome (62).

416 We find higher levels of long ROH (≥1cM) in Cabo Verdeans compared to most other analyzed
417 populations, including ASW and ACB (**Figure 4A** and **Appendix 4-figure 1**). We find the highest levels of
418 long-ROH in individuals born on Maio, Boa Vista, Sal, São Nicolau, São Vincente, and Santo Antão, with a
419 mean individual length of long-ROHs around 3cM (**Figure 4B**), and the lowest levels of long-ROH in Santiago
420 and Brava-born individuals. Among long ROH (**Appendix 4-figure 2C**), we find little to no correlation with
421 total non-ROH levels for African local-ancestry segments (Pearson ρ=-0.06689, p=0.3179), European
422 (ρ=0.1551, p=0.01989), or East Asian (ρ=0.06239, p=0.3516). Of all ROH identified, the mean proportion of
423 ROH that were long ranged from 0.065 to 0.280 (**Figure 4-source data 1**).

424 In admixed populations, we expected that some of the long ROH spanned local ancestry breakpoint
425 switches (see **Materials and Methods 4**), indicating that the most recent common ancestor existed after the
426 initial admixture event having generated local-ancestry patterns. Furthermore, we expected that these
427 "spanning" ROH whould be among the longest ROH observed if admixture occurred only in the past few
428 generations. We find that (**Figure 4C**), almost uniformly across Cabo Verde, the longest ROH identified
429 indeed spanned at least one ancestry breakpoint, excluding the very few East Asian ancestry regions identified.
430 Furthermore, correcting ancestry-specific long-ROH sizes (**Figure 4-figure supplement 1**) for individuals'
431 total ancestry fraction of that ancestry, we find that individuals born in Fogo have, on average, an
432 overrepresentation of European ancestry (and a corresponding underrepresentation of African ancestry) in
433 long-ROH (**Figure 4D**; permutation $p < 10^{-4}$; **Figure 4-figure supplement 2, Figure 4-source data 2**), and
434 that individuals from Santo Antão and São Vincente have, conversely, an apparent overrepresentation of
435 African ancestry and underrepresentation of European ancestry in long ROH (permutation $p = 10^{-4}$ and $p < 10^{-}$
436 ^{4}, respectively; **Figure 4-figure supplement 2, Figure 4-source data 2**). Finally, we find that individuals from
437 Brava, Santiago, Maio, Boa Vista, São Nicolau, and Sal have relatively similar long-ROH levels in African
438 and European segments (permutation p > 0.01; **Figure 4-figure supplement 2, Figure 4-source data 2**). This
439 latter pattern may be consistent with these populations being founded by admixed individuals, while the former
440 patterns could indicate, in addition to such admixture founding effects, more recent or recurring contributions
441 from the sources (60).
442

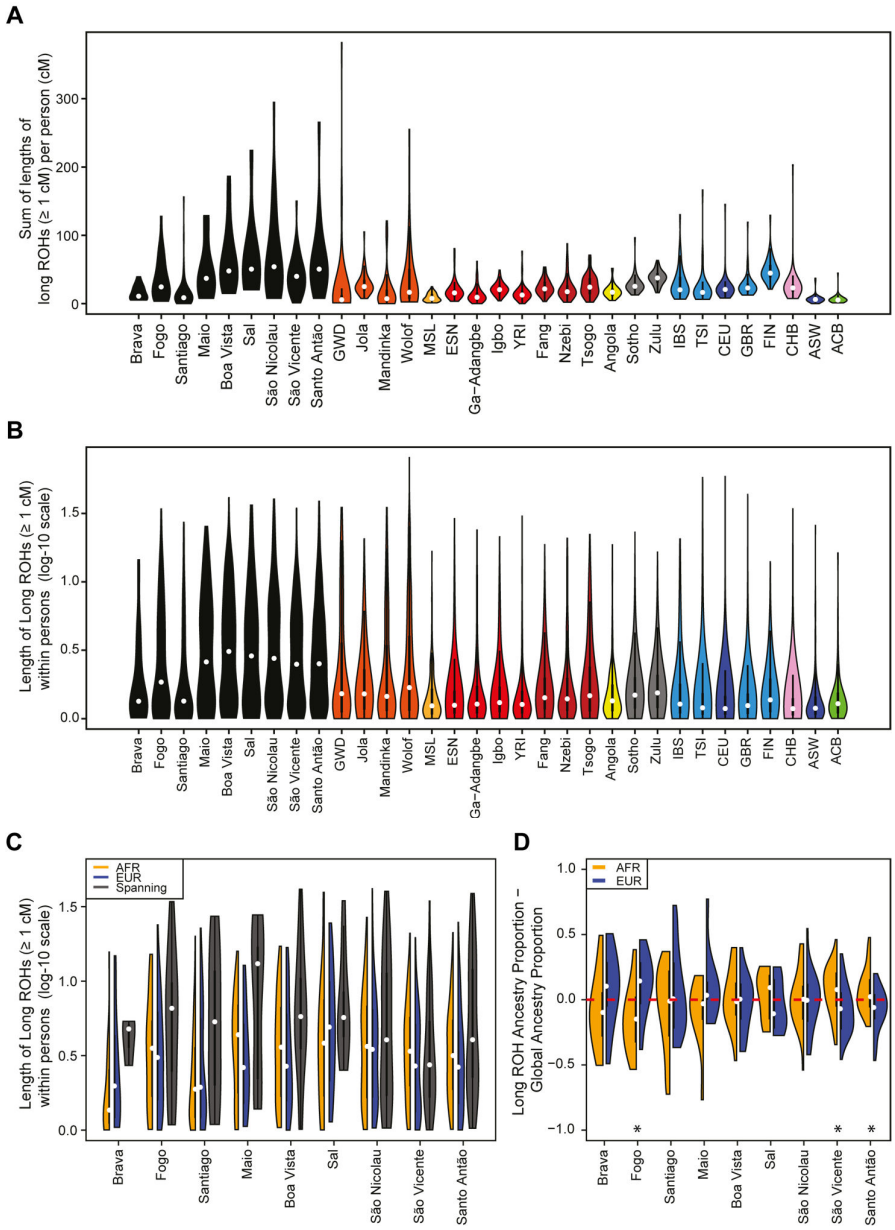

Figure 4:

Distributions of long ROHs (≥ 1 cM) in Cabo Verde.

A) The distribution of the sum of long-ROH (≥ 1 cM) lengths per person for each Cabo Verdean birth-island and other populations. **B)** The length distribution (log-10 scale) of individual long-ROHs identified within samples for each Cabo Verdean birth-island and other populations (e.g., for a distribution with mass at 1.0, this suggests individual ROHs of length 10 cM were identified among samples from that group). **C)** The length distribution of ancestry-specific and ancestry-spanning individual long-ROHs for each Cabo Verdean birth-island. **D)** The distribution of differences between individuals' long-ROH ancestry proportion and their global ancestry proportion, for African and European ancestries separately and for each Cabo Verdean birth-island. * indicates significantly ($\alpha < 1\%$) different proportions of ancestry-specific long-ROH, based on non-parametric permutation tests, see **Material and Methods 4**, **Figure 4-source data 2, and Figure 4-figure supplement 2**.

Figure 4-figure supplement 1:

The distribution of total ancestry in long ROH per individual for each Cabo Verdean birth-island.

Figure 4-figure supplement 2:

460 **Permutation distributions for over/under representation of ancestry in long ROH (≥ 1 cM) for each Cabo Verdean island of**
461 **birth.**
462
463 **Figure 4-source data 1:** ***provided in .xls format***
464 **Mean proportion of total length of ROH that are classified as long (cM≥1) for each Cabo Verdean island of birth.**
465
466 **Figure 4-source data 2:** ***provided in .xls format***
467 **Permutation tests' p-values for over/under representation of ancestry in long ROH (cM≥1) for each Cabo Verdean island of**
468 **birth.**
469
470 **Figure 4-source data 3:** ***provided in .xls format***
471 **Mean proportion of total length of long ROH (cM≥1) that have heterozygous ancestry (AFR and EUR), for each Cabo Verdean**
472 **island of birth.**
473
474

475 **Figure 4-figure supplement 1:**
476 **The distribution of total ancestry in long ROH per individual for each Cabo Verdean birth-island.**
477

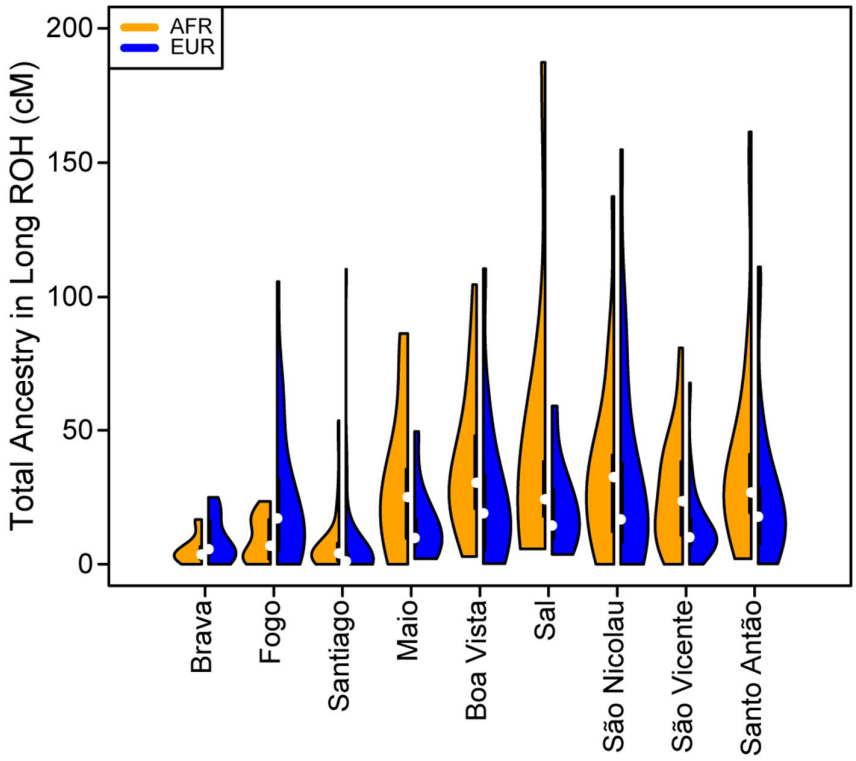

478
479
480

481 **Figure 4-figure supplement 2:**
482 **Permutation distributions for over/under representation of ancestry in long ROH (≥ 1 cM) for each Cabo Verdean island of**
483 **birth.**
484 As mentioned in **Material and Methods 4**, for each individual in each island, we randomly permuted the location of all long ROH
485 (ensuring that no permuted ROH overlap), re-computed the local AFR ancestry proportion falling within these permuted ROH, and
486 then subtracted the global ancestry proportion. We then take the mean of this difference across all individuals for each island and repeat
487 the process 10,000 times. As there is negligible ASN ancestry across these individuals, the AFR and EUR proportions essentially add
488 to 1, and therefore we consider an over/under representation of AFR ancestry in long ROH to be equivalent to an under/over represen-
489 tation of EUR ancestry in long ROH. Observed values in the real data set are provided as a red vertical line for each island of birth
490 separately. Permutation p-values are reported in **Figure 4-source data 2**.
491

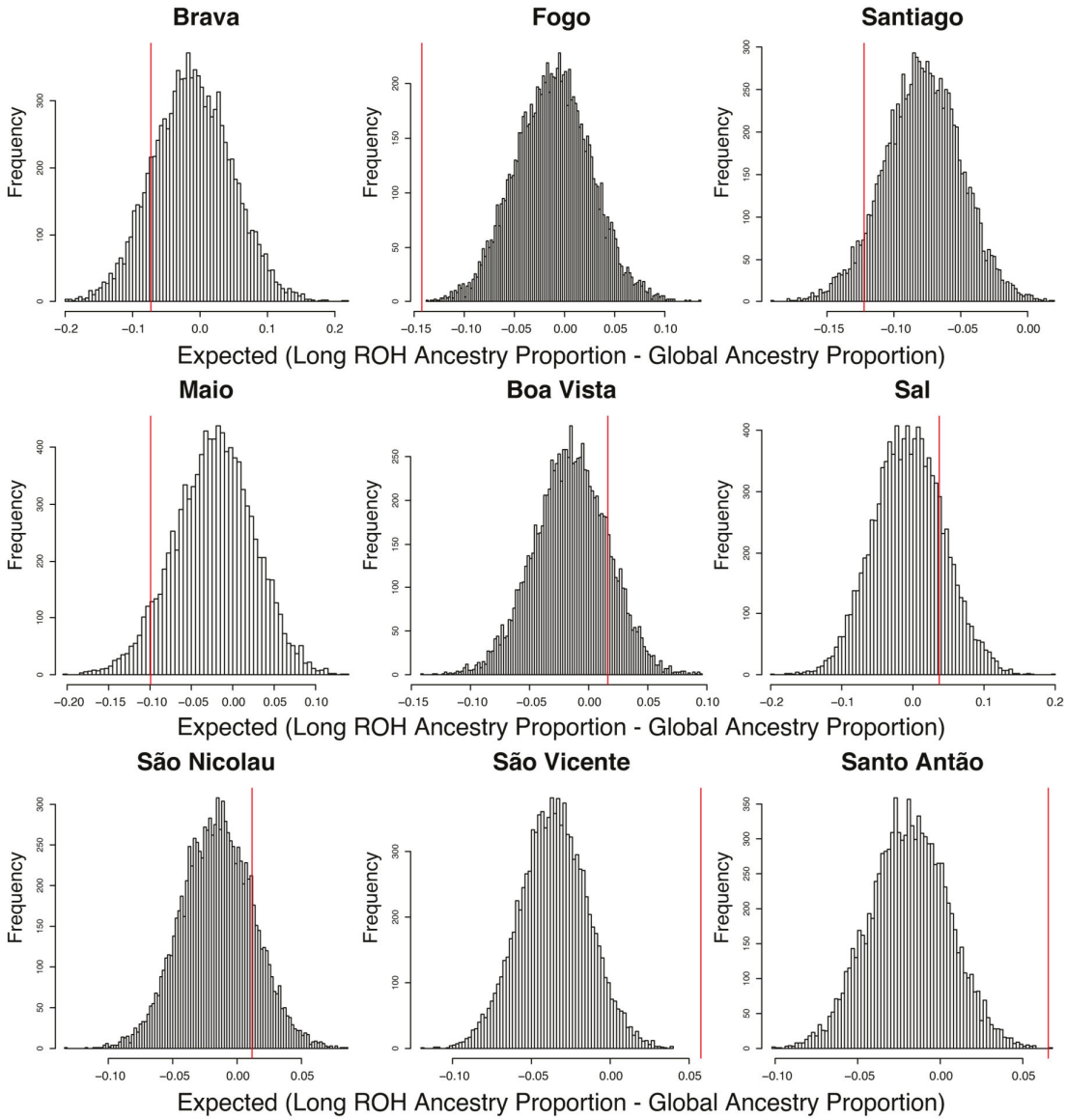

492
493

494 **5. Genetic and linguistic isolation-by-distance within Cabo Verde**
495 The above ASD-MDS, ADMIXTURE, local-ancestry inferences, and ROH results suggest substantial genetic
496 differentiation at a very reduced geographical scale within the archipelago across Cabo Verdean birth-islands
497 of individuals. Following previous linguistic investigations highlighting Kriolu qualitative linguistic variation
498 across islands within the archipelago (15,17,29,30), we aim at further characterizing possible patterns of joint
499 genetic and linguistic isolation (39) at very reduced geographical scale across islands as well as within islands.
500 Indeed, while the geographic distribution of genetic diversity has been previously extensively explored across
501 human populations to reveal population migration routes, in particular in island and archipelago contexts (e.g.
502 (63,64)), the underlying parent-offspring genetic and linguistic dispersal mechanisms have been seldom ex-
503 plored in humans at extremely local scales to our knowledge (39,42–44). Nevertheless, knowledge about such
504 dispersal mechanisms can be built by exploring the influence of isolation-by-distance mechanisms on genetic
505 and linguistic diversity distributions at very reduced geographical scales (~50km) within a population (39–41).
506 We thus explored both pairwise ASD and inter-individual variation in manners of speaking Kriolu (character-
507 ized as differences in the frequencies of use of Kriolu utterances among individual discourses; see **Material**
508 **and Methods 1.c-d**), in the same set of 225 Cabo Verde-born individuals. To do so, we used MDS and Mantel
509 testing of correlations between, respectively, genetic and linguistic pairwise differentiation, and socio-cultural
510 and geographical covariates including age, duration of academic education, residence locations, birth-places,
511 and parental birth-places (**Figure 5**, **Table 1**, and **Table 1-source data 1**).
512 The first ASD-MDS axis differentiates mainly individuals born on Brava and Fogo compared to Santiago
513 (**Figure 5A-B**). The second axis mainly differentiates individuals from Santiago, Fogo, and Brava from all
514 other islands, while the third axis differentiates individuals from Boa Vista, São Nicolau, Sal, and Maio from
515 all other birth-islands. Furthermore, we find a significant positive correlation between ASD and actual indi-
516 vidual birth-locations across Cabo Verde (**Table 1**; Spearman ρ=0.2916, two-sided Mantel $p<2\text{x}10^{-4}$). This
517 correlation increases when considering only within-islands pairwise comparisons and excluding all inter-island
518 comparisons (Spearman ρ=0.3460, two-sided Mantel $p<2\text{x}10^{-4}$), thus illustrating the strong signal of genetic
519 isolation-by-distance (39) within Cabo Verde at very reduced geographical scales.
520 Furthermore, the first utterance-MDS axis of pairwise inter-individual Euclidean distances between utter-
521 ance frequencies mainly differentiates Santiago and Santo Antão/São Vicente-born individuals' speech-varie-
522 ties; all other Cabo Verdeans cluster intermediately (**Figure 5C-D**). The third axis further separates speech-
523 varieties recorded in individuals from Fogo, Maio, and Brava. Analogously to genetic differentiation patterns,
524 we find a positive correlation between differences in utterance frequencies and actual birth-places' distances
525 (Spearman ρ=0.2794, two-sided Mantel $p<2\text{x}10^{-4}$), as well as paternal and maternal birth-places respectively
526 (**Table 1**). However, unlike for to ASD, we find that utterance-frequencies differences stem from inter-birth-
527 islands' distances, rather than shorter distances within islands only. Extending previous results from Santiago
528 only (23), these results altogether show that speech-varieties are significantly transmitted from one generation
529 to the next throughout Cabo Verde, anchored in individuals' birth-places. Importantly, note, however, that this
530 vertical transmission of manners of speaking Kriolu does not account for the majority of observed linguistic
531 variation across individuals in our dataset. Indeed, we find that age-differences also substantially correlate with
532 utterance-frequency differences even when correcting for individual birth-places (Spearman ρ=0.2294, two-
533 sided partial-Mantel $p<2\text{x}10^{-4}$). Finally, while we might intuitively expect that academic education influences
534 idiolects, we find instead that differences in education-duration do not correlate with Kriolu utterance-frequen-
535 cies differences, whether correcting for residence or birth-places distances, or not (**Table 1**). This shows the
536 modest influence of academic education on Kriolu variation. Altogether, our results highlight strong genetic
537 and linguistic isolation-by-distance patterns at reduced geographic distances within Cabo Verde.
538 Altogether, we find here genetic and linguistic isolation-by-distance anchored in inter-individual birth-
539 places distances across, and sometimes within, Cabo Verdean islands. These results demonstrate the reduced

dispersal of Cabo Verdeans at very local scales within the archipelago, both genetically and linguistically, a fundamental mobility-behavior mechanism likely explaining genetic and linguistic isolation across islands and sometimes even within islands despite the large self-reported exploration mobility of Cabo Verdeans.

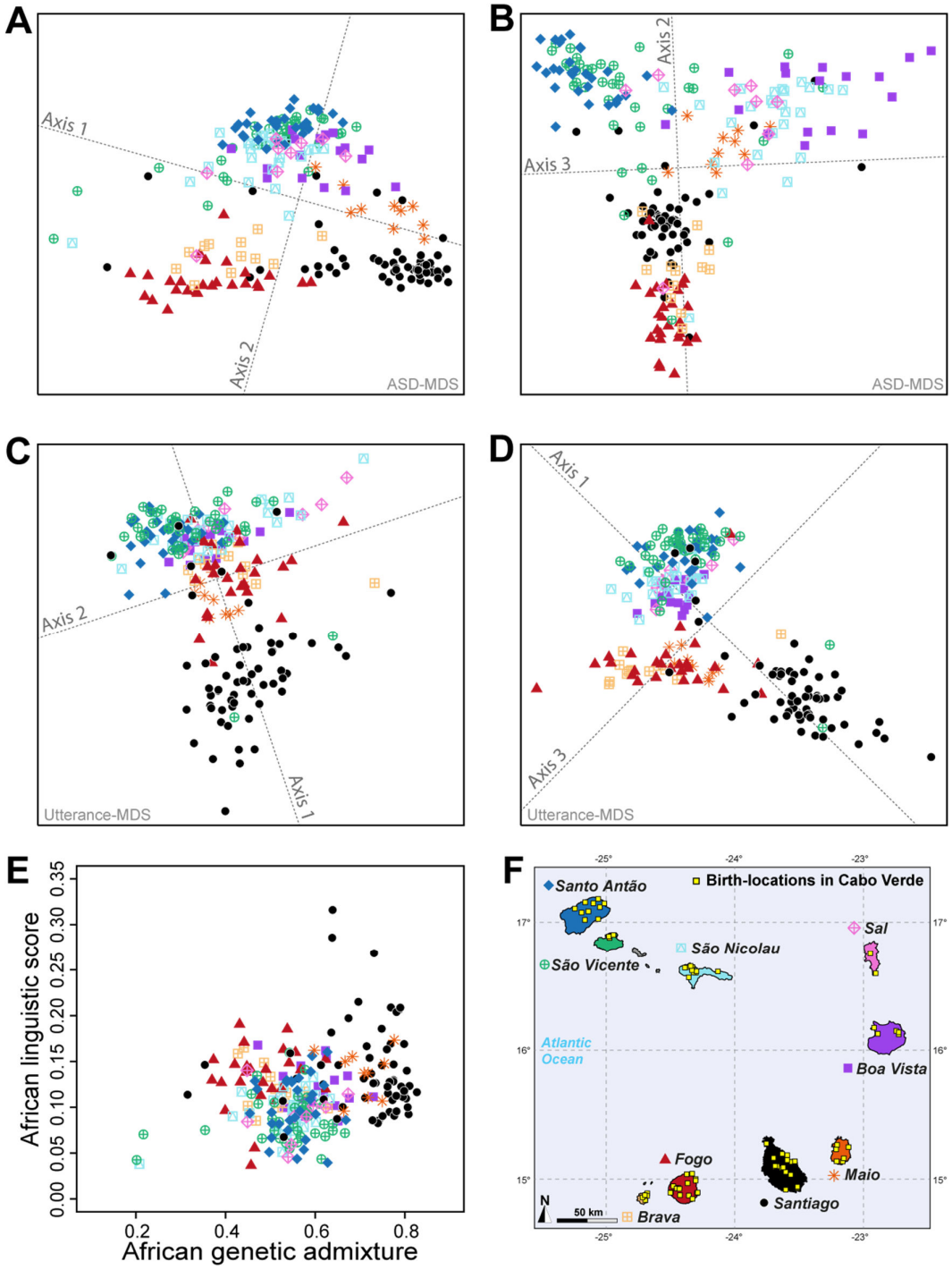

Figure 5:

Utterance and genetic diversity and admixture within Cabo Verde.

A-B) 3D MDS projection of Allele Sharing Dissimilarities computed among 225 unrelated Cabo-Verde-born individuals using 1,899,878 autosomal SNPs. Three-dimensional Euclidean distances between pairs of individuals in this MDS significantly correlated with ASD (Spearman ρ=0.6863; p<2.2x10^{-16}). **C-D)** 3D MDS projection of individual pairwise Euclidean distances between uttered

551 linguistic items frequencies based on the 4831 unique uttered items obtained from semi-spontaneous discourses. Three-dimensional
552 Euclidean distances between pairs of individuals in this MDS significantly correlated with the utterance-frequencies distances (Spear-
553 man ρ=0.8647; $p<2.2\text{x}10^{-16}$). **E)** Spearman correlation between individual African utterance scores and individual genetic African
554 admixture rates obtained with ADMIXTURE at *K*=2. **F)** Birth-locations of 225 individuals in Cabo Verde. Symbols for individuals'
555 birth-island in panels **A**-**E** are shown in panel **F**. Panel **A-D** were Procrustes-transformed according to individual actual birth-places'
556 geographical locations in panel **F** (65).

Mantel variable	Partial-Mantel control	n	Geographic scale	Genetic ASD - 1,899,978 SNPs		Utterance-frequency Euclidean distances - 4831 uttered items	
				Spearman rho	10000 Mantel two-sided permutation p	Spearman rho	10000 Mantel two-sided permutation p
abs(Age difference)	--	225	within and between islands	**0.1303**	**< 2.10^{-4}**	**0.2215**	**< 2.10^{-4}**
abs(Age difference)	log(Birth-loc. dist.)	225	within and between islands	**0.1348**	**< 2.10^{-4}**	**0.2294**	**< 2.10^{-4}**
log(Birth-loc. dist.)	--	225	within and between islands	**0.2916**	**< 2.10^{-4}**	**0.2794**	**< 2.10^{-4}**
log(Birth-loc. dist.)	abs(Age difference)	225	within and between islands	**0.2935**	**< 2.10^{-4}**	**0.2855**	**< 2.10^{-4}**
abs(Education duration difference)	--	186	within and between islands	*0.0168*	*0.2730*	*0.0962*	*0.0024*
abs(Education duration difference)	log(Birth-loc. dist.)	186	within and between islands	*-0.0023*	*0.4900*	*0.0834*	*0.0071*
abs(Education duration difference)	--	185	within and between islands	*0.0159*	*0.2825*	*0.1001*	*0.0014*
abs(Education duration difference)	log(Residence dist.)	185	within and between islands	*-0.0041*	*0.4651*	*0.0824*	*0.0068*
log(Residence dist.)	--	224	within and between islands	**0.1658**	**< 2.10^{-4}**	**0.2145**	**< 2.10^{-4}**
log(Residence dist.)	log(Birth-loc. dist.)	224	within and between islands	**-0.0488**	**0.0005**	*0.0306*	*0.0682*
log(Birth-loc. dist.)	--	224	within and between islands	**0.2889**	**< 2.10^{-4}**	**0.2800**	**< 2.10^{-4}**
log(Birth-loc. dist.)	log(Residence dist.)	224	within and between islands	**0.2445**	**< 2.10^{-4}**	**0.1863**	**< 2.10^{-4}**
log(Father Birth-loc. dist.)	--	222	within and between islands	**0.2424**	**< 2.10^{-4}**	**0.1704**	**< 2.10^{-4}**
log(Father Birth-loc. dist.)	log(Birth-loc. dist.)	222	within and between islands	*0.0846*	*0.0014*	*0.0066*	*0.3915*
log(Mother Birth-loc. dist.)	--	224	within and between islands	**0.2619**	**< 2.10^{-4}**	**0.2634**	**< 2.10^{-4}**
log(Mother Birth-loc. dist.)	log(Birth-loc. dist.)	224	within and between islands	*0.0748*	*0.0057*	*0.0853*	*0.0071*
abs(Age difference)	--	225	within islands only	**0.2124**	**0.0006**	**0.2727**	**< 2.10^{-4}**
abs(Age difference)	log(Birth-loc. dist.)	225	within islands only	*0.1648*	*0.0041*	**0.2546**	**< 2.10^{-4}**
log(Birth-loc. dist.)	--	225	within islands only	**0.3460**	**< 2.10^{-4}**	*0.1412*	*0.0401*
log(Birth-loc. dist.)	abs(Age difference)	225	within islands only	**0.3212**	**< 2.10^{-4}**	*0.0990*	*0.1030*
abs(Education duration difference)	--	186	within islands only	*-0.0370*	*0.3077*	*0.1287*	*0.0440*
abs(Education duration difference)	log(Birth-loc. dist.)	186	within islands only	*-0.0537*	*0.2330*	*0.1239*	*0.0496*
abs(Education duration difference)	--	185	within islands only	*-0.0382*	*0.3037*	*0.1421*	*0.0292*
abs(Education duration difference)	log(Residence dist.)	185	within islands only	*-0.0491*	*0.2566*	*0.1202*	*0.0546*
log(Residence dist.)	--	224	within islands only	*-0.0667*	*0.1907*	*0.0982*	*0.0911*
log(Residence dist.)	log(Birth-loc. dist.)	224	within islands only	*-0.0549*	*0.2319*	*0.1063*	*0.0704*
log(Birth-loc. dist.)	--	224	within islands only	**0.3465**	**< 2.10^{-4}**	*0.1537*	*0.0282*
log(Birth-loc. dist.)	log(Residence dist.)	224	within islands only	**0.3446**	**< 2.10^{-4}**	*0.1589*	*0.0230*
log(Father Birth-loc. dist.)	--	222	within islands only	**0.2660**	**0.0006**	*0.0160*	*0.4123*
log(Father Birth-loc. dist.)	log(Birth-loc. dist.)	222	within islands only	*0.2187*	*0.0045*	*-0.0111*	*0.4546*
log(Mother Birth-loc. dist.)	--	224	within islands only	*0.2240*	*0.0034*	*0.1283*	*0.0423*
log(Mother Birth-loc. dist.)	log(Birth-loc. dist.)	224	within islands only	*0.1563*	*0.0303*	*0.1000*	*0.0925*

Table 1:
Mantel and partial-Mantel correlations between utterance frequency differences and covariables, and between genetic ASD and the same covariables, in 225 genetically unrelated Cabo Verde-born Kriolu-speaking individuals.
Spearman correlations ρ are indicated in bold when significant at $\alpha<0.001$, and in italics otherwise. Spearman correlations and Mantel-tests among covariables are provided in **Table 1-source data 1**.

Table 1-source data 1: ***provided in .xls format***
Mantel correlations among individual birth-places, residence-places, maternal and paternal birth places, age, and academic education duration.

566 **6. Geographic distribution of genetic and linguistic admixture within Cabo Verde**
567 Based on these results of genetic and linguistic diversity isolation-by-distance patterns anchored in individual's
568 birth-places, we aim at investigating whether individual genetic and/or linguistic admixture levels also exhibit
569 isolation-by-distance patterns across and within islands, beyond the qualitative observation that genetic and
570 linguistic admixture patterns vary across different islands of Cabo Verde obtained above and in previous results
571 (23,34). Interestingly, we find that absolute differences in inter-individual genetic admixture levels from Africa,
572 estimated with ADMIXTURE or ASD-MDS, significantly correlate with actual birth-places distance across
573 islands (Spearman ρ=0.1865, two-sided Mantel $p<2x10^{-4}$ and ρ=0.1813, $p<2x10^{-4}$, respectively), but not
574 within-islands only (ρ=0.0342 p=0.3094 and ρ=0.0282 p=0.3385, respectively). This shows that two individ-
575 uals born on far-away islands are likely to differ more in African genetic admixture levels, than two individuals
576 born on close-by islands, a form of isolation-by-distance pattern for genetic admixture across Cabo Verdean
577 islands.
578 We explored inter-individual variation in Kriolu utterance frequencies specifically for uttered items of
579 clearly African and dual European-African origins (utterance categories A and B; **Material and Methods 1.e**)
580 providing an estimate of individual African linguistic-admixture scores (23). We find that African linguistic-
581 admixture score differences significantly correlate with actual birth-places' distances throughout Cabo Verde
582 (Spearman ρ=0.1297, two-sided Mantel $p<2x10^{-4}$), and even marginally significantly correlate with birth-
583 places' distances at short distances within birth-islands (Spearman ρ=0.1209, two-sided Mantel p=0.0419).
584 Finally, we find a significant positive correlation (Spearman ρ=0.2070, p=0.0018) between genetic and
585 linguistic admixture in Cabo Verde (**Figure 5E**), indicating that individuals who frequently use African-related
586 utterances in their manner of speaking Kriolu are more likely to exhibit higher levels of African genetic-ad-
587 mixture. This correlation remains, respectively, marginally significant and significant when considering utter-
588 ances of strictly African-origin (Category A) or utterances with a dual European-African etymology (Category
589 B) separately (Spearman ρ=0.1631, p=0.0143, and ρ=0.1829, p=0.0059, respectively). These positive correla-
590 tions between genetic and linguistic admixture generalize to the whole archipelago our previous results ob-
591 tained in Santiago only (23), and further suggest that genetic and linguistic admixture histories may have oc-
592 curred in parallel all throughout Cabo Verde.
593 Therefore, not only we identify isolation-by-distance patterns within Cabo Verdean islands for genetic
594 and linguistic diversities, but also identify a form of isolation-by-distance for genetic and linguistic admixture
595 levels at very reduced geographical scales. This suggests that processes of reduced dispersal of individuals can
596 also be identified in the genetic and linguistic admixture patterns, which has never been previously observed
597 in human admixed populations to our knowledge, nor previously suspected whether genetically or linguisti-
598 cally in Cabo Verde (3,15,17,23,30,33).
599 Together with the above LAI and ROH results, the various isolation-by-distance patterns here identified
600 suggest that different founding events followed by local isolation due to reduced genetic and linguistic disper-
601 sal ranges, as well as different admixture histories, are at the root of patterns of genetic and linguistic diversity
602 and admixture throughout Cabo Verde, anchored in individual birth places across islands, and even sometimes
603 within islands.
604

605 **7. Genetic admixture histories in Cabo Verde inferred with *MetHis*-ABC**
606 Highly complex admixture histories, with more than two separate pulses and/or periods of recurring admixture
607 from each source population, are often impossible to infer from observed genetic data using maximum-likeli-
608 hood approaches; whether the likelihood itself cannot be explicitly formulated or whether its maximization is
609 computationally intractable for such high levels of complexity (8,9,66,67). Instead, Approximate Bayesian
610 Computation allows, in principle, formal comparison of competing scenarios underlying the observed data and
611 estimation of the posterior distribution of the parameters under the winning model (68,69). The user simulates
612 numerous genetic datasets under competing scenarios, drawing randomly the parameter values of each simu-
613 lation in prior distributions. ABC then allows to formally compare a set of summary statistics calculated on
614 the observed data with the same set of summary statistics calculated on each simulated genetic dataset sepa-
615 rately, in order to identify which of the competing scenarios produces simulations for which summary-statistics
616 are closest to the observed ones. Under the winning scenario, ABC then estimates the joint posterior distribu-
617 tion of parameter values which produced simulations whose summary statistics most resemble the observed
618 ones. Therefore, ABC allows, in principle, to infer arbitrarily complex demographic models underlying the
619 data, provided that data can be efficiently simulated under these scenarios drawing randomly parameter values
620 from prior distributions explicitly set by the user, and provided that calculated summary statistics are indeed
621 informative about the scenarios' parameters (70).
622 We reconstruct the admixture histories of each Cabo Verde island separately using the *MetHis*-ABC
623 framework (45,71,72). It was recently developed to investigate highly complex admixture histories using ma-
624 chine-learning ABC, by simulating independent autosomal SNPs forward-in-time in an admixed population
625 under any two source-population versions of a general admixture model (73), and calculating, for each simu-
626 lation, sets of summary statistics shown to be informative about the underlying admixture models' parameters
627 for ABC inferences (45). See **Material and Methods 7** and **Appendix 1** for the detailed description of simu-
628 lations and ABC machine-learning scenario-choice and posterior parameter estimation procedures.
629
630 <u>*MetHis*–ABC prior checking</u>
631 We considered four competing genetic-admixture scenarios described in **Figure 6** and **Table 2**, tested
632 separately for individuals born on each Cabo Verdean island and for the 225 Cabo Verde-born unrelated indi-
633 viduals grouped altogether, with *MetHis*–ABC machine-learning scenario-choice and posterior parameter in-
634 ferences (45,71,72). ABC inferences are based on 42 summary statistics (**Table 3**), calculated for each simu-
635 lation under each competing scenario separately using 60,000 independent autosomal SNPs in Cabo Verdean
636 individuals, the African Mandinka and the European Iberian-IBS proxy source populations.
637 Note that we did not explicitly simulate genotype data in the European and African source-populations.
638 Instead, we built gamete reservoirs at each 21 generation of the forward-in-time admixture process, matching
639 in frequency the observed allele frequencies at the 60,000 independent SNPs for the Iberian IBS and Mandinka
640 populations, respectively. As in our previous *MetHis*-ABC investigation of the admixture history of the Afri-
641 can-American ASW and Barbadian ACB populations (45), we therefore consider that the African and Euro-
642 pean proxy populations at the source of the admixture history of Cabo Verde are large and unaffected by
643 mutation during the 21 generations of the admixture process; this assumption is reasonable provided that we
644 consider only independent genotyped SNPs and the very recent demographic history of the archipelago, dis-
645 covered un-inhabited and first settled in the 1460's. Therefore, although we cannot reconstruct the evolutionary
646 history of the African and European source populations with our design, we nevertheless implicitly take the
647 real demographic histories of these source populations into account in our simulations, as we use observed
648 genetic patterns themselves, the product of this demographic history, to create the virtual source populations
649 at the root of the admixture history of Cabo Verde.

We find that the summary-statistics calculated from the observed datasets fall well within the space of summary-statistics obtained from 10,000 simulated-datasets under each of the four competing scenarios (**Appendix 1-figure 3**, **Appendix 1-figure 3-figure supplement 1-10**), considering non-significant ($\alpha > 5\%$) goodness-of-fit, visual inspection of summary-statistics PCA-projections, and each summary-statistic's distribution, for each Cabo Verdean birth-island and for all Cabo Verde-born individuals grouped in a single population, separately. Prior-checks thus demonstrate that *MetHis* simulations are appropriate for further ABC scenario-choice and posterior parameter inferences using observed data in the African Mandinka and the European Iberian IBS source populations and each Cabo Verde islands separately or grouped altogether, as they allow to mimic the observed summary-statistics, despite the assumption that the European and African proxy source populations are at the drift-mutation equilibrium over the last 21 generations.

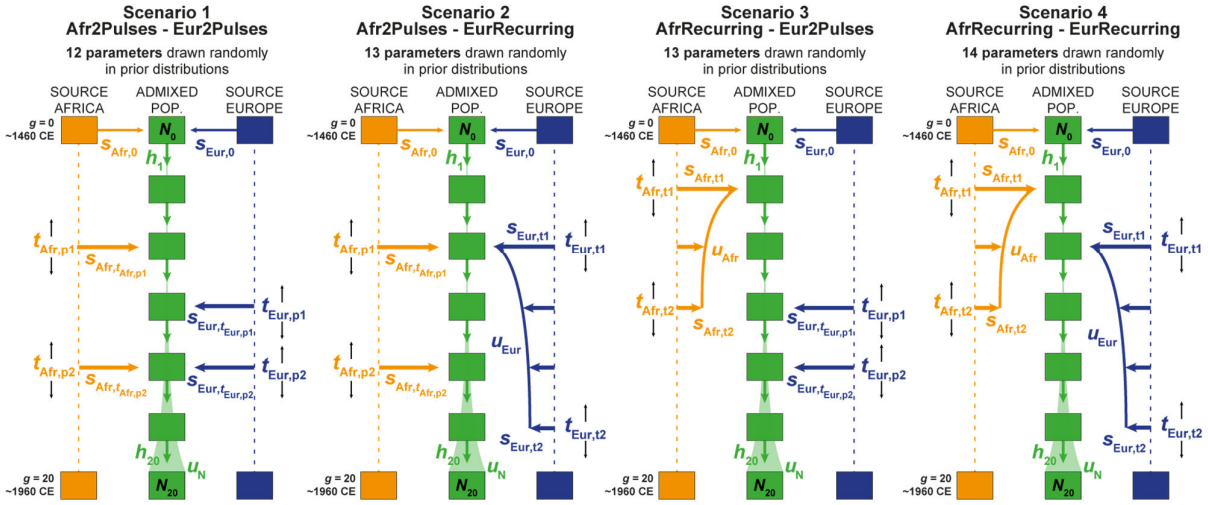

Figure 6:

Four competing scenarios for the genetic admixture histories of each Cabo Verde island.

For all scenarios, the duration of the admixture process is set to 20 generations after the initial founding admixture event occurring at generation 0, which corresponds roughly to the initial peopling of Cabo Verde in the 1460's, considering 25 years per generation and sampled individuals born on average between the 1960s and 1980's.

Scenario 1 Afr2Pulses-Eur2Pulses: after the initial founding pulse of admixture, the admixed population receives two separate introgression pulses from the African and European sources, respectively. ***Scenario 2 Afr2Pulses-EurRecurring***: after the initial founding pulse of admixture, the admixed population receives two separate introgression pulses from the African source, and a period of monotonically constant or decreasing recurring introgression from the European source. ***Scenario 3 AfrRecurring-Eur2Pulses***: after the initial founding pulse of admixture, the admixed population receives a period of monotonically constant or decreasing recurring introgression from the African source, and two separate introgression pulses from the European source. ***Scenario 4 AfrRecurring-EurRecurring***: after the initial founding pulse of admixture, the admixed population receives a period of monotonically constant or decreasing recurring introgression from the African source, and, separately, a period of monotonically constant or decreasing recurring introgression from the European source.

For all scenarios, we consider demographic models corresponding to either a constant reproductive population size N_g between the founding event and the present, or, instead, a linear or hyperbolic increase between N_0 and N_{20}, depending on the values of N_0, N_{20}, and u_N used for each simulation respectively.

Time for admixture pulses or time for the onset and offset of admixture periods are schematically represented as $t_{\mathrm{Source,g}}$. We define (73), $s_{\mathrm{Afr,g}}$, $s_{\mathrm{Eur,g}}$, and h_{g} as the proportion of parents of individuals in the admixed population at generation g coming from, respectively, the African source population, the European one, and the admixed population itself at the previous generation. Thus, for $g = 0$, $s_{\mathrm{Afr,0}} + s_{\mathrm{Eur,0}} = 1$, and for each value of g in [1,20], $s_{\mathrm{Afr,g}} + s_{\mathrm{Eur,g}} + h_{\mathrm{g}} = 1$. The number of "free" scenario-parameters drawn randomly in prior distributions set by the user for simulations and subsequent Approximate Bayesian Computation inferences is indicated below the name of each scenario respectively.

See **Table 2** for parameter prior distributions, and **Materials and Methods 7** for detailed descriptions of scenario-parameters.

Description	Scenario	Model parameter	Prior	Conditions
African admixture-pulse times	1, 2	$t_{Afr,p1}$	Uniform [1 , 20] in discrete generations, a range corresponding to between ~1485 and ~1960 in years CE	$t_{Afr,p1} > t_{Afr,p2}$
		$t_{Afr,p2}$		
European admixture-pulse times	1, 3	$t_{Eur,p1}$	Uniform [1 , 20] in discrete generations, a range corresponding to between ~1485 and ~1960 in years CE	$t_{Eur,p1} > t_{Eur,p2}$
		$t_{Eur,p2}$		
African admixture period start and end times	2, 4	$t_{Afr,t1}$	Uniform [1 , 20] in discrete generations, a range corresponding to between ~1485 and ~1960 in years CE	$t_{Afr,t1} > t_{Afr,t2}$
		$t_{Afr,t2}$		
European admixture period start and end times	3, 4	$t_{Eur,t1}$	Uniform [1 , 20] in discrete generations, a range corresponding to between ~1485 and ~1960 in years CE	$t_{Eur,t1} > t_{Eur,t2}$
		$t_{Eur,t2}$		
African admixture-pulse intensities	1, 2	$s_{Afr,tAfr,p1}$	Uniform [0 , 1]	$s_{Afr,g} + s_{Eur,g} = 1 - h_g$, with h_g in [0,1]
		$s_{Afr,tAfr,p2}$		
European admixture-pulse intensities	1, 3	$s_{Eur,tEur,p1}$	Uniform [0 , 1]	
		$s_{Eur,tEur,p2}$		
African admixture period intensity parameters	2, 4	$s_{Afr,tAfr,t1}$	Uniform [0 , 1]	$s_{Afr,tAfr,t1} \geq s_{Afr,tAfr,t2}$
		$s_{Afr,tAfr,t2}$	Uniform [0 , 1]	$s_{Afr,g} + s_{Eur,g} = 1 - h_g$, with h_g in [0,1]
		u_{Afr}	Uniform [0 , 0.5]	
European admixture period intensity parameters	3, 4	$s_{Eur,tEur,t1}$	Uniform [0 , 1]	$s_{Eur,tEur,t1} \geq s_{Eur,tEur,t2}$
		$s_{Eur,tEur,t2}$	Uniform [0 , 1]	$s_{Afr,g} + s_{Eur,g} = 1 - h_g$, with h_g in [0,1]
		u_{Eur}	Uniform [0 , 0.5]	
Admixture pulse at the foundation	1, 2, 3, 4	$s_{Afr,0}$	Uniform [0 , 1]	$S_{Eur,0} = 1 - s_{Afr,0}$
Founding reproductive population size	1, 2, 3, 4	N_0	Uniform [10 , 1000]	
Current reproductive population size	1, 2, 3, 4	N_{20}	Uniform [100 , 100000]	$N_0 \leq N_{20}$
Steepness of the reproductive population size increase	1, 2, 3, 4	u_N	Uniform [0 , 0.5]	

693
694 **Table 2:**
695 **Prior distributions for the parameters of four competing scenarios for the admixture history of Cabo Verde islands.**
696 Parameters are presented in **Figure 6** and described in **Materials and Methods 7**.
697

Summary Statistics for ABC inference		Nunber of statistics	Reference
within population	Mean ASD within population H	1	(46)
	Mean Heterozygosity (SNP by SNP) within population H	1	(74)
	Variance Heterozygosity (SNP by SNP) within population H	1	(74)
	Mean inbreeding F within population H	1	(75)
	Variance inbreeding F within population H	1	(75)
admixture pattern	Mode ASD-MDS African admixture proportions in population H	1	(45,73)
	Mean ASD-MDS African admixture proportions in population H	1	(45,73)
	Variance ASD-MDS African admixture proportions in population H	1	(45,73)
	Skewness ASD-MDS African admixture proportions in population H	1	(45,73)
	Kurtosis ASD-MDS African admixture proportions in population H	1	(45,73)
	Min ASD-MDS African admixture proportions in population H	1	(45,73)
	Max ASD-MDS African admixture proportions in population H	1	(45,73)
	Deciles of ASD-MDS African admixture proportions in population H	9	(45,73)
	Mode ASD-MDS "African-European angles" in population H	1	This study; **Appendix 1-figure 2**
	Mean ASD-MDS "African-European angles" in population H	1	This study; **Appendix 1-figure 2**
	Variance ASD-MDS "African-European angles" in population H	1	This study; **Appendix 1-figure 2**
	Skewness ASD-MDS "African-European angles" in population H	1	This study; **Appendix 1-figure 2**
	Kurtosis ASD-MDS "African-European angles" in population H	1	This study; **Appendix 1-figure 2**
	Min ASD-MDS "African-European angles" in population H	1	This study; **Appendix 1-figure 2**
	Max ASD-MDS "African-European angles" in population H	1	This study; **Appendix 1-figure 2**
	Deciles of ASD-MDS "African-European angles" in population H	9	This study; **Appendix 1-figure 2**
between populations	FST(African Source - Population H)	1	(76)
	FST(European Source - Population H)	1	(76)
	Mean ASD (African Source - Population H)	1	(46)
	Mean ASD (European Source - Population H)	1	(46)
	f3 (Population H ; European Source, African Source)	1	(50)

698

699 **Table 3:**

700 **Summary-statistics used for *MetHis*-machine-learning ABC inferences.**

701 All 42 statistics were computed using the summary-statistics computation tool embedded in *MetHis* (45).

702

703

704 *MetHis*–Random Forest (RF)-ABC scenario-choices
705 Overall (**Figure 7B**), *MetHis*-RF-ABC scenario-choices indicate that multiple pulses of admixture from the
706 European and African source populations (after the founding admixture pulse, two independent admixture
707 pulses from both Africa and Europe: "Afr2Pulses-Eur2Pulses" scenarios, **Figure 6 – Scenario 1**), best explain
708 the genetic history of individuals born on six of nine Cabo Verdean islands. Furthermore, we find that even
709 more complex scenarios involving a period of recurring admixture from either source best explain the history
710 of the remaining three islands. Scenarios with periods of recurring admixture from both Africa and Europe
711 ("AfrRecurring-EurRecurring", **Figure 6 – Scenario 4**) are the least favored across Cabo Verde.
712 RF-ABC cross-validation prior-errors for each of the 40,000 simulations used, in-turn, as pseudo-ob-
713 served data indicate a reasonably good, albeit not perfect, discriminatory power of the RF (**Appendix 1-figure**
714 **4A**). RF-ABC scenario-choices identify the correct scenario in the majority of cross-validations for most sce-
715 narios and most islands. Furthermore, asymmetrical scenarios are the least confused with one-another (AfrRe-
716 current-Eur2Pulses vs Afr2Pulses-EurRecurring, or Afr2Pulses-Eur2Pulses vs AfrRecurring-EurRecurring).
717 As expected and previously shown empirically with *MetHis*-RF-ABC scenario-choice (45,77), these results
718 are consistent with increased assignation-errors in the parts of the parameter-space where the different scenar-
719 ios are highly nested and thus biologically equivalent. Finally (**Appendix 1-figure 4B**), the mean, variance,
720 skewness, kurtosis, minimum, and maximum of individual admixture proportions' distributions are systemat-
721 ically among the most informative summary-statistics for RF-ABC scenario-choice in every island or in Cabo
722 Verde as a whole, consistently with theoretical expectations (45,73).
723 Finally, when considering all Cabo Verde-born individuals as a single random-mating population without
724 distinguishing birth-islands, our *MetHis*-RF-ABC scenario-choice identifies the Afr2Pulses-Eur2Pulses sce-
725 nario as the winning scenario (**Appendix 1-figure 4B**), thus consistent with the scenario most often found as
726 the winner among Cabo Verde islands considered as the target admixed population in nine separate *MetHis*-
727 RF-ABC analyses.
728
729 *MetHis*–Neural Network (NN)-ABC posterior parameter estimations
730 For individuals on each Cabo Verdean birth island separately, we performed NN-ABC joint posterior param-
731 eter estimation based on 100,000 *MetHis* simulations under the winning scenario (45): Afr2Pulses-Eur2Pulses
732 in Santiago, Fogo, Santo Antão São Nicolau, Brava, and Maio; Afr2Pulses-EurRecurring in Boa Vista and Sal;
733 and AfrRecurring-Eur2Pulses in São Vicente (**Figure 7B**). For each island separately, detailed posterior pa-
734 rameters' distributions, Credibility Intervals (CI), and cross-validation errors are provided in **Figure 7-figure**
735 **supplement 1-3** and **Appendix 5-table 1-10**. We synthesized our results considering median point-estimates
736 and 50%-CI for each scenario parameter in the admixture history of each island in **Figure 7C-D**. We detailed
737 our results and discussion for admixture history inferences for each island separately in **Appendix 5,** in the
738 light of historical data about the peopling of Cabo Verde (**Figure 7-source data 1**).
739 **Figure 7C** shows that the reproductive population size of Cabo Verde islands remained very low until a
740 strong increase in the last three generations for all islands but Santiago and Brava. In Santiago the population
741 expansion was more linear since the founding of Cabo Verde in the 1460's, while the reproductive size of
742 Brava remained almost constant and low until today.
743 In summary, **Figure 7D** shows that European and African admixture events throughout the archipelago
744 occurred first during the early peopling history of each island, before the mid-17th century massive expansion
745 of the TAST due to the expansion of the plantation economy (1). We find that other admixture events from
746 Europe or Africa, or both, likely occurred much later during, or immediately after, the 19th century abolition
747 of the TAST and of slavery in European colonial empires. Altogether our *MetHis*-ABC results support limited
748 historical admixture having occurred in Cabo Verde during the most intense periods of the TAST between the

749 mid-17th and early 19th centuries. Furthermore, note that we find admixture events often earlier than, or con-
750 comitant with, the first perennial peopling of an island. For the islands of Santiago, Fogo, Santo Antão and, to
751 a lesser extent, São Nicolau, initial historical admixture events occurred synchronously to the first perennial
752 settlement of the island. For the islands of Brava, Maio, Boa Vista, and São Vicente, early admixture events
753 occurred long before their first perennial peopling, thus showing that their founding was already largely com-
754 posed of already admixed individuals. Importantly, note that our *MetHis*-NN-ABC posterior parameter infer-
755 ences cannot infer all scenario-parameters accurately, as some parameters hardly depart from their respective
756 priors (**Figure 7-figure supplement 1-3**), and the admixture history of the island of Sal remains overall poorly
757 inferred.
758 Interestingly, *MetHis*-NN-ABC posterior parameter inference results obtained for the 225 Cabo Verde-
759 born individuals grouped in a single random-mating population instead of separately for each island of birth,
760 are largely undifferentiated from their prior distributions, and have very wide CI and large cross-validation
761 errors, for all admixture-history parameters except for the two parameters associated with the most recent pulse
762 of admixture from the African source (**Figure 7-figure supplement 1-3**; **Appendix 5-table 10**). This contrasts
763 with the substantial number of informative posterior-parameter estimations obtained for all islands of birth
764 separately except Sal (**Figure 7**, **Figure 7-figure supplement 1-3; Appendix 5-table 1-9**), despite the much
765 smaller sample sizes used in each one of these separate analyses compared to the analysis considering Cabo
766 Verde as a single population. These results further show that the history of admixture substantially differs
767 across Cabo Verde islands and that considering the Cabo Verde archipelago as a single random mating popu-
768 lation is inadequate to successfully infer the parameters of its admixture history, consistently with our results
769 from ADMIXTURE, LAI, ROH and Isolation-By-Distance analyses.
770

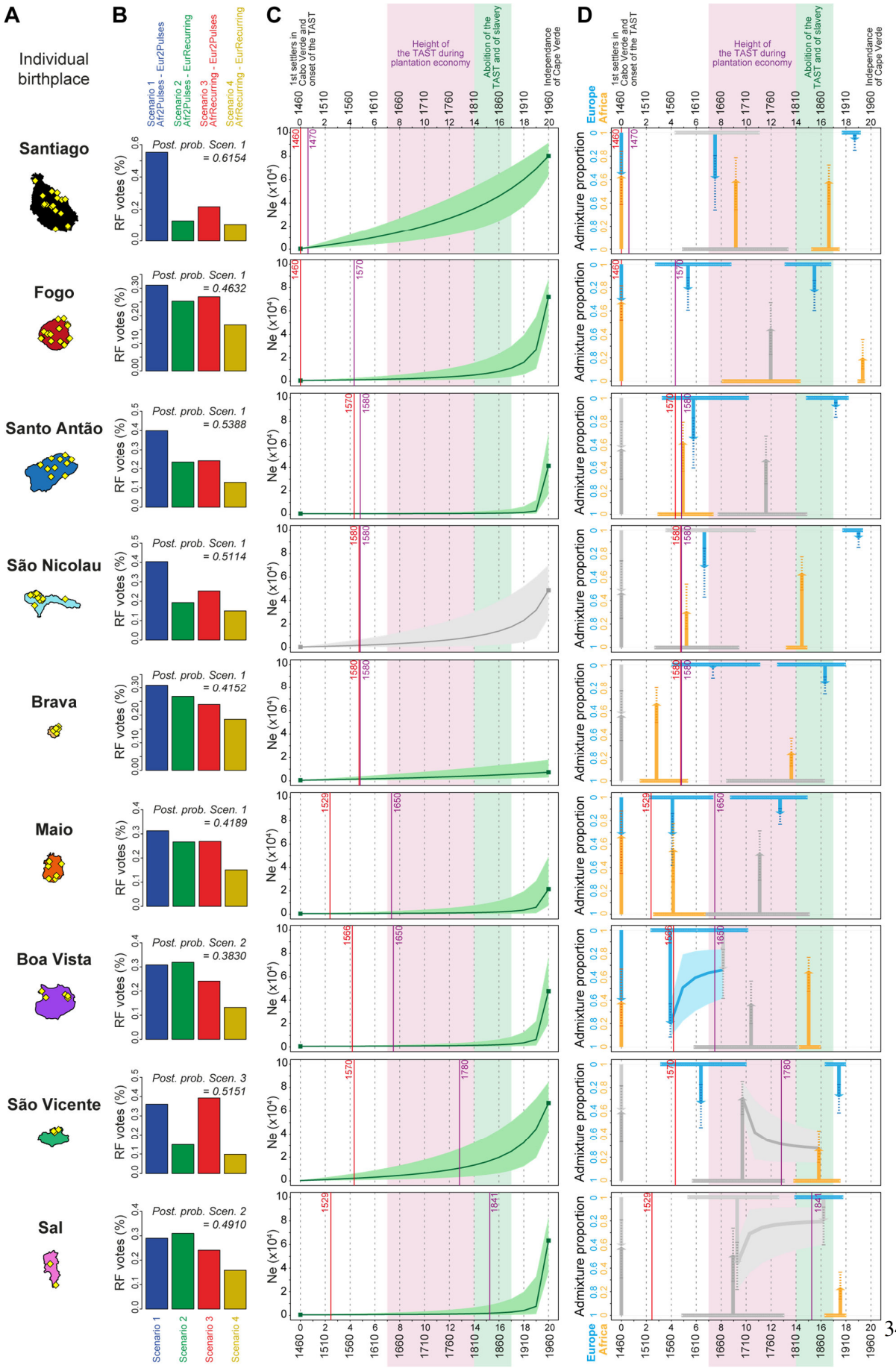
A
Individual birthplace
B
Scenario 1 Afr2Pulses - Eur2Pulses
Scenario 2 Afr2Pulses - EurRecurring
Scenario 3 AfrRecurring - Eur2Pulses
Scenario 4 AfrRecurring - EurRecurring
C
1st settlers in Cabo Verde and onset of the TAST
Height of the TAST during plantation economy
Abolition of the TAST and of slavery
Independance of Cape Verde
D
Europe
Africa
Santiago
Post. prob. Scen. 1 = 0.6154
Fogo
Post. prob. Scen. 1 = 0.4632
Santo Antão
Post. prob. Scen. 1 = 0.5388
São Nicolau
Post. prob. Scen. 1 = 0.5114
Brava
Post. prob. Scen. 1 = 0.4152
Maio
Post. prob. Scen. 1 = 0.4189
Boa Vista
Post. prob. Scen. 2 = 0.3830
São Vicente
Post. prob. Scen. 3 = 0.5151
Sal
Post. prob. Scen. 2 = 0.4910
RF votes (%)
Ne (x10⁴)
Admixture proportion
Scenario 1
Scenario 2
Scenario 3
Scenario 4

771

Figure 7:

Genetic admixture histories of Cabo Verde islands inferred with *MetHis*-Approximate Bayesian Computation.

Elements of the peopling-history of Cabo Verde islands are synthesized in **Figure 7-source data 1**, stemming from historical work cited therein. Islands are ordered from top to bottom in the chronological order of the first historical census perennially above 100 individuals within an island, indicated with the purple vertical lines. First historical records of the administrative, political, and religious, settlement of an island are indicated with the red vertical lines.

A) Within-island birth-places of 225 Cabo-Verde-born individuals. **B)** *MetHis*-Random Forest-ABC scenario-choice vote results for each island separately in histogram format. Posterior probabilities of correctly identifying a scenario if correct are indicated for the winning scenario as "Post. prob. Scen.", above each histogram. **C)** *MetHis*-Neural Network-ABC posterior parameter distributions with 50% Credibility Intervals for the reproductive population size history of each birth-island separately. **D)** Synthesis of *MetHis*-NN-ABC posterior parameter median point-estimates and associated 50%CI, for the admixture history of each island under the winning scenario identified with RF-ABC in panel **B**. European admixture history appears in blue, African admixture history in orange. Horizontal bars indicate 50%CI for the admixture time parameters, vertical arrows correspond to median admixture intensity estimates with 50%CI in doted lines.

For **C)** and **D)**, posterior parameter distributions showing limited departure from their respective priors and large CI are greyed, as they were largely unidentifiable in our ABC procedures. Detailed parameter posterior distributions, 95%CI, and cross-validation errors are provided in **Figure 7-figure supplement 1-3** and **Appendix 5-table1-9**. Detailed results description for each island are provided in **Appendix 5**.

C-D) The period between the 1630's and the abolition of the TAST in the 1810's, when most enslaved-Africans were deported from Africa by European empires concomitantly to the expansion of the plantation economy (1,2), is indicated in light-pink. The period between the abolition of the TAST in the 1810's and the abolition of slavery enacted between 1856 and 1878 throughout the Portuguese empire is indicated in light-green (25). The independence of Cabo Verde occurred in 1975.

Figure 7-figure supplement 1:

Reproductive-size posterior parameter distributions and associated priors obtained with Neural Network ABC inference for each island, and for the 225 Cabo Verde-born individuals grouped in a single random mating population "Cabo Verde", separately.

Figure 7-figure supplement 2:

African admixture histories posterior parameter distributions and associated priors obtained with Neural Network ABC inference for each island, and for the 225 Cabo Verde-born individuals grouped in a single random mating population "Cabo Verde", separately.

Figure 7-figure supplement 3:

European admixture histories posterior parameter distributions and associated priors obtained with Neural Network ABC inference for each island, and for the 225 Cabo Verde-born individuals grouped in a single random mating population "Cabo Verde", separately.

Figure 7-source data 1: ***provided in .xls format***

Historical landmark chronology for the peopling history of Cabo Verde as provided by previous historical work, respectively for each island.

Figure 7-figure supplement 1:

Reproductive-size posterior parameter distributions and associated priors obtained with Neural Network ABC inference for each island separately.

We considered, for each island separately, and for all 225 Cabo Verde-born individuals grouped in a single random mating population separately, Neural Network tolerance levels and number of neurons in the hidden layer, for each island and for Cabo Verde as a whole, separately, are chosen based on posterior parameter cross-validation error minimization procedures conducted on 1,000 random simulations used in-turn, as pseudo observed data (see **Appendix 1**, and **Appendix 1-table 1**). For each island and for Cabo Verde as a whole, separately, posterior parameter distributions correspond to the solid lines and corresponding priors correspond to the doted black lines. Density distributions are based on the logit transformation of parameter values (see **Appendix 1**) using an Epanechnikov kernel between the corresponding prior bounds. See **Results 7**, main **Discussion**, and **Appendix 5** for descriptions and discussions of the results. Synthesis in **Figure 7**.

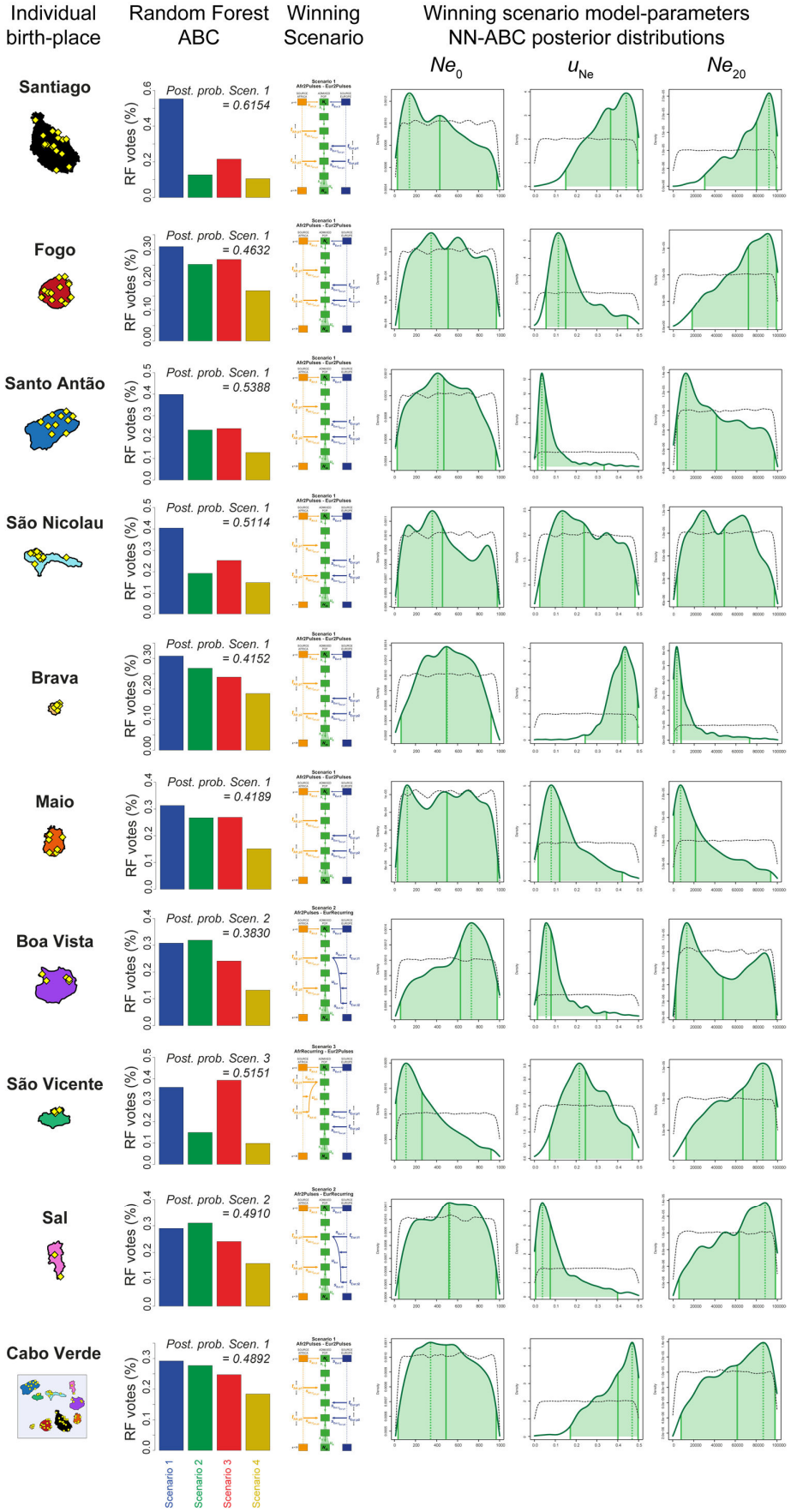
Individual birth-place
Random Forest ABC
Winning Scenario
Winning scenario model-parameters NN-ABC posterior distributions
Ne_0
u_{Ne}
Ne_{20}
Santiago
Post. prob. Scen. 1 = 0.6154
Fogo
Post. prob. Scen. 1 = 0.4632
Santo Antão
Post. prob. Scen. 1 = 0.5388
São Nicolau
Post. prob. Scen. 1 = 0.5114
Brava
Post. prob. Scen. 1 = 0.4152
Maio
Post. prob. Scen. 1 = 0.4189
Boa Vista
Post. prob. Scen. 2 = 0.3830
São Vicente
Post. prob. Scen. 3 = 0.5151
Sal
Post. prob. Scen. 2 = 0.4910
Cabo Verde
Post. prob. Scen. 1 = 0.4892
RF votes (%)
Scenario 1
Scenario 2
Scenario 3
Scenario 4

829

830 **Figure 7-figure supplement 2:**
831 **African admixture histories posterior parameter distributions and associated priors obtained with Neural Network ABC in-**
832 **ference for each island separately.**
833 We considered, for each island separately, and for all 225 Cabo Verde-born individuals grouped in a single random mating population
834 separately, Neural Network tolerance levels and number of neurons in the hidden layer, for each island and for Cabo Verde as a whole,
835 separately, are chosen based on posterior parameter cross-validation error minimization procedures conducted on 1,000 random simu-
836 lations used in-turn, as pseudo observed data (see **Appendix 1**, and **Appendix 1-table 1**). For each island and for Cabo Verde as a
837 whole, separately, posterior parameter distributions correspond to the solid lines and corresponding priors correspond to the doted
838 black lines. Density distributions are based on the logit transformation of parameter values (see **Appendix 1**) using an Epanechnikov
839 kernel between the corresponding prior bounds. See **Results 7**, main **Discussion**, and **Appendix 5** for descriptions and discussions of
840 the results. Synthesis in **Figure 7**.
841

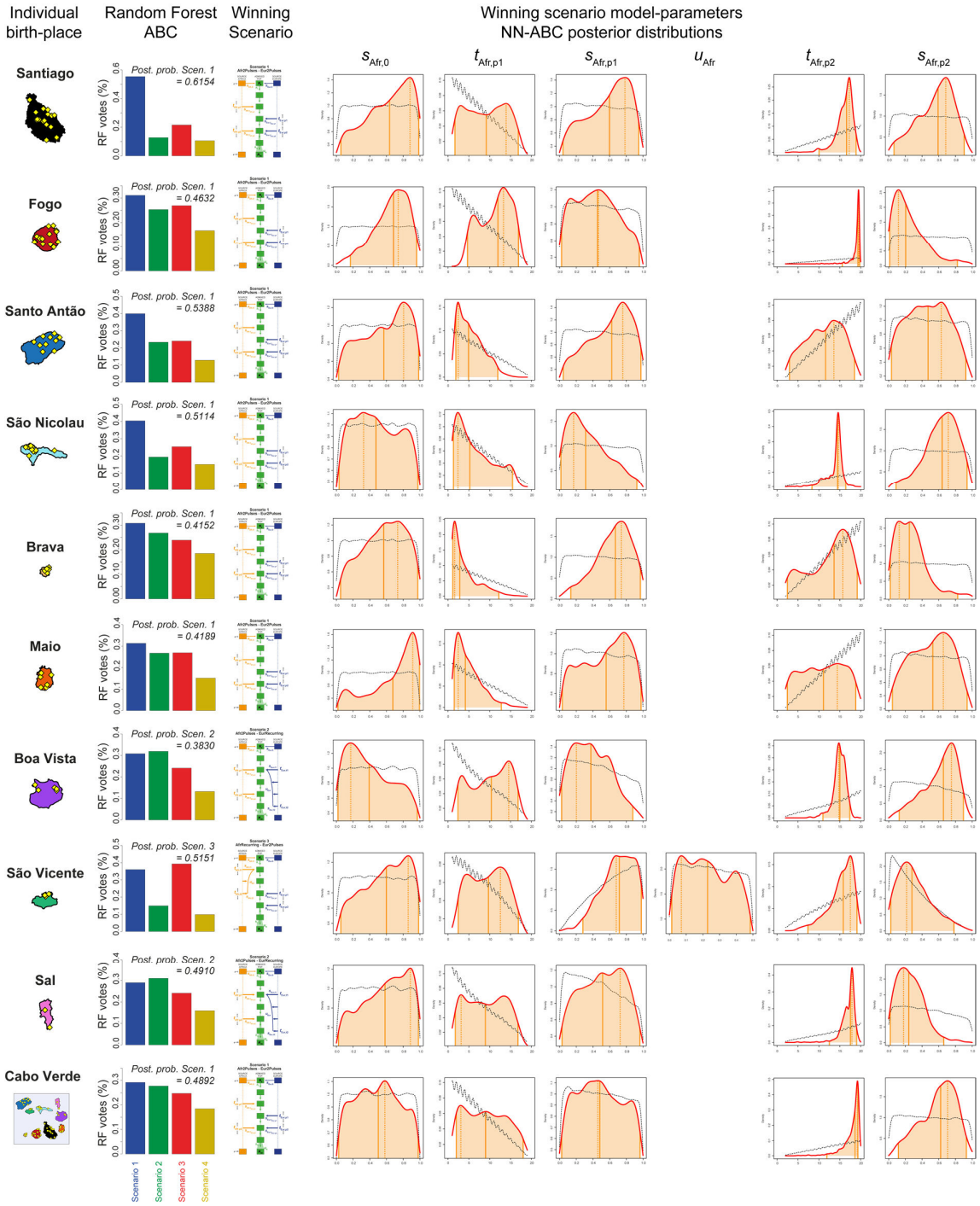
Individual birth-place
Random Forest ABC
Winning Scenario
Winning scenario model-parameters NN-ABC posterior distributions
$s_{Afr,0}$
$t_{Afr,p1}$
$s_{Afr,p1}$
u_{Afr}
$t_{Afr,p2}$
$s_{Afr,p2}$
Santiago
Post. prob. Scen. 1 = 0.6154
Fogo
Post. prob. Scen. 1 = 0.4632
Santo Antão
Post. prob. Scen. 1 = 0.5388
São Nicolau
Post. prob. Scen. 1 = 0.5114
Brava
Post. prob. Scen. 1 = 0.4152
Maio
Post. prob. Scen. 1 = 0.4189
Boa Vista
Post. prob. Scen. 2 = 0.3830
São Vicente
Post. prob. Scen. 3 = 0.5151
Sal
Post. prob. Scen. 2 = 0.4910
Cabo Verde
Post. prob. Scen. 1 = 0.4892
RF votes (%)
Scenario 1
Scenario 2
Scenario 3
Scenario 4

842

843 **Figure 7-figure supplement 3:**
844 **European admixture histories posterior parameter distributions and associated priors obtained with Neural Network ABC**
845 **inference for each island separately.**
846 We considered, for each island separately, and for all 225 Cabo Verde-born individuals grouped in a single random mating population
847 separately, 100,000 simulations computed under the winning scenario obtained with RF-ABC scenario-choice procedures and provided
848 on the left of the figure. Neural Network tolerance levels and number of neurons in the hidden layer, for each island and for Cabo
849 Verde as a whole, separately, are chosen based on posterior parameter cross-validation error minimization procedures conducted on
850 1,000 random simulations used in-turn, as pseudo observed data (see **Appendix 1**, and **Appendix 1-table 1**). For each island and for
851 Cabo Verde as a whole, posterior parameter distributions correspond to the solid lines and corresponding priors correspond to the doted
852 black lines. Density distributions are based on the logit transformation of parameter values (see **Appendix 1**) using an Epanechnikov
853 kernel between the corresponding prior bounds. See **Results 7**, main **Discussion**, and **Appendix 5** for descriptions and discussions of
854 the results. Synthesis in **Figure 7**.
855

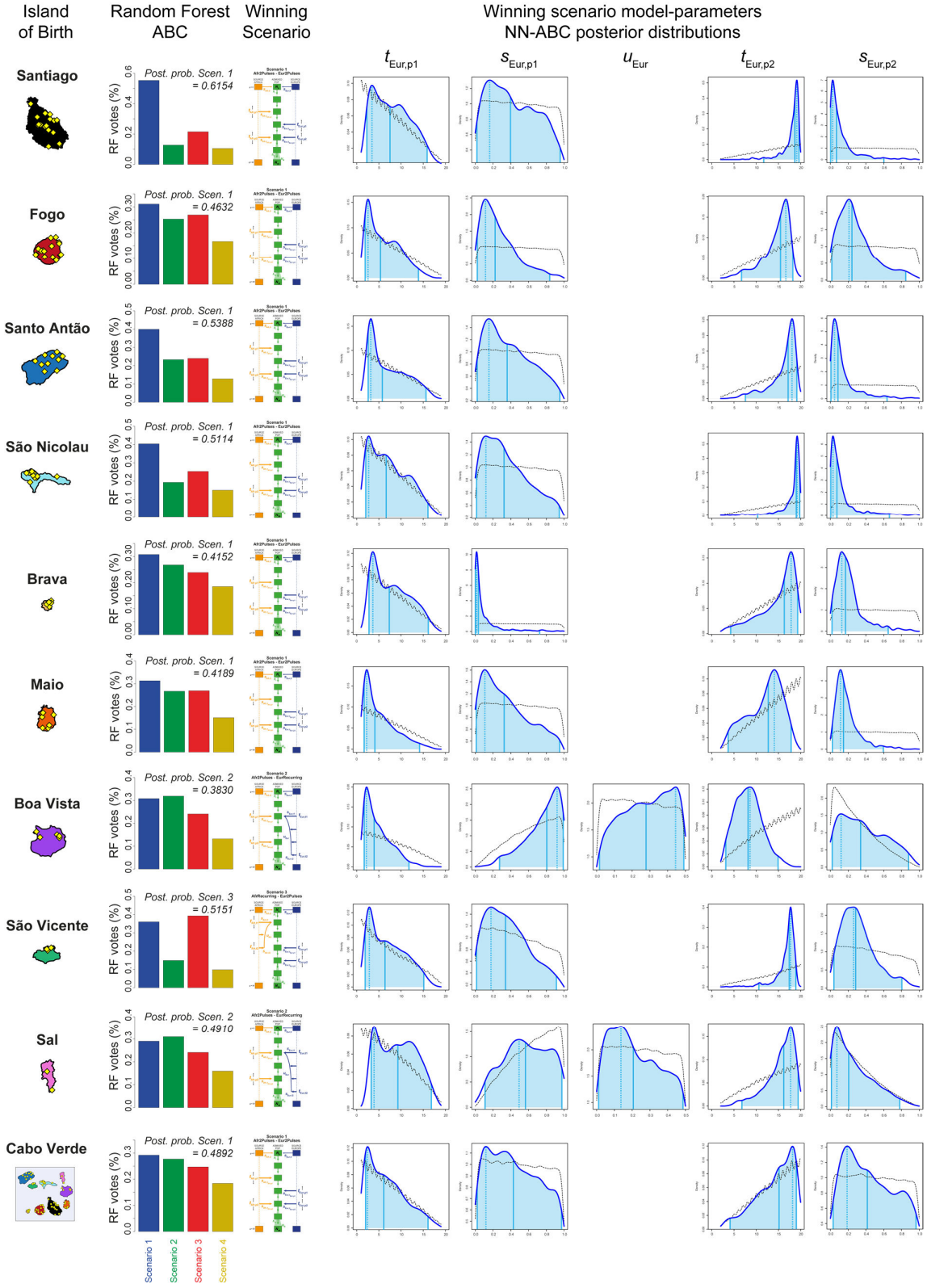
Island of Birth
Random Forest ABC
Winning Scenario
Winning scenario model-parameters NN-ABC posterior distributions
$t_{Eur,p1}$
$s_{Eur,p1}$
u_{Eur}
$t_{Eur,p2}$
$s_{Eur,p2}$
Santiago
Post. prob. Scen. 1 = 0.6154
Fogo
Post. prob. Scen. 1 = 0.4632
Santo Antão
Post. prob. Scen. 1 = 0.5388
São Nicolau
Post. prob. Scen. 1 = 0.5114
Brava
Post. prob. Scen. 1 = 0.4152
Maio
Post. prob. Scen. 1 = 0.4189
Boa Vista
Post. prob. Scen. 2 = 0.3830
São Vicente
Post. prob. Scen. 3 = 0.5151
Sal
Post. prob. Scen. 2 = 0.4910
Cabo Verde
Post. prob. Scen. 1 = 0.4892
RF votes (%)
Scenario 1
Scenario 2
Scenario 3
Scenario 4

856

857 **DISCUSSION**
858
859 **Which African and European populations contributed genetically to Cabo Verde?**
860
861 *The genetic heritage of continental Africa in Cabo Verde*
862 Numerous enslaved-African populations from Western, Central, and South-Western Central Africa were for-
863 cibly deported during the TAST to both Cabo Verde and the Americas, as shown by historical demographic
864 records (1,25). There is still extensive debate about whether enslaved-Africans remained or more briefly trans-
865 ited in Cabo Verde during the most intense period of the TAST, in the 18th and 19th centuries, when the archi-
866 pelago served as a slave-trade platform between continents (25,78,79); the question of the duration of stay of
867 enslaved individuals at a given location being also of major interest throughout the Americas during the TAST
868 (18,37). In this context, previous genetic studies considering a relatively limited number of populations from
869 mainland Europe and Africa, and/or limited numbers of Cabo Verdean islands of birth, suggested that mainly
870 continental West Africans and South Europeans were at the root of Cabo Verde genetic landscape (3,23,34).
871 In this context, our genetic results favor scenarios where mostly certain West Western African Senegam-
872 bian populations only (Mandinka and Wolof in our study) contribute to the genetic makeup of Cabo Verde
873 (**Figure 2-3**). Other Western, Central, and South-Western African populations historically also forcibly de-
874 ported during the TAST seem to have had very limited contributions to the genomic diversity of most Cabo
875 Verde islands, and virtually no contribution to that of Brava, Fogo, and Santiago.
876 This could be due to Cabo Verde being only a temporarily waypoint for these latter enslaved-African
877 populations between Africa, the Americas, and Europe, but would also be consistent with additional socio-
878 historical processes (see below). Interestingly, and further echoing these genetic results, the Cabo Verdean
879 Kriolu language carries specific signatures mainly from the Mande language-family, and Wolof and Temne
880 languages from Western Africa, and largely more limited signatures of Kikongo and Kimbundu Bantu lan-
881 guages from Central and South-Western Africa (15,30).
882 These results contrast with the admixture patterns identified in other enslaved-African descendant popu-
883 lations in the Americas in our dataset (African-American and Barbadian, **Figure 2-3**), and in previous studies
884 (3,4,10,38,80). Indeed, the origins of African ancestries in numerous populations throughout the Caribbean
885 and the Americas traced to varied continental African regions, from Western to South-Western Africa, thus
886 qualitatively consistent with the known diversity of slave-trade routes used between continents and within the
887 Americas after the Middle Passage.
888
889 *The genetic heritage of continental Europe in Cabo Verde*
890 After the initial settlement of Cabo Verde by Portuguese migrants, temporary changes of European dominion
891 in certain islands, newly developing commercial opportunities, and intense piracy during the 16th and 17th
892 centuries have triggered different European populations to migrate to the archipelago (26,27,36).
893 Nevertheless, these latter historical events do not seem to have left a major signature in the genetic land-
894 scape of Cabo Verde (**Figure 2-3**). Instead, we find that Cabo Verdean-born individuals in our dataset share
895 virtually all their European genetic ancestry with Iberian populations, with extremely limited evidence of con-
896 tributions from other European regions, consistent with previous studies (3,23). Interestingly, the reduced di-
897 versity of European populations' contributions to the genomic landscape of Cabo Verde is also identified in
898 other enslaved-African descendant populations in our study, as well as in previous studies in Caribbean and
899 American populations (11,12,38). Our results thus show that European admixture in enslaved-African de-
900 scendant populations on both sides of the Atlantic, as represented here by Cabo Verde, the Barbadians ACB
901 and the African American ASW, mainly stem from the gene-pool of the European empires historically and
902 socio-economically dominant locally, rather than subsequent European migrations (2).

903 Altogether, note that, in our local-ancestry inferences, we considered as reference source populations var-
904 ied existing populations from continental mainland Africa and Europe, categorized as such from sampling
905 information and geographic location only, prior to any genetic investigation. Therefore, in these analyses, we
906 cannot disentangle the fraction of European admixture in Cabo Verdean genomes stemming directly from
907 European migrations after the 1460's, from the fraction stemming from the European genetic legacy in conti-
908 nental African source populations acquired whether during more ancient migrations which occurred before the
909 peopling of Cabo Verde (e.g. (81)), or since then during the European colonial expansion in Sub-Saharan
910 Africa. Symmetrically, we cannot disentangle the fraction of African admixture in Cabo Verde stemming di-
911 rectly from continental Africa after the 1460's, from the fraction inherited from Africa-Europe admixture
912 events that may have occurred in Europe prior to the peopling of Cabo Verde or during the colonial era until
913 today. Disentangling both genetic heritages will require, in future studies, the explicit modelling of such pos-
914 sible admixture histories within African and European ancestral populations at the source of the Cabo Verde
915 genetic landscape, and would also benefit from including data from North-African populations in our reference
916 panels.
917
918 **Genetic and linguistic isolation-by-distance and recent demographic expansion in Cabo Verde**
919 A scenario of island peopling via a series of founding events followed by slow-growing population sizes and
920 local isolation due to reduced genetic and linguistic parent-offspring dispersal would consistently explain the
921 increasing differentiation of island-specific patterns with increasing values of *K* found with ADMIXTURE,
922 ASD-MDS, and isolation-by-distance results (**Figure 2-5**, **Table 1**), as well as *MetHis*-ABC demographic
923 inferences (**Figure 7C**).
924 Indeed, *MetHis*-ABC results (**Figure 7C**) show the long period of small relatively constant reproductive
925 sizes until the very recent strong, hyperbolic, increases in most Cabo Verdean islands; with the notable excep-
926 tions of, *i)* the linear increase in Santiago, the political and commercial center of Cabo Verde throughout the
927 colonial history of the archipelago, and *ii)* the relatively constant reduced reproductive sizes in Brava until
928 today. Altogether, this result was expected as the dry Sahelian climate of Cabo Verde with scarcely accessible
929 water resources, recurring famines and epidemic outbreaks, and the Portuguese crown maintaining a strong
930 control over population movements within Cabo Verde, rendered difficult the perennial peopling of most is-
931 lands (see **Figure 7-source data 1** and references therein, **Appendix 5**). Furthermore, such demographic sce-
932 narios are also consistent with long-ROH patterns reflecting isolation on each Cabo Verdean islands, whereas
933 elevated shorter ancestry-specific ROH patterns likely stemmed from admixture (**Figure 4**), similarly to our
934 results in the ASW and ACB populations and as previously identified (61). Note, however, that while we
935 explored and found, *a posteriori*, a different demographic regime for each Cabo Verde island separately, with
936 constant, hyperbolic, or linear increases of reproductive sizes, we did not consider possible demographic bot-
937 tlenecks which may also have occurred as a result of the difficult settlement history of Cabo Verde described
938 above. Such possible bottleneck events will need to be explored in the future, a particularly challenging task
939 given the extensive number of competing models to be considered and given that bottleneck intensities and
940 duration parameters have to be co-estimated with admixture parameters over a very short history of 21 gener-
941 ations.
942 Investigating isolation-by-distance anchored in individual birth-places at a very reduced geographical
943 scale (39–41) within a population and a language allowed us to reveal that effective dispersal from one gener-
944 ation to the next across Cabo Verde islands, and sometimes even within-islands, was surprisingly reduced
945 compared to the large mobility self-reported by participants (**Figure 5**, **Table 1**). Patterns of parent-offspring
946 dispersal at a very local scale ~50 km within populations has seldom been tested using genetics, to our
947 knowledge, in human populations (39,42–44); although isolation-by-distance genetic patterns have been ex-
948 tensively explored to investigate serial founding events and migrations across human populations at varied

949 geographical scales, including in archipelagos contexts (20,63,64,82). Furthermore, while the geographic dis-
950 tribution of genetic admixture patterns have been explored at much larger geographical scales (e.g 55,78,79),
951 and in particular in enslaved-African descendant populations (11,12), isolation-by-distance patterns for inter-
952 individual differences of genetic admixture fractions at very reduced geographical scales have never been
953 reported to our knowledge.
954 We also found substantial signals of isolation-by-distance among Kriolu idiolects (i.e. individual manners
955 of uttering Cabo Verdean Kriolu), also anchored in individual birth-places (**Figure 5**, **Table 1**), thus showing
956 striking parallels between the history of biological and cultural dispersal and isolation in Cabo Verde at a
957 micro-geographical scale. Our results show that linguistic admixture patterns were isolated-by-distance within
958 the archipelago, similarly to genetic admixture patterns, which was previously unsuspected in both genetics
959 and linguistic studies of Cabo Verde (15,23,29,34).
960 Altogether, these joint genetic-linguistic patterns highlight the limited effective genetic and linguistic dis-
961 persal from one generation to the next within Cabo Verde, including for genetic and linguistic admixture levels,
962 despite extended mobility of individuals within the archipelago. Both mechanisms may thus underline indi-
963 vidual linguistic identity construction processes and the genetic relative isolation across and within Cabo Verd-
964 ean islands.
965 Importantly, we considered only random mating processes in our inferences and interpretations. However,
966 the almost complete lack of identifiability of the admixture-history parameters obtained when considering
967 Cabo Verde as a single random-mating population in our ABC inferences (**Figure 7-figure supplement 1-3**,
968 **Appendix 5-table 1-9**), and our ROH results together with recent work (85), altogether suggest that non-
969 random matting processes significantly influenced Cabo Verdean genetic patterns. Therefore, future studies
970 will need to evaluate how possible deviations from random-mating in Cabo Verde, such as assortative mating
971 (85,86), may have influenced our results and interpretations. Note that this is a conceptually particularly chal-
972 lenging task in a small census-size population with strong marital stratification where mate-choices have been,
973 by definition, limited during most of the TAST (87). Nevertheless, such complex processes may also underlie
974 the joint genetic-linguistic isolation-by-distance patterns anchored in birth-place distances here observed for
975 both diversity and admixture patterns; and would also explain that genetic and linguistic histories of admixture
976 apparently occurred in parallel in Cabo Verde.
977
978 **Histories of genetic admixture in Cabo Verde**
979 *Early admixture in Cabo Verde, limited admixture during the plantation economy era*
980 While we expected recurring African admixture processes due to the known history of regular forced migra-
981 tions from Africa during most of Cabo Verde history (25), our *MetHis*–ABC scenario-choices indicate that,
982 qualitatively, these demographic migrations did not necessarily translate into clearly recurring gene-flow pro-
983 cesses to shape genetic patterns in most of Cabo Verde islands (**Figure 7B**). Indeed, African admixture pro-
984 cesses in all islands, except São Vicente, seem to have occurred during much more punctual periods of Cabo
985 Verdean history. Our *MetHis*–ABC posterior parameter estimations further highlighted often largely differing
986 admixture histories across Cabo Verde islands (**Figure 7C-D** and **Appendix 5**).
987 We find that admixture from continental Europe and Africa occurred first early during the TAST history,
988 concomitantly with the successive settlement of each Cabo Verdean island between the 15th and the early 17th
989 centuries (**Figure 7D**). Furthermore, we find that the most intense period of enslaved-African deportations
990 during the TAST via Cabo Verde, between the mid-17th and early-19th centuries during the expansion of the
991 plantation economic system in the Americas and Africa (1,25–27), seem to have left a limited signature in the
992 admixture patterns of most Cabo Verdean islands today. Interestingly, previous studies also highlighted that
993 admixture in enslaved-African descendants in the Caribbean may have occurred first early in the European
994 colonial expansion in the region in the 16th century, and then much later towards the end of the TAST at the

end of the 18th century, and had thus been relatively limited during most of the plantation economy era (11,88). Together with our results, this illustrates the apparent discrepancy between intense demographic forced migrations during the TAST and genetic admixture signatures at least in certain populations on both sides of the Atlantic. Indeed, in contrast with these results, numerous other enslaved-African populations in the Americas have, instead, shown substantial historical admixture inferred to have occurred during the plantation economy era, hence exemplifying the diversity of admixture histories experienced locally by enslaved-Africans descendant populations during the TAST (4,12).

The inferred lack of admixture events in Cabo Verde during the height of the TAST could be due to newly deported enslaved-Africans being only transiting via Cabo Verde before being massively re-deported to other European colonies during this era (25,78,79). Furthermore, and not mutually exclusive with this latter hypothesis, historians reported, in Cabo Verde and other European colonies in the Americas, that relationships between enslaved and non-enslaved communities largely changed with the expansion of plantation economy at the end of the 17th century. These changes are often referred to as the shift from Societies-with-Slaves to Slave-Societies (1,19,89). Slave-Societies legally enforced the socio-marital and economic segregation between communities, and coercively controlled relationships between new enslaved-African migrants and pre-existing enslaved-African descendant communities more systematically and violently than Societies-with-Slaves (19)$^{-p.15-46,95-108,}$(25)$^{-p.281-319}$. The high prevalence of segregation during the height of the plantation economy could have limited genetic admixture between enslaved-African descendants and non-enslaved communities of European origin, as well as admixture between new migrants, forced or voluntary, and pre-existing Cabo Verdeans; notwithstanding the known history of dramatic sexual abuses during and before this era. This could consistently explain our observations of a relative lack of diverse African or European origins in Cabo Verdean genomes despite the known geographical diversity of populations deported and emigrated to the archipelago throughout the TAST. Furthermore, with legally enforced segregation, we might expect more marital pairings than before to occur among individuals with common origins; i.e. between two individuals with the same continental African or European origin. Such ancestry-specific marriages triggered by socio-cultural segregation would be consistent with our ROH patterns (**Figure 4**), also depending on how long such mate-choice behaviors persisted after the end of legal segregation. We note, however, that we have not formally tested this influence on ROH and ancestry patterns and that a careful consideration of alternate explanations, such as temporally varying admixture contributions over time or a severe bottleneck in one of the ancestral populations, would be important to consider in such future analyses.

In this context, the diversified African ancestries here found in the Americas (**Figure 2-3**), consistently with previous studies showing admixture events occurring before or during the height of plantation economy in the Americas (3,4,12), would suggest that the gene-pool of enslaved-Africans communities admixing with Europeans in the Americas since the 16th century often involved, at a local scale, multiple African source populations, thus reflecting the multiple slave-trade routes between continents and within the Americas. Conversely in Cabo Verde, the early onset of the TAST during the 15th century likely privileged commercial routes with nearby Senegambia (25)$^{-p.31-54,281-319}$, thus favoring almost exclusively admixture events with individuals from this region and from certain populations only. Altogether, our results in Cabo Verde contrasting with certain other enslaved-African descendant populations in the Americas, highlight the importance of early admixture processes and socio-cultural constraints changes on intermarriages throughout the TAST, which likely durably influenced genomic diversities in descendant populations locally, on both sides of the Atlantic.

Admixture in Cabo Verde after the abolition of the TAST and of Slavery

Finally, we find that recent European and African admixture in Cabo Verde occurred mainly during the complex historical transition after the abolition of the TAST in European colonial empires in the 1800's and the subsequent abolition of slavery between the 1830's and the 1870's (**Figure 7D**). Historians have showed

that these major historical shifts strongly disrupted pre-existing segregation systems between enslaved and non-enslaved communities (1)[-p.271-290,](25)[-p.335-362,](90). In addition, an illegal slave-trade flourished during this era, bringing numerous enslaved-Africans to Cabo Verde outside of the official routes (25)[-p.363-384] (91). Altogether, our results indicate increased signals of European and African admixture events in almost every island of Cabo Verde during this period, and were thus consistent with a change of the social constraints regarding admixture and forced displacements of enslaved-descendants that had prevailed over the preceding 200 years of the TAST. These results were largely consistent with previous studies elsewhere in the Caribbean (11,88), and Central and South America (4,38); showing, at a local scale, the major influence of this recent and global socio-historical change in inter-community relationships in European colonial empires on either sides of the ocean.

Perspectives

Altogether, our results highlight both the unity and diversity of the genetic peopling and admixture histories of Cabo Verde islands, the first colony peopled by Europeans in Sub-Saharan Africa, resulting from the sociocultural and historical complexity of the Trans-Atlantic Slave Trade and European colonial expansions since the 15th century. Our results obtained at a micro-geographical scale reveal the fundamental importance of the early TAST history, before the expansion of the plantation economy, in durably shaping the genomic and cultural diversities of enslaved-African descendant populations in both Africa and the Americas.

Importantly, we considered only the genome-wide autosomal admixture history of Cabo Verde in this study, and therefore did not explore possible sex-biased admixture processes. However, previous studies demonstrated the strong sex-biased admixture processes involved in Cabo Verde using sex-specific genetic markers (32,33), similarly as in other enslaved-African descendant populations in the Americas (2). Furthermore, previous theoretical work considering sex-specific mechanistic admixture models showed that sex-biased admixture processes may possibly bias historical inferences based only on autosomal data (92). It will thus be important, in future studies, to explore how this sex-biased admixture history may have influenced the ABC inferences here conducted; for instance, via sex-specific developments of *MetHis*-ABC.

Future work will need to formally test the serial-founder hypothesis here proposed to be at the root of the observed genetic and linguistic patterns within Cabo Verde, and thus compare the numerous possible routes for such a peopling history across islands within the archipelago. In particular, it will be of interest to investigate, then, the series of bottlenecks concomitant to each genetic and linguistic founding event; a much needed but challenging task considering the very recent history of the archipelago founded only 21 generations ago, and the historically-known small census sizes echoed in the relatively small reproductive sizes here identified in almost every island until the 20th century.

Our novel results together with their methodological limitations massively beg for future work further complexifying the admixture models here considered, as well as incorporating other summary-statistics such as admixture-LD and sex-specific statistics. This will allow to further dissect the admixture processes that gave birth to enslaved-African descendant populations, on both sides of the Atlantic.

1080 **MATERIALS AND METHODS**
1081
1082 **1. Cabo Verde genetic and linguistic datasets**
1083 We conducted joint sampling of anthropological, genetic, and linguistic data in Cabo Verde with the only
1084 inclusion criteria that volunteer-participants be healthy adults with Cabo Verdean citizenship and self-report-
1085 ing speaking Kriolu (23). Between 2010 and 2018, six interdisciplinary sampling-trips were conducted to in-
1086 terview 261 participants from more than thirty interview-locations throughout the archipelago (**Figure 1**).
1087
1088 **1.a. Familial anthropology and geography data**
1089 The 261 Cabo Verdean individuals were each interviewed to record a classical familial anthropology question-
1090 naire on self-reported life-history mobility. In particular, we recorded primary residence location, birth location,
1091 parental and grand-parental birth and residence locations, and history of islands visited in Cabo Verde and
1092 foreign experiences (23). Furthermore, we also recorded age, sex, marital status, and cumulative years of
1093 schooling and higher education (for 211 individuals only), and languages known and their contexts of use.
1094 GPS coordinates for each reported location were acquired on site during field-work, supplemented by
1095 paper maps and Google Earth™ for non-Caboverdean locations and islands that we did not visit (Sal and Maio).
1096 While participants' birth-locations were often precise, increasing levels of uncertainty arose for the reported
1097 parental and grand-parental locations. We arbitrarily assigned the GPS coordinates of the main population
1098 center of an island when only the island of birth or residence could be assessed with some certainty by partic-
1099 ipants. All other uncertain locations where recorded as missing data. Figure maps were designed with the
1100 software *QuantumGIS* v3.10 "București" and using Natural Earth free vector and raster map data
1101 (https://www.naturalearthdata.com).
1102
1103 **1.b. Genome-wide genotyping data**
1104 The 261 participants each provided 2mL saliva samples collected with DNAGenotek™ OG-250 kits, and com-
1105 plete DNA was extracted following manufacturer's recommendations. DNA samples were genotyped using
1106 an Illumina HumanOmni2.5Million-BeadChip genotyping array following manufacturer's instructions. We
1107 followed the quality-control procedures for genotypic data curation using Illumina's GenomeStudio® Geno-
1108 typing Module v2.0 described in (23). Genotype-calling, population-level quality-controls, and merging pro-
1109 cedures are detailed in **Appendix 1-figure 1**.
1110 In summary, we extracted a preliminary dataset of 259 Cabo Verdean Kriolu-speaking individuals, in-
1111 cluding relatives, genotyped at 2,118,835 polymorphic di-allelic autosomal SNPs genome-wide. We then
1112 merged this dataset with 2,504 worldwide samples from the 1000 Genomes Project Phase 3 (93); with 1,307
1113 continental African samples from the African Genome Variation Project (94,95) (EGA accession number
1114 EGAD00001000959); and with 1,235 African samples (7,96) (EGA accession number EGAS00001002078).
1115 We retained only autosomal SNPs common to all data sets, and excluded one individual for each pair of indi-
1116 viduals related at the 2nd degree (at least one grand-parent in common) as inferred with KING (97), following
1117 previous procedures (23).
1118 After merging all datasets (**Appendix 1-figure 1**), we considered a final working-dataset of 5,157 world-
1119 wide unrelated samples, including 233 unrelated Cabo Verdean Kriolu-speaking individuals, of which 225
1120 were Cabo-Verde-born, genotyped at 455,705 autosomal bi-allelic SNPs (**Figure 1**; **Figure 1-source data 1**).
1121 Note that, for this working-dataset, the fraction of missing genotypes was very low and equaled 7.0×10^{-4} on
1122 average within Cabo Verdean islands of birth (SD = 3.0×10^{-4} across islands).
1123
1124 **1.c. Individual utterances of Kriolu**

We collected linguistic data for each of the 261 Cabo Verdean individuals using anthropological linguistics questionnaires, and semi-directed interviews. Each participant was shown a brief (~6 min) speech-less movie, *"The Pear Story"* (98), after which they were asked to narrate the story as they wanted in "the Kriolu they speak every day at home". Discourses were fully recorded without interruption, whether individuals' discourses were related to the movie or not. Then each discourse was separately fully transcribed using the orthographic convention of the Cabo Verdean Kriolu official alphabet "Alfabeto Unificado para a Escrita da Língua Cabo-verdiana (ALUPEC)" (Decreto-Lei nº 67/98, 31 de Dezembro 1998, I Série nº 48, Sup. B. O. da República de Cabo Verde).

Building on the approach of (23), we were interested in inter-individual variation of "ways of speaking Kriolu" rather than in a prescriptivist approach to the Kriolu language. Thus, we considered each utterance as defined in (99)[-p.107]: "a particular instance of actually-occurring language as it is pronounced, grammatically structured, and semantically interpreted in its context". Transcripts were parsed together and revealed 4831 (L=4831) unique uttered items among the 92,432 uttered items transcribed in total from the 225 discourses from the genetically-unrelated Cabo Verde-born individuals. To obtain these counts, we considered phonetic, morphological, and syntactic variation of the same lexical root items that were uttered/pronounced differently, and we excluded from the utterance-counts onomatopoeia, interjections, and names. Note that we were here interested in the diversity of realizations in the Kriolu lexicon, including within the same individuals. In other words, we are interested in both between-speaker and within-speaker variation. Also note that a very limited number of English words were pronounced by particular individuals (10 utterances each occurring only once), and were kept in utterance-counts.

1.d. Individual Kriolu utterance frequencies

The list of unique uttered items was then used to compute individual's specific vectors of uttered items' relative frequencies as, for each genetically unrelated Cabo Verde-born individual i (in [1, 225]) and each unique uttered item l (in [1, L=4831]), $f_{i,l} = n_{i,l}/\sum_{j=1}^{L} n_{i,j}$, where $n_{i,l}$ is the absolute number of times individual i uttered the unique item l over her/his entire discourse, f_i being the vector $(f_{i,1}, f_{i,2}, \dots, f_{i,L})$. We compared vectors of individuals' utterance-frequencies by computing the inter-individual pairwise Euclidean distance matrix as, for all pairs of individuals i and j, $d(f_i, f_j) = \sqrt{\sum_{l=1}^{L}(f_{i,l} - f_{j,l})^2}$ (23).

1.e. African origin of Kriolu utterances

We categorized each of the 4831 unique uttered items separately into five linguistic categories (23). Category A included only unique utterances directly tracing to a known African language and comprised 88 unique items occurring 3803 times out of the 92,432 utterances. Category B included only items with a dual African and European etymology, i.e. items of a European linguistic origin strongly influenced in either meaning, syntax, grammar, or form by African languages or vice versa, attesting to the intense linguistic contacts at the origins of Cabo Verdean Kriolu, and comprised 254 unique items occurring 6960 times. Category C included 4432 items (occurring 73,799 times) with strictly Portuguese origin and not carrying identifiable traces of significant African linguistic origin or influence. Category D included 26 items occurring 6762 times with potential, not attested by linguists, traces of African languages' phonetic or morphologic influences. Finally, Category U included the 10 English utterances occurring 10 times and the 21 unique Kriolu utterances occurring 1089 times of unknown origin as they could not be traced to African or European languages.

Following (23), we defined an "African-utterances score" based, conservatively, on the utterance frequencies obtained separately for items in Category A, Category B, and merging Categories A and B, as, for individual i and the set of utterances in each category denoted Cat (in [A; B; A&B]), $Z_{i,Cat} = \sum_{l=1}^{L_{Cat}} f_{i,l}$, with L_{Cat} the number of uttered items in the corresponding category, and $f_{i,l}$ defined as previously.

2. Population genetics descriptions

2.a. Allele Sharing Dissimilarities, Multidimensional Scaling, and ASD-MDS admixture estimates

We calculated pairwise Allele Sharing Dissimilarities (46) using the *asd* software (v1.1.0a; https://github.com/szpiech/asd), among the 5,157 individuals in our worldwide dataset (**Figure 1**; **Figure 1-source data 1**), using 455,705 autosomal SNPs, considering, for a given pair of individuals, only the SNPs with no missing data. We then projected this dissimilarity matrix in three dimensions with metric Multidimensional Scaling using the *cmdscale* function in R (100). We conducted successive MDS analyses on different individual subsets of the original ASD matrix, by excluding, in turn, groups of individuals and recomputing each MDS separately (**Appendix 2-figure 1-4**; **Figure 2-figure supplement 1**). Lists of populations included in each analysis can be found in **Figure 1-source data 1**. 3D MDS animated plots in *gif* format for **Figure 2**, **Figure 2-figure supplement 1**, and **Appendix 2-figure 1-4** were obtained with the *plot3d* and *movie3d* functions from the R packages *rgl* and *magick*.

Recently admixed individuals are intuitively expected to be at intermediate distances between the clusters formed by their putative proxy source populations on ASD-MDS two-dimensional plots. A putative estimate of individual admixture rates can then be obtained by projecting admixed individuals orthogonally on the line joining the respective centroids of each proxy-source populations and, then, calculating the distance between the projected points and either centroid, scaled by the distance between the two centroids (**Appendix 1-figure 2**; (45,101)). We estimated such putative individual admixture rates in Cabo Verdean, ASW, and ACB individuals, considering sets of individuals for the putative proxy-source populations identified visually and resulting from our ASD-MDS decomposition (**Appendix 2**).

2.b. ADMIXTURE-CLUMPP-DISTRUCT and f_3-admixture analyses

Based on ASD-MDS explorations, we focused on the genetic structure of individuals born in Cabo Verde compared to that of other admixed populations related to TAST migrations. Therefore, we conducted ADMIXTURE analyses (48) using 1,100 individuals from 22 populations: four from Europe, 14 from Africa, the USA-CEU, the African-American ASW, the Barbadian-ACB populations, and the North Chinese-CHB population as an outgroup (**Figure 1-source data 1**). To limit clustering biases due to uneven sampling, we randomly resampled without replacement 50 individuals, once, for each one of these 22 populations. Furthermore, we also included all 44 Angolan individuals from four populations in the analyses, as no other samples from the region were available in our dataset. In addition to the 1,100 individuals hence obtained, we included the 225 Cabo Verde-born individuals.

Following constructor recommendations, we pruned the initial 455,705 SNPs set for low LD using *plink* (102) function *--indep-pairwise* for a 50 SNP-window moving in increments of 10 SNPs and a r^2 threshold of 0.1. We thus conducted all subsequent ADMIXTURE analyses considering 1,369 individuals genotyped at 102,543 independent autosomal SNPs.

We performed 30 independent runs of ADMIXTURE for values of K ranging from 2 to 15. For each value of K separately, we identified groups of runs providing highly similar results (ADMIXTURE "modes"), with Symmetric Similarity Coefficient strictly above 99.9% for all pairs of runs within a mode, using CLUMPP (103). We plotted each modal result comprising two ADMIXTURE runs or more, for each value of K sepa-

1211 rately, using DISTRUCT (104). We evaluated within-population variance of individual membership propor-
1212 tions as F_{ST}/F_{ST}^{max} values using FSTruct (105) with 1000 Bootstrap replicates per population, for the ADMIX-
1213 TURE mode result at *K=2* (**Figure 3-figure supplement 1**).
1214 Finally, we computed, using ADMIXTOOLS (50,106), f_3-admixture tests considering as admixture tar-
1215 gets each Cabo Verdean birth-island, the ASW, and the ACB separately, with, as admixture sources, in turn
1216 all 108 possible pairs of one continental European population (Source 1) and one continental African popula-
1217 tion (Source2), or the East Asian CHB (Source1) and one continental African population (Source2). For all
1218 tests we used the same individuals, population groupings, and genotyping dataset as in the previous ADMIX-
1219 TURE analyses (**Figure 3-figure supplement 2**), and considered the no-inbreeding option in ADMIXTOOLS.
1220
1221 **3. Local-ancestry inferences**
1222 To identify all populations sharing a likely common ancestry with the Cabo Verdean, ASW or ACB individuals
1223 in our dataset using local-ancestry haplotypic inferences, we considered the same sample-set as for the AD-
1224 MIXTURE analysis (**Figure 1-source data 1**), including all 455,705 SNPs from the merged dataset.
1225
1226 *Phasing with ShapeIT2*
1227 We first phased individual genotypes using SHAPEIT2 (57) for the 22 autosomal chromosomes separately
1228 using the joint Hap Map Phase 3 Build GRCh38 genetic recombination map (107). We considered default
1229 parameters using phasing windows of 2Mb and 100 states per SNP. We considered by default 7 burn-in itera-
1230 tions, 8 pruning iterations, 20 main iterations, and missing SNPs were imputed as monomorphic. Finally, we
1231 considered a "Ne" parameter of 30,000, and all individuals were considered unrelated.
1232
1233 *Chromosome painting with ChromoPainter2*
1234 We determined the possible origins of each Cabo Verdean, ASW, and ACB individual pair of phased haplo-
1235 types among European, African, USA-CEU, and Chinese-CHB populations using CHROMOPAINTER v2
1236 (56) with the same recombination map used for phasing. Following authors' recommendations, we conducted
1237 a first set of 10 replicated analyses on a random subset of 10% of the individuals for chromosomes 2, 5, 12,
1238 and 19, which provided a posteriori Ne=233.933 and θ=0.0004755376, on average by chromosome weighted
1239 by chromosome sizes, to be used in the subsequent analysis. We then conducted a full CHROMOPAINTER
1240 analysis using these parameters to paint all individuals in our dataset, in turn set as Donor and Recipient, except
1241 for Cabo Verde, ACB, and ASW individuals set only as Recipient. Finally, we combined painted chromosomes
1242 for each individual in the Cabo Verdean, ASW, and ACB population, separately.
1243
1244 *Estimating possible source populations for the Cabo Verde gene-pool using SOURCEFIND*
1245 We used CHROMOPAINTER results aggregated for each Cabo Verdean, ACB, and ASW individual sepa-
1246 rately and conducted two SOURCEFIND (58) analyses using all other populations in the dataset as a possible
1247 source, separately for four or six possible source populations ("surrogates"), to allow *a priori* for symmetric
1248 or asymmetric numbers of African and European source populations for each target admixed population. We
1249 considered 400,000 MCMC iteration steps (including 100,000 burn-in) and kept only one MCMC step every
1250 10,000 steps for final likelihood estimation. Each individual genome was divided in 100 slots with possibly
1251 different ancestry, with an expected number of surrogates equal to 0.5 times the number of surrogates, for each
1252 SOURCEFIND analysis. We aggregated results obtained for all individuals in the ACB, ASW, and each Cabo
1253 Verdean birth-island, separately. We present the highest likelihood results across 20 separate iterations of the
1254 SOURCEFIND analysis in **Figure 3B.** The second-best results were highly consistent and thus not shown.
1255
1256 **4. Runs of homozygosity (ROH)**

1257
1258 **4.a. Calling ROHs**
1259 Considering the same sample and SNP set as in the above local-ancestry analyses (**Figure 1-source data 1**),
1260 we called ROH with GARLIC (108). For each population separately, we ran GARLIC using the weighted
1261 logarithm of the odds (wLOD) score-computation scheme, with a genotyping-error rate of 10^{-3} (a likely
1262 overestimate), and using the same recombination map as for phasing, window sizes ranging from 30 to 90
1263 SNPs in increments of 10 SNPs, 100 resampling to estimate allele frequencies, and all other GARLIC
1264 parameters set to default values. We only considered results obtained with a window size of 40 SNPs, which
1265 was the largest window size associated with a bimodal wLOD score distribution and a wLOD score cutoff
1266 between the two modes, for all populations.
1267 For each population and Cabo Verdean island separately, we considered three classes of ROH that
1268 correspond to the approximate time to the most recent common ancestor of the IBD haplotypes, which can be
1269 estimated from the equation $g=100/2l$, where l is the ROH length in cM and g is the number of generations to
1270 the most recent common ancestor of the haplotypes (59). Short ROH are less than 0.25cM, reflecting
1271 homozygosity of haplotypes from more than 200 generations ago; medium ROH are between 0.25cM and 1cM
1272 reflecting demographic events having occurred between approximately 200 and 50 generations ago; and long
1273 ROH are longer than 1cM, reflecting haplotypes with a recent common ancestor less than 50 generations ago.
1274 In **Figure 4A-B** and **Appendix 4-figure 1**, we plot the distribution of the summed length of ROH per individual
1275 per size-classes.
1276
1277 **4.b. Intersecting ROH and local ancestry painting**
1278 Using the same phasing results as described above, we conducted 10 EM iterations of the RFMIX2 (109)
1279 algorithm to assign, for each Cabo Verdean individual and each SNP on each chromosome, separately, its
1280 putative source population of origin among the 24 African, European, Chinese-CHB, and USA-CEU popula-
1281 tions. We collapsed the local ancestry assignments for each SNP in each Cabo Verdean individual hence ob-
1282 tained into three continental regions, representing broadly African, broadly European, and broadly East Asian
1283 ancestries respectively. Any ancestry call that was assigned a population from the African continent was as-
1284 signed a category of AFR, any ancestry call that was assigned a population from the European continent was
1285 assigned a category of EUR, and any ancestry call that was assigned a population from the East Asian continent
1286 was assigned a category of ASN. We considered an approach similar to previous work (61), and intersected
1287 local ancestry calls with ROH calls (**Figure 4C-D**).
1288 RFMIX2 only makes local ancestry calls at loci that are present in the dataset. Therefore, a gap of unclas-
1289 sified ancestry exists where inferred ancestry switches between two successive genotyped loci as called by
1290 RFMIX2. These gaps necessarily each contain an odd number of ancestry switch points ($\geq$1) absent from our
1291 marker set. Therefore, when computing the total ancestry content of an ROH that overlaps one of these ancestry
1292 breakpoints, we assign half of the length of this gap to each ancestry classification, effectively extending each
1293 local ancestry segment to meet at the midpoint.
1294 We then plotted the length distribution of long ROH for each island and we break out the distributions by
1295 ancestral haplotype background: those with only African ancestry, those with only European ancestry, and
1296 those that span at least one ancestry breakpoint (**Figure 4C**). We excluded long ROH in East Asian ancestry
1297 segments from this and the following analyses, as we found such ancestry overall very limited in the samples
1298 (**Appendix 4-figure 2**). We also excluded ROH called with heterozygous ancestry calls (e.g., called with one
1299 haplotype called as AFR and the other as EUR). These regions were also rare (**Figure 4-source data 3**).
1300 Finally, we explored how total African/European ancestry in long ROH varies between islands. For each
1301 individual we summed the total amount of each ancestry in long-ROH and plot the distributions across islands
1302 (**Figure 4-figure supplement 1**). High levels of a given ancestry in long ROH could stem from an overall high

level of that ancestry in that individual. Therefore, for each individual, we computed their global ancestry proportions by summing up the total length of the genome inferred as a given ancestry and dividing by the length of the genome. We then plotted (**Figure 4D**), the difference of an individual's long-ROH ancestry proportion and their global ancestry proportion, for African and European ancestries separately. Values above zero indicated that a given ancestry is overrepresented in long-ROH relative to genome-wide proportions of that ancestry.

To assess the significance of these deviations, we performed a non-parametric permutation test. For each individual in each island, we randomly permuted the location of all long ROH (ensuring that no permuted ROH overlap), re-computed the local AFR ancestry proportion falling within these permuted ROH, and then subtracted the global ancestry proportion. We then took the mean of this difference across all individuals for each island and repeated the process 10,000 times. As there is negligible ASN ancestry across these individuals, the AFR and EUR proportions essentially add to 1, and therefore we consider an over/under representation of AFR ancestry in long ROH to be equivalent to an under/over representation of EUR ancestry in long ROH. Permutation distributions with observed values are plotted in **Figure 4-figure supplement 2** and permutation p-values are given in **Figure 4-source data 2**.

5. Isolation-by-distance: genetic and linguistic diversity within Cabo Verde

We explored genetic pairwise levels of differentiation calculated with ASD as previously, considering the 1,899,878 non-monomorphic SNPs within Cabo Verde obtained after QC Stage 3 (**Appendix 1-figure 1**). We projected the matrix for the 225 unrelated Cabo Verde-born individuals using metric MDS as above. Note that pruning this data set for very low LD using *plink* function *--indep-pairwise* for a 50 SNPs window moving in increments of 10 SNPs and a r^2 threshold of 0.025 resulted in 85,425 SNPs for which the ASD matrix was highly correlated with the one using all SNPs (Spearman ρ=0.8745, $p<2.2\text{x}10^{-16}$). In parallel, we described the diversity of Kriolu idiolects (i.e. individuals' manners of speaking Kriolu) among the 225 genetically unrelated Cabo Verde-born individuals by projecting, with metric MDS, the matrix of pairwise Euclidean distances between vectors of individuals' utterance-frequencies (**Material and Methods 1.d**), considering the 4831 unique uttered items.

We then conducted a series of Mantel and partial Mantel correlation tests (Legendre and Legendre 1998), using the *partial.mantel.test* function in the R package *ncf*, with Spearman correlation and 10,000 Mantel permutations, to explore possible isolation-by-distance (39) patterns as well as correlations with other variables of interest. We conducted correlation tests between either the pairwise Euclidean distances between vectors of individuals' utterance-frequencies or genetic ASD separately, and individual pairwise matrices of *i)* absolute age differences, *ii)* absolute differences in academic education duration, *iii)* geographic distances between residence-locations (logarithmic scale), *iv)* between birth-locations, *v)* between mothers' birth-locations, *vi)* between fathers' birth-locations (**Table 1**, **Table 1-source data 1**). All pairwise geographic distances were calculated with the Haversine great-circle distance formulation (110), taking 6,371 km for the radius of the Earth, using the *rdist.earth* function in the R package *fields*. Before computing logarithmic distances, we added 1km to all pairwise distances.

6. Isolation-by-distance: genetic and linguistic admixture within Cabo Verde

We further explored isolation-by-distance patterns within Cabo Verde specifically for African genetic and linguistic individual admixture levels. We considered African genetic admixture levels estimated from ADMIXTURE at K=2 or ASD-MDS approaches (**Material and Methods 2-3**, **Figure 3, Appendix 1-figure 2**), and individual African linguistic admixture as "African-utterances scores" $Z_{i,Cat}$ as defined in **Material and Methods 1.e** for utterance lists contained in Category A, Category B, or Category A&B respectively (23). For

genetic or linguistic admixture levels separately, we computed the pairwise matrix of individual absolute admixture levels differences, and conducted Mantel testing with the different geographical distance matrices as above. Finally, we compared African genetic and linguistic admixture scores using Spearman correlations, throughout Cabo Verde and within all birth-islands, separately.

7. Inferring genetic admixture histories in Cabo Verde with *MetHis*-ABC

We aimed at reconstructing the detailed genetic admixture history of each Cabo Verde island separately. To do so, we first design *MetHis* v1.0 (45) forward-in-time simulations of four competing complex admixture scenarios. We then couple *MetHis* simulation and summary-statistics calculation tools with ABC Random-Forest scenario-choice implemented in the R package *abcrf* (71), followed by Neural-Network posterior parameter estimation with the R package *abc* (72), under the winning scenario for each island separately.

7.a. Simulating four competing scenarios of complex historical admixture for each Cabo Verde island

ABC inference relies on simulations conducted with scenario-parameter values drawn randomly within prior distributions set explicitly by the user. We used *MetHis* v1.0 (45) to simulate 60,000 independent autosomal SNP markers in the admixed population H, forward-in-time and individual centered, under the four competing scenarios presented in **Figure 6** and **Table 2** and explicated below. In all four scenarios (**Figure 6**; **Table 2**), we considered, forward-in-time, that the admixed population (Population H) is founded at generation 0, 21 generations before present. Generation 0 thus roughly corresponds to the 15th century when considering an average generation-time of 25 years and sampled individuals born on average between the 1960's and the 1980's and no later than 1990 in our dataset. This is reasonable as historical records showed that Cabo Verde was likely un-inhabited before its initial colonial settlement established in the 1460s on Santiago (26). Due to the recent admixture history of Cabo Verde and as we considered only independent genotyped SNPs, we neglected mutation in our simulations for simplicity.

Following our descriptive analyses results, we considered scenarios with only one "European" and one "African" source population, and each Cabo Verde island, separately, as the "Admixed" recipient population H. This corresponds to the "two-source" version of the general admixture model from Verdu and Rosenberg (73), also explored with *MetHis* previously (45).We therefore considered a single African and European population at the source of all admixture in Cabo Verde, and further considered that both source populations were very large and at the drift-mutation equilibrium during the 21 generations of the admixture process until present. Furthermore, we considered that these source populations were accurately represented, respectively, by the Mandinka from Senegambia and the Iberian-IBS populations in a random genotyping dataset of 60,000 independent autosomal SNPs (see **Results 1-3**).

In brief (see below), at each generation, *MetHis* performs simple Wright-Fisher (111,112) forward-in-time discrete simulations, individual-centered, in a randomly-mating (without selfing) admixed population of N_g diploid individuals. Separately for each N_g individual in the admixed population at generation g, *MetHis* draws parents randomly from the source populations and the admixed population itself at the previous generation according to given parameter-values drawn from prior distributions separately for each simulation.

Hyperbolic increase, linear increase, or constant reproductive population size in the admixed population

We considered, for the admixed population H, a reproductive population size of N_0 diploid individuals at generation 0, with N_0 in [10,1000], and N_{20} in [100,100,000] at generation 20, such that $N_0 < N_{20}$. In between these two values, we considered for the N_g values at each generation the discrete numerical solutions of an increasing rectangular hyperbola function of parameter u_N in [0,1/2] (45). Therefore, values of the demographic parameters $N_0 \sim N_{20}$ correspond to simulations with a constant admixed-population H reproductive population size of N_0 diploid individuals during the entire 21 generations of the admixture process, whichever the value of u_N.

Instead, parameter values $N_0 \neq N_{20}$ necessarily correspond to simulations with an increase in reproductive size between N_0 and N_{20}, steeper with values of u_N closer to 0. Note, thus, that parameter values $N_0 \neq N_{20}$ and u_N close to 0 correspond to simulations where the reproductive size of the admixed population H is roughly constant and equal to N_0 at each generation until a very sharp increase to reach N_{20} at the last generation before present. Instead, parameter values $N_0 \neq N_{20}$ and u_N close to 1/2 correspond to simulations with a linear increase in reproductive size between N_0 and N_{20}.

Therefore, while we do not formally compare competing scenarios with different demographic regimes in this work, each scenario comprises simulations whose parameter values correspond to a variety of constant, hyperbolic increase, or linear increase in reproductive size over the course of the admixture history of each Cabo Verdean island separately. Therefore, ABC parameter estimation of the demographic parameters N_0, N_{20}, and u_N should determine, *a posteriori*, which of the three demographic regimes best explain our data, whichever is the winning admixture scenario among the four in competition.

Founding the admixed population

At generation 0 (**Figure 6**), the admixed population of size N_0 diploid individuals drawn in [10,1000] is founded with a proportion $s_{Eur,0}$ of admixed individuals' parents originating from the European source drawn in [0,1], and a proportion of $s_{Afr,0}$ parents from the African source drawn in [0,1], with $s_{Eur,0} + s_{Afr,0}=1$. Note that parameter-values of $s_{Afr,0}$, or $s_{Eur,0}$, close to 0 correspond to simulations where the "admixed" population is initially founded by only one of the sources, and that genetic admixture *per se* may only occur at the following admixture event.

After the founding of the admixed population H, we considered two different admixture scenarios for either source population's contribution to the gene-pool of population H. In all cases, for all generations g in [1,20] after the initial founding of the admixed population at $g = 0$, *MetHis* randomly draws parents from the African source, the European source and the admixed population H respectively in proportions $s_{Afr,g}$, $s_{Eur,g}$, and h_g, each in [0,1] and satisfying $s_{Afr,g} + s_{Eur,g} + h_g = 1$. Then, the software randomly builds gametes for each parent and randomly pairs them, without selfing, to produce N_g diploid individuals in the admixed population.

Two admixture pulses after foundation

For a given source population hereafter designated "Source" ("European" or "African" in our case), after founding at generation 0, we considered scenarios with two additional pulses of admixture ("Source"-2Pulses scenarios). The two pulses occur, respectively, at generation $t_{Source,p1}$ and $t_{Source,p2}$ in [1,20], with $t_{Source,p1} \neq t_{Source,p2}$; and with intensity $s_{Source,tSource,p1}$ and $s_{Source,tSource,p2}$ in [0,1], respectively.

Note that simulations considering values of parameters $t_{Source,p1}= t_{Source,p2} + 1$, and simulations with either $s_{Source,tSource,p1}$ or $s_{Source,tSource,p2}$ close to 0, may strongly resemble those expected under scenarios with only one pulse of admixture after the founding of the admixed population H.

A period of recurring admixture after foundation

For a given Source population, after founding at generation 0, we considered scenarios with a possible period of recurring admixture, where, during this period, admixture intensity followed a monotonically decreasing trend ("Source"-Recurring scenarios). The period of admixture occurs between times $t_{Source,t1}$ and $t_{Source,t2}$ in [1,20] with $t_{Source,t2} \geq t_{Source,t1} + 1$. The beginning of the admixture period at $t_{Source,t1}$ is associated with admixture intensity $s_{Source,tSource,t1}$ in [0,1]. The end of the admixture period at $t_{Source,t2}$ is associated with intensity $s_{Source,tSource,t2}$ in [0,1] such that $s_{Source,tSource,t1} \geq s_{Source,tSource,t2}$. In between, the admixture intensity values at each generation of the admixture period are the discrete numerical solutions of a decreasing rectangular hyperbola function of parameter u_{Source} in [0,1/2] (45).

Intuitively, a u parameter value close to 0 corresponds to a sharp pulse of admixture occurring at the beginning of the admixture period of intensity $s_{Source,tSource,t1}$, followed at the next generation by constant recurring admixture of intensity $s_{Source,tSource,t2}$ until the end of the admixture period. Alternatively, a u parameter value close to 1/2 corresponds to a linearly decreasing admixture at each generation of the admixture period, from $s_{Source,tSource,t1}$ to $s_{Source,tSource,t2}$.

Note that in the limit when $s_{Source,tSource,t1} \sim s_{Source,tSource,t2}$, Recurring scenarios correspond to constant recurring admixture of that intensity. Furthermore, simulations with u and $s_{Source,tSource,t2}$ parameter values both close to 0 correspond to scenarios with a single pulse of admixture from a given source after the founding pulse, occurring at time $t_{Source,t1}$ and with intensity $s_{Source,tSource,t1}$.

Four competing scenarios of admixture from two-source populations in each Cabo Verde island

Finally, we combined the 2Pulses and Recurring scenarios from either the African and European Source populations in order to produce four competing scenarios of admixture for the genetic history of Cabo Verde (**Figure 6**), with the only constraint that at each generation g between 1 and 20, $s_{Afr,g} + s_{Eur,g}=1 - h_g$, where h_g is the contribution of the admixed population H to itself at the following generation in [0,1].

Simulating the admixed population from source-populations for 60,000 independent SNPs with MetHis

As introduced previously, our results showed that the Mandinka from West Western Africa and the Iberian IBS from South West Europe were reasonable proxies of the main source populations for the gene-pool of Cabo Verde, at least when considering a relatively small number of independent autosomal SNPs. We decided to consider both populations as very large and at the drift-mutation equilibrium since the 1460's and the initial founding of Cabo Verde. We thus chose not to explicitly simulate the evolutionary history of the two European and African populations at the source of the genetic history of the Cabo Verde islands.

Instead, we first randomly drew 60,000 independent SNPs, avoiding singletons, from the LD-pruned 102,543 independent SNPs employed for the ADMIXTURE analyses. We then built a single reservoir of "African" gametes comprising 20,000 haploid genomes of 60,000 independent SNP-sites each, where each allele at each site of a gamete was randomly drawn in the site frequency spectrum observed for the corresponding SNP in the Mandinka proxy source population. Separately, we proceeded similarly to build a reservoir of 20,000 European gametes matching instead the site-frequency spectrum observed in the Iberian IBS at the 60,000 SNPs.

For a given simulation with, at generation 0, given parameter values $s_{Afr,0}$ and $s_{Eur,0}$, each in [0,1] such that $s_{Afr,0} + s_{Eur,0}=1$, and a given value (in [10,1000]) of N_0 diploid individuals in the admixed population H, *MetHis* randomly draws two different gametes in the African gamete-reservoir and randomly pairs them to produce one parent from the African source and repeats the process $s_{Afr,0}$ x $2N_0$ times to obtain that number of African parents. In parallel and using the same procedure, *MetHis* randomly builds $s_{Eur,0}$ x $2N_0$ parents from the European gamete-reservoirs. For each of N_0 individuals in the admixed population separately, *MetHis* then draws randomly a pair of parents among the European and African parents hence obtained, and for each parent separately, builds one haploid gamete by randomly drawing one allele for each 60,000 genotypes. Finally, *MetHis* pairs both hence obtained gametes to create the novel individual in the admixed population at the following generation, and repeats the procedure (replacing the pair of parents after each random draw in the parental pool) for each of N_0 individuals separately.

Then, for the same given simulation, admixture from a source population is set to occur at a given generation g (in [1,20]) associated with a given intensity $s_{source,g}$, keeping in mind that at all g in [1,20], $s_{Afr,g} + s_{Eur,g} + h_g = 1$. *MetHis* then builds anew $s_{source,g}$ x $2N_g$ reproductive parents from this source population's gamete-reservoir as previously, and in parallel randomly draws h_g x $2N_g$ parents from the admixed population H itself at the previous generation. Then, for each of N_g individuals in the admixed population separately, *MetHis*

1485 randomly draws a pair of different parents (replacing the pair of parents after each random draw in the parental
1486 pool), randomly builds haploid gametes from each parent, and pairs them similarly as previously to obtain a
1487 new individual at the following generation.
1488 Thus, note that while our source-populations' gamete reservoirs were fixed during the admixture process,
1489 the African or the European diploid parents possibly contributing to the gene-pool of the admixed population
1490 are randomly built anew, and each produce novel gametes, at each generation and in each simulation separately.
1491 Importantly, note that recombination is thus not a parameter in *MetHis* simulations as all SNPs are considered
1492 statistically independent.
1493
1494 *Sampling simulated source and admixed populations*
1495 At the end of each simulation, we randomly drew individual samples from each source and the admixed pop-
1496 ulation H matching observed sample sizes. We randomly sampled 60 individuals in the African source gamete
1497 reservoirs, 60 individuals in the European source, and the number of admixed individuals corresponding to the
1498 sample size of each Cabo Verde island of birth of individuals or to all 225 Cabo Verde-born individuals
1499 grouped in a single random mating population, in turn (**Figure 1-source data 1**). We sampled individuals
1500 without grand-parents in common, as allowed in *MetHis* by explicit genealogical flagging of individuals during
1501 the last two generations of the admixture process, hence mimicking our observed family unrelated dataset
1502 within Cabo Verde.
1503
1504 *Number of simulations and scenario-parameter priors for ABC inference*
1505 We performed 10,000 such *MetHis* simulations under each of four admixture scenarios for each of the nine
1506 birth-islands of Cabo Verde and for all Cabo Verde-born individuals grouped in a single population, separately.
1507 Each simulation was performed under a vector of scenario parameters drawn from prior distributions described
1508 above and in **Table 2,** using *MetHis parameter generator* tools. Separately for each island and for Cabo Verde
1509 as a single population, we used this set of simulations to determine which scenario best explained the observed
1510 data using Random-Forest ABC (see below). Under the winning scenario for each birth-island and separately
1511 for Cabo Verde as a whole, we then performed an additional 90,000 simulations each corresponding to a dif-
1512 ferent vector of parameter values drawn randomly from the priors set by the user for this scenario, to produce
1513 a total of 100,000 simulations to be used for Neural-Network ABC posterior parameter estimation, for each
1514 ten – 9 islands and Cabo Verde as a whole, separately – analysis separately.
1515
1516 **7.b. *MetHis*-ABC Random Forest scenario-choice and Neural Network posterior parameter estimations**
1517 To reconstruct highly complex admixture histories in Cabo Verde using genetic data, we conducted machine-
1518 learning Approximate Bayesian Computation inferences based on the simulations produced with *MetHis* as
1519 described above under the four competing admixture history scenarios. We performed Random-Forest ABC
1520 scenario-choice (71), and Neural Network ABC posterior parameter inferences (72), for each Cabo Verde
1521 island and for all Cabo Verde-born individuals grouped in a single population, separately. We followed the
1522 *MetHis*-ABC approach proposed in (45) for summary-statistics calculation, prior-checking, out-of-bag cross-
1523 validation, machine-learning ABC predictions and inferences parameterization, and posterior parameter cross-
1524 validation error calculations.
1525 All the details and results of these ABC procedures can be found in corresponding **Appendix 1**, **Appendix**
1526 **1-table 1**, **Appendix 5-table 1-10**, **Appendix 1-figure 3-4**, **Appendix 1-figure 3-figure supplement 1-10**,
1527 and **Figure 7-figure supplement 1-3**. Briefly, we performed 10,000 simulations of 60,000 independent SNPs
1528 under each of the four competing scenarios described above, drawing parameter values in prior distributions
1529 detailed in **Table 2**. As listed in **Table 3** and described in details in **Appendix 1**, we then computed 42 sum-

1530 mary-statistics separately for each simulated dataset comprising 60,000 independent SNPs, by drawing ran-
1531 domly 60 parents in the African and European source populations, and randomly drawing sample-sets match-
1532 ing the observed sample-sizes of each Cabo Verde birth-island or all Cabo Verde-born individuals as a single
1533 population, separately. Note that we considered summary-statistics specifically aiming at describing the dis-
1534 tribution of individual admixture fractions in the sample set, known theoretically and empirically to be highly
1535 informative about complex admixture history parameters (45,73). We thus performed RF-ABC scenario-
1536 choices using 40,000 vectors of 42 summary-statistics (10,000 under each four competing scenarios), each
1537 corresponding to a vector of parameter values randomly drawn in prior distributions and used for *MetHis*
1538 simulations, for each nine birth-island and for Cabo Verde as a whole, separately. We then performed NN-
1539 ABC joint posterior parameter inferences of all scenario-parameters under the winning scenarios obtained with
1540 RF-ABC, using 100,000 vectors of 42 summary statistics obtained from additional *MetHis* simulations under
1541 the winning scenarios respectively for each nine birth-island and for Cabo Verde as a whole, separately.
1542
1543

ACKNOWLEDGEMENTS

The authors would like to warmly thank all Cabo Verdean participants to this study as well as the UniCV for facilitating the project. This project was funded in part by the French "Agence Nationale pour la Recherche" grant ANR METHIS 15-CE32-0009-1, and by a grant from the France-Stanford Center for Interdisciplinary Studies. MB was supported in part by the Linguistics Department at the University of Michigan (MI, USA). ZAS was supported in part by startup funds from the Department of Biology at the Pennsylvania State University (PA, USA), and by the NIH grant R35 GM146926. CAFL was supported in part by the Marcus Borgströms Foundation for Genetic Research and the Bertil Lundman Foundation for Anthropological Studies (Sweden). We thank the platform "Paléogénomique et génétique moléculaire" (P2GM) of the French Muséum National d'Histoire Naturelle at the Musée de l'Homme for support handling biological samples and generating genetic data. We thank the BIOMICS platform from the Pasteur institute for performing genotyping analyses. Finally, the authors warmly thank two independent reviewers and the editors of *eLife*, as well as Frank Alvarez-Pereyre, Erkan O. Buzbas, Marta Ciccarella, Pierre Darlu, Evelyne Heyer, Ethan M. Jewett, Marie-France Mifune, Etienne Patin, Jorge M. Rocha, Lara Rubio Arauna, and Bruno Toupance, for useful comments and discussions about this work.

CONFLICT OF INTEREST STATEMENT

The authors declare no conflict of interests for this work.

1565 **REFERENCES**

1566

1567 1. Eltis D, Richardson D. Atlas of the transatlantic slave trade. 2015. 336 p.

1568 2. Fortes-Lima C, Verdu P. Anthropological genetics perspectives on the transatlantic slave
1569 trade. Human Molecular Genetics [Internet]. 2021 Apr 26 [cited 2021 Jun 4];30(R1):R79–87.
1570 Available from: https://academic.oup.com/hmg/article/30/R1/R79/6040749

1571 3. Micheletti SJ, Bryc K, Ancona Esselmann SG, Freyman WA, Moreno ME, Poznik GD, et al.
1572 Genetic Consequences of the Transatlantic Slave Trade in the Americas. The American
1573 Journal of Human Genetics [Internet]. 2020 Aug [cited 2021 Jun 4];107(2):265–77. Available
1574 from: https://linkinghub.elsevier.com/retrieve/pii/S0002929720302007

1575 4. Ongaro L, Scliar MO, Flores R, Raveane A, Marnetto D, Sarno S, et al. The Genomic Impact
1576 of European Colonization of the Americas. Current Biology [Internet]. 2019 Dec [cited 2022
1577 Apr 8];29(23):3974-3986.e4. Available from:
1578 https://linkinghub.elsevier.com/retrieve/pii/S0960982219313065

1579 5. Winkler CA, Nelson GW, Smith MW. Admixture Mapping Comes of Age. Annu Rev Genom
1580 Hum Genet [Internet]. 2010 Sep [cited 2021 Jun 4];11(1):65–89. Available from:
1581 http://www.annualreviews.org/doi/10.1146/annurev-genom-082509-141523

1582 6. Wojcik GL, Graff M, Nishimura KK, Tao R, Haessler J, Gignoux CR, et al. Genetic analyses
1583 of diverse populations improves discovery for complex traits. Nature [Internet]. 2019 Jun
1584 [cited 2021 Jun 4];570(7762):514–8. Available from: http://www.nature.com/articles/s41586-
1585 019-1310-4

1586 7. Patin E, Lopez M, Grollemund R, Verdu P, Harmant C, Quach H, et al. Dispersals and genetic
1587 adaptation of Bantu-speaking populations in Africa and North America. Science [Internet].
1588 2017 May 5 [cited 2021 Jun 4];356(6337):543–6. Available from:
1589 https://www.sciencemag.org/lookup/doi/10.1126/science.aal1988

1590 8. Gravel S. Population Genetics Models of Local Ancestry. Genetics [Internet]. 2012 Jun 1
1591 [cited 2021 Jun 4];191(2):607–19. Available from:
1592 https://academic.oup.com/genetics/article/191/2/607/5935164

1593 9. Hellenthal G, Busby GBJ, Band G, Wilson JF, Capelli C, Falush D, et al. A Genetic Atlas of
1594 Human Admixture History. Science [Internet]. 2014 Feb 14 [cited 2021 Jun
1595 4];343(6172):747–51. Available from:
1596 https://www.sciencemag.org/lookup/doi/10.1126/science.1243518

1597 10. Mathias RA, Taub MA, Gignoux CR, Fu W, Musharoff S, O'Connor TD, et al. A continuum
1598 of admixture in the Western Hemisphere revealed by the African Diaspora genome. Nat
1599 Commun [Internet]. 2016 Nov [cited 2021 Jun 4];7(1):12522. Available from:
1600 http://www.nature.com/articles/ncomms12522

1601 11. Moreno-Estrada A, Gravel S, Zakharia F, McCauley JL, Byrnes JK, Gignoux CR, et al.
1602 Reconstructing the Population Genetic History of the Caribbean. Tarazona-Santos E, editor.
1603 PLoS Genet [Internet]. 2013 Nov 14 [cited 2021 Jun 4];9(11):e1003925. Available from:
1604 https://dx.plos.org/10.1371/journal.pgen.1003925

1605 12. Baharian S, Barakatt M, Gignoux CR, Shringarpure S, Errington J, Blot WJ, et al. The Great

Migration and African-American Genomic Diversity. Gibson G, editor. PLoS Genet [Internet]. 2016 May 27 [cited 2021 Jun 4];12(5):e1006059. Available from: https://dx.plos.org/10.1371/journal.pgen.1006059

13. Holm JA. An introduction to pidgin and creoles. Cambridge [England] ; New York: Cambridge University Press; 2000. 282 p. (Cambridge textbooks in linguistics).

14. Escure G, Schwegler A. Creoles, contact, and language change: linguistics and social implications. Amsterdam ; Philadelphia: John Benjamins Pub; 2004. 354 p. (Creole language library).

15. Quint N. Le cap-verdien: origines et devenir d'une langue métisse. Paris, France: L'Harmattan; 2000. 353 p.

16. Essegbey J, Migge B, Winford D. Cross-linguistic influence in language creation: Assessing the role of the Gbe languages in the formation of the Creoles of Suriname. Lingua [Internet]. 2013 May [cited 2021 Jun 4];129:1–8. Available from: https://linkinghub.elsevier.com/retrieve/pii/S002438411300048X

17. Baptista M. Continuum and variation in Creoles: Out of many voices, one language. JPCL [Internet]. 2015 Oct 20 [cited 2021 Jun 4];30(2):225–64. Available from: http://www.jbe-platform.com/content/journals/10.1075/jpcl.30.2.02bap

18. Eltis D, editor. Coerced and free migration: global perspectives. Stanford, Calif: Stanford University Press; 2002. 447 p. (The making of modern freedom).

19. Berlin I. Many Thousands Gone: the First Two Centuries of Slavery in North America. [Internet]. Cambridge: Harvard University Press; 2009 [cited 2021 Jun 7]. 512 p. Available from: https://public.ebookcentral.proquest.com/choice/publicfullrecord.aspx?p=3300728

20. Creanza N, Ruhlen M, Pemberton TJ, Rosenberg NA, Feldman MW, Ramachandran S. A comparison of worldwide phonemic and genetic variation in human populations. Proc Natl Acad Sci USA [Internet]. 2015 Feb 3 [cited 2022 Nov 30];112(5):1265–72. Available from: https://pnas.org/doi/full/10.1073/pnas.1424033112

21. Cavalli-Sforza LL, Piazza A, Menozzi P, Mountain J. Reconstruction of human evolution: bringing together genetic, archaeological, and linguistic data. Proc Natl Acad Sci USA [Internet]. 1988 Aug [cited 2023 Jan 20];85(16):6002–6. Available from: https://pnas.org/doi/full/10.1073/pnas.85.16.6002

22. Ansari-Pour N, Moñino Y, Duque C, Gallego N, Bedoya G, Thomas MG, et al. Palenque de San Basilio in Colombia: genetic data support an oral history of a paternal ancestry in Congo. Proc R Soc B [Internet]. 2016 Mar 30 [cited 2021 Jun 4];283(1827):20152980. Available from: https://royalsocietypublishing.org/doi/10.1098/rspb.2015.2980

23. Verdu P, Jewett EM, Pemberton TJ, Rosenberg NA, Baptista M. Parallel Trajectories of Genetic and Linguistic Admixture in a Genetically Admixed Creole Population. Current Biology [Internet]. 2017 Aug [cited 2022 Feb 2];27(16):2529-2535.e3. Available from: https://linkinghub.elsevier.com/retrieve/pii/S096098221730859X

24. Hagemeijer T, Rocha J. Creole languages and genes: the case of São Tomé and Príncipe. Faits Lang [Internet]. 2019 Aug 23 [cited 2021 Jun 4];49(1):167–82. Available from:

https://brill.com/view/journals/fdl/49/1/article-p167_11.xml

25. Carreira A. Cabo Verde: formação e extinção de uma sociedade escravocrata (1460-1878). 3rd ed. Praia, Cabo Verde: IPC; 2000. 522 p. (Estudos e ensaios).

26. Albuquerque L de, Santos MEM, editors. História geral de Cabo Verde T1. Vol. 1. Lisboa : Praia [Cape Verde]: Centro de Estudos de História e Cartografia Antiga, Instituto de Investigação Científica Tropical ; Instituto Nacional da Cultura de Cabo Verde; 1991. 523 p.

27. Albuquerque L de, Santos MEM, editors. História geral de Cabo Verde T2. 2. ed. Vol. 2. Lisboa: Centro de Estudos de História e Cartogr. Antiga; 1995. 596 p.

28. Albuquerque L de, Santos MEM, editors. História concisa de Cabo Verde (Resumo da História geral de Cabo Verde T1-3). Lisboa: Inst. de Investigação Científica Tropical; 2007. 427 p.

29. Baptista M. The syntax of Cape Verdean Creole: the Sotavento varieties. Amsterdam ; Philadelphia: John Benjamins Pub; 2002. 289 p. (Linguistik aktuell = Linguistics today).

30. Lang J. Les langues des autres dans la créolisation: théorie et exemplification par le créole d'empreinte wolof à l'île Santiago du Cap Vert. Tübingen: Narr; 2009. 275 p.

31. Brehm A, Pereira L, Bandelt HJ, Prata MJ, Amorim A. Mitochondrial portrait of the Cabo Verde archipelago: the Senegambian outpost of Atlantic slave trade. Ann Hum Genet [Internet]. 2002 Jan [cited 2021 Jun 4];66(1):49–60. Available from: http://doi.wiley.com/10.1017/S0003480001001002

32. Gonçalves R, Rosa A, Freitas A, Fernandes A, Kivisild T, Villems R, et al. Y-chromosome lineages in Cabo Verde Islands witness the diverse geographic origin of its first male settlers. Human Genetics [Internet]. 2003 Nov 1 [cited 2021 Jun 4];113(6):467–72. Available from: http://link.springer.com/10.1007/s00439-003-1007-4

33. Beleza S, Campos J, Lopes J, Araújo II, Hoppfer Almada A, e Silva AC, et al. The Admixture Structure and Genetic Variation of the Archipelago of Cape Verde and Its Implications for Admixture Mapping Studies. Relethford JH, editor. PLoS ONE [Internet]. 2012 Nov 30 [cited 2021 Jun 4];7(11):e51103. Available from: https://dx.plos.org/10.1371/journal.pone.0051103

34. Beleza S, Johnson NA, Candille SI, Absher DM, Coram MA, Lopes J, et al. Genetic Architecture of Skin and Eye Color in an African-European Admixed Population. Spritz RA, editor. PLoS Genet [Internet]. 2013 Mar 21 [cited 2021 Jun 4];9(3):e1003372. Available from: https://dx.plos.org/10.1371/journal.pgen.1003372

35. Hamid I, Korunes KL, Beleza S, Goldberg A. Rapid adaptation to malaria facilitated by admixture in the human population of Cabo Verde. eLife [Internet]. 2021 Jan 4 [cited 2021 Jun 4];10:e63177. Available from: https://elifesciences.org/articles/63177

36. Soares MJ. The British Presence on the Cape Verdean Archipelago (Sixteenth to Eighteenth centuries). African Economic History. 2011;39:129–46.

37. Berlin I. The making of African America: the four great migrations. New York: Penguin Books; 2010. 304 p.

38. Gouveia MH, Borda V, Leal TP, Moreira RG, Bergen AW, Kehdy FSG, et al. Origins,

Admixture Dynamics, and Homogenization of the African Gene Pool in the Americas. Nielsen R, editor. Molecular Biology and Evolution. 2020 Jun 1;37(6):1647–56.

39. Rousset F. Genetic Differentiation and Estimation of Gene Flow from *F* -Statistics Under Isolation by Distance. Genetics [Internet]. 1997 Apr 1 [cited 2022 Feb 2];145(4):1219–28. Available from: https://academic.oup.com/genetics/article/145/4/1219/6018124

40. Barbujani G. Autocorrelation of Gene Frequencies Under Isolation by Distance. Genetics [Internet]. 1987 Dec 1 [cited 2022 Nov 30];117(4):777–82. Available from: https://academic.oup.com/genetics/article/117/4/777/5997427

41. Malécot G. Heterozygosity and relationship in regularly subdivided populations. Theoretical Population Biology [Internet]. 1975 Oct [cited 2022 Nov 30];8(2):212–41. Available from: https://linkinghub.elsevier.com/retrieve/pii/0040580975900337

42. Barbujani G, Sokal RR. Genetic population structure of Italy. II. Physical and cultural barriers to gene flow. Am J Hum Genet. 1991 Feb;48(2):398–411.

43. Cavalli-Sforza LL, Moroni A, Zei G. Consanguinity, Inbreeding, and Genetic Drift in Italy. Princeton: Princeton University Press; 2004.

44. Verdu P, Leblois R, Froment A, Théry S, Bahuchet S, Rousset F, et al. Limited dispersal in mobile hunter–gatherer Baka Pygmies. Biol Lett [Internet]. 2010 Dec 23 [cited 2022 Nov 30];6(6):858–61. Available from: https://royalsocietypublishing.org/doi/10.1098/rsbl.2010.0192

45. Fortes-Lima CA, Laurent R, Thouzeau V, Toupance B, Verdu P. Complex genetic admixture histories reconstructed with Approximate Bayesian Computation. Mol Ecol Resour [Internet]. 2021 May [cited 2021 Jun 4];21(4):1098–117. Available from: https://onlinelibrary.wiley.com/doi/10.1111/1755-0998.13325

46. Bowcock AM, Ruiz-Linares A, Tomfohrde J, Minch E, Kidd JR, Cavalli-Sforza LL. High resolution of human evolutionary trees with polymorphic microsatellites. Nature [Internet]. 1994 Mar [cited 2022 Feb 2];368(6470):455–7. Available from: http://www.nature.com/articles/368455a0

47. Hastie T, Tibshirani R, Friedman JH, Friedman JH. The elements of statistical learning: data mining, inference, and prediction. Vol. 2. Springer; 2009.

48. Alexander DH, Novembre J, Lange K. Fast model-based estimation of ancestry in unrelated individuals. Genome Research [Internet]. 2009 Sep 1 [cited 2021 Jun 4];19(9):1655–64. Available from: http://genome.cshlp.org/cgi/doi/10.1101/gr.094052.109

49. Morrison ML, Alcala N, Rosenberg NA. FSTruct: An FST-based tool for measuring ancestry variation in inference of population structure. Molecular Ecology Resources [Internet]. 2022 Oct [cited 2023 Jan 20];22(7):2614–26. Available from: https://onlinelibrary.wiley.com/doi/10.1111/1755-0998.13647

50. Patterson N, Moorjani P, Luo Y, Mallick S, Rohland N, Zhan Y, et al. Ancient Admixture in Human History. Genetics [Internet]. 2012 Nov 1 [cited 2022 Feb 2];192(3):1065–93. Available from: https://academic.oup.com/genetics/article/192/3/1065/5935193

51. Pritchard JK, Stephens M, Donnelly P. Inference of population structure using multilocus genotype data. Genetics. 2000 Jun;155(2):945–59.

52. Rosenberg NA. Genetic Structure of Human Populations. Science [Internet]. 2002 Dec 20 [cited 2021 Jun 4];298(5602):2381–5. Available from: https://www.sciencemag.org/lookup/doi/10.1126/science.1078311

53. Falush D, Stephens M, Pritchard JK. Inference of population structure using multilocus genotype data: linked loci and correlated allele frequencies. Genetics. 2003 Aug;164(4):1567–87.

54. Lawson DJ, van Dorp L, Falush D. A tutorial on how not to over-interpret STRUCTURE and ADMIXTURE bar plots. Nat Commun [Internet]. 2018 Dec [cited 2021 Jun 4];9(1):3258. Available from: http://www.nature.com/articles/s41467-018-05257-7

55. Peter BM. A geometric relationship of F_2, F_3 and F_4-statistics with principal component analysis. Phil Trans R Soc B [Internet]. 2022 Jun 6 [cited 2023 Jan 20];377(1852):20200413. Available from: https://royalsocietypublishing.org/doi/10.1098/rstb.2020.0413

56. Lawson DJ, Hellenthal G, Myers S, Falush D. Inference of Population Structure using Dense Haplotype Data. Copenhaver GP, editor. PLoS Genet [Internet]. 2012 Jan 26 [cited 2021 Jun 4];8(1):e1002453. Available from: https://dx.plos.org/10.1371/journal.pgen.1002453

57. Delaneau O, Marchini J, Zagury JF. A linear complexity phasing method for thousands of genomes. Nat Methods [Internet]. 2012 Feb [cited 2021 Jun 4];9(2):179–81. Available from: http://www.nature.com/articles/nmeth.1785

58. Chacón-Duque JC, Adhikari K, Fuentes-Guajardo M, Mendoza-Revilla J, Acuña-Alonzo V, Barquera R, et al. Latin Americans show wide-spread Converso ancestry and imprint of local Native ancestry on physical appearance. Nat Commun [Internet]. 2018 Dec [cited 2021 Jun 4];9(1):5388. Available from: http://www.nature.com/articles/s41467-018-07748-z

59. Thompson EA. Identity by Descent: Variation in Meiosis, Across Genomes, and in Populations. Genetics [Internet]. 2013 Jun 1 [cited 2021 Jun 4];194(2):301–26. Available from: https://academic.oup.com/genetics/article/194/2/301/6065409

60. Mooney JA, Huber CD, Service S, Sul JH, Marsden CD, Zhang Z, et al. Understanding the Hidden Complexity of Latin American Population Isolates. The American Journal of Human Genetics [Internet]. 2018 Nov [cited 2022 Feb 2];103(5):707–26. Available from: https://linkinghub.elsevier.com/retrieve/pii/S0002929718303513

61. Szpiech ZA, Mak ACY, White MJ, Hu D, Eng C, Burchard EG, et al. Ancestry-Dependent Enrichment of Deleterious Homozygotes in Runs of Homozygosity. The American Journal of Human Genetics [Internet]. 2019 Oct [cited 2021 Jun 4];105(4):747–62. Available from: https://linkinghub.elsevier.com/retrieve/pii/S0002929719303374

62. Pemberton TJ, Absher D, Feldman MW, Myers RM, Rosenberg NA, Li JZ. Genomic Patterns of Homozygosity in Worldwide Human Populations. The American Journal of Human Genetics [Internet]. 2012 Aug [cited 2022 Nov 30];91(2):275–92. Available from: https://linkinghub.elsevier.com/retrieve/pii/S0002929712003230

63. Arauna LR, Bergstedt J, Choin J, Mendoza-Revilla J, Harmant C, Roux M, et al. The genomic

landscape of contemporary western Remote Oceanians. Current Biology [Internet]. 2022 Nov [cited 2022 Nov 30];32(21):4565-4575.e6. Available from: https://linkinghub.elsevier.com/retrieve/pii/S096098222201377X

64. Hunley K, Dunn M, Lindström E, Reesink G, Terrill A, Healy ME, et al. Genetic and Linguistic Coevolution in Northern Island Melanesia. Pritchard JK, editor. PLoS Genet [Internet]. 2008 Oct 31 [cited 2022 Nov 30];4(10):e1000239. Available from: https://dx.plos.org/10.1371/journal.pgen.1000239

65. Wang C, Szpiech ZA, Degnan JH, Jakobsson M, Pemberton TJ, Hardy JA, et al. Comparing Spatial Maps of Human Population-Genetic Variation Using Procrustes Analysis. Statistical Applications in Genetics and Molecular Biology [Internet]. 2010 Jan 27 [cited 2022 Apr 27];9(1). Available from: https://www.degruyter.com/document/doi/10.2202/1544-6115.1493/html

66. Foll M, Shim H, Jensen JD. WFABC: a Wright-Fisher ABC-based approach for inferring effective population sizes and selection coefficients from time-sampled data. Mol Ecol Resour [Internet]. 2015 Jan [cited 2022 Nov 30];15(1):87–98. Available from: https://onlinelibrary.wiley.com/doi/10.1111/1755-0998.12280

67. Ni X, Yuan K, Liu C, Feng Q, Tian L, Ma Z, et al. MultiWaver 2.0: modeling discrete and continuous gene flow to reconstruct complex population admixtures. Eur J Hum Genet [Internet]. 2019 Jan [cited 2022 Nov 30];27(1):133–9. Available from: http://www.nature.com/articles/s41431-018-0259-3

68. Tavaré S, Balding DJ, Griffiths RC, Donnelly P. Inferring coalescence times from DNA sequence data. Genetics. 1997 Feb;145(2):505–18.

69. Beaumont MA, Zhang W, Balding DJ. Approximate Bayesian computation in population genetics. Genetics. 2002 Dec;162(4):2025–35.

70. Sisson SA, Fan Y, Beaumont MA, editors. Handbook of Approximate Bayesian Computation [Internet]. 1st ed. Boca Raton, Florida : CRC Press, [2019]: Chapman and Hall/CRC; 2018 [cited 2022 Nov 30]. Available from: https://www.taylorfrancis.com/books/9781439881514

71. Pudlo P, Marin JM, Estoup A, Cornuet JM, Gautier M, Robert CP. Reliable ABC model choice via random forests. Bioinformatics [Internet]. 2016 Mar 15 [cited 2021 Jun 4];32(6):859–66. Available from: https://academic.oup.com/bioinformatics/article/32/6/859/1744513

72. Csilléry K, François O, Blum MGB. abc: an R package for approximate Bayesian computation (ABC): *R package: abc*. Methods in Ecology and Evolution [Internet]. 2012 Jun [cited 2021 Jun 4];3(3):475–9. Available from: http://doi.wiley.com/10.1111/j.2041-210X.2011.00179.x

73. Verdu P, Rosenberg NA. A General Mechanistic Model for Admixture Histories of Hybrid Populations. Genetics [Internet]. 2011 Dec 1 [cited 2021 Jun 4];189(4):1413–26. Available from: https://academic.oup.com/genetics/article/189/4/1413/6089061

74. Nei M. Estimation of average heterozygosity and genetic distance from a small number of individuals. Genetics [Internet]. 1978 Jul 20 [cited 2022 Feb 2];89(3):583–90. Available from: https://academic.oup.com/genetics/article/89/3/583/5992737

75. Danecek P, Auton A, Abecasis G, Albers CA, Banks E, DePristo MA, et al. The variant call format and VCFtools. Bioinformatics [Internet]. 2011 Aug 1 [cited 2022 Feb 2];27(15):2156–8. Available from: https://academic.oup.com/bioinformatics/article-lookup/doi/10.1093/bioinformatics/btr330

76. Weir BS, Cockerham CC. Estimating F-statistics for the analysis of population-structure. Evolution [Internet]. 1984 Nov [cited 2022 Feb 2];38(6):1358–70. Available from: https://onlinelibrary.wiley.com/doi/10.1111/j.1558-5646.1984.tb05657.x

77. Robert CP, Mengersen K, Chen C. Model choice versus model criticism. Proceedings of the National Academy of Sciences [Internet]. 2010 Jan 19 [cited 2021 Jun 4];107(3):E5–E5. Available from: http://www.pnas.org/cgi/doi/10.1073/pnas.0911260107

78. Patterson KD. Epidemics, Famines, and Population in the Cape Verde Islands, 1580-1900. The International Journal of African Historical Studies [Internet]. 1988 [cited 2021 Jun 4];21(2):291. Available from: https://www.jstor.org/stable/219938?origin=crossref

79. Brooks GE. Cabo Verde: Gulag of the South Atlantic: Racism, Fishing Prohibitions, and Famines. Hist Afr. 2006;33:101–35.

80. Martin AR, Gignoux CR, Walters RK, Wojcik GL, Neale BM, Gravel S, et al. Human Demographic History Impacts Genetic Risk Prediction across Diverse Populations. The American Journal of Human Genetics [Internet]. 2017 Apr [cited 2022 Apr 8];100(4):635–49. Available from: https://linkinghub.elsevier.com/retrieve/pii/S0002929717301076

81. Busby GB, Band G, Si Le Q, Jallow M, Bougama E, Mangano VD, et al. Admixture into and within sub-Saharan Africa. eLife [Internet]. 2016 Jun 21 [cited 2022 Feb 2];5:e15266. Available from: https://elifesciences.org/articles/15266

82. Ramachandran S, Deshpande O, Roseman CC, Rosenberg NA, Feldman MW, Cavalli-Sforza LL. Support from the relationship of genetic and geographic distance in human populations for a serial founder effect originating in Africa. Proc Natl Acad Sci USA [Internet]. 2005 Nov [cited 2022 Nov 30];102(44):15942–7. Available from: https://pnas.org/doi/full/10.1073/pnas.0507611102

83. Bradburd GS, Ralph PL, Coop GM. A Spatial Framework for Understanding Population Structure and Admixture. Slatkin M, editor. PLoS Genet [Internet]. 2016 Jan 15 [cited 2022 Nov 30];12(1):e1005703. Available from: https://dx.plos.org/10.1371/journal.pgen.1005703

84. Gnecchi-Ruscone GA, Jeong C, De Fanti S, Sarno S, Trancucci M, Gentilini D, et al. The genomic landscape of Nepalese Tibeto-Burmans reveals new insights into the recent peopling of Southern Himalayas. Sci Rep [Internet]. 2017 Dec [cited 2022 Nov 30];7(1):15512. Available from: http://www.nature.com/articles/s41598-017-15862-z

85. Korunes KL, Soares-Souza GB, Bobrek K, Tang H, Araújo II, Goldberg A, et al. Sex-biased admixture and assortative mating shape genetic variation and influence demographic inference in admixed Cabo Verdeans. Hernandez R, editor. G3 Genes|Genomes|Genetics [Internet]. 2022 Sep 30 [cited 2023 Jan 20];12(10):jkac183. Available from: https://academic.oup.com/g3journal/article/doi/10.1093/g3journal/jkac183/6647844

86. Zaitlen N, Huntsman S, Hu D, Spear M, Eng C, Oh SS, et al. The Effects of Migration and Assortative Mating on Admixture Linkage Disequilibrium. Genetics [Internet]. 2017 Jan 1

[cited 2021 Jun 4];205(1):375–83. Available from: https://academic.oup.com/genetics/article/205/1/375/6095598

87. Versluys TMM, Mas-Sandoval A, Flintham EO, Savolainen V. Why do we pick similar mates, or do we? Biol Lett [Internet]. 2021 Nov [cited 2022 Feb 2];17(11):20210463. Available from: https://royalsocietypublishing.org/doi/10.1098/rsbl.2021.0463

88. Fortes-Lima C, Bybjerg-Grauholm J, Marin-Padrón LC, Gomez-Cabezas EJ, Bækvad-Hansen M, Hansen CS, et al. Exploring Cuba's population structure and demographic history using genome-wide data. Sci Rep [Internet]. 2018 Dec [cited 2021 Jun 4];8(1):11422. Available from: http://www.nature.com/articles/s41598-018-29851-3

89. Chaudenson R, Mufwene SS. Creolization of language and culture. London ; New York: Routledge; 2001. 340 p.

90. Cooper F, Holt TC, Scott RJ. Beyond slavery: explorations of race, labor, and citizenship in postemancipation societies. Chapel Hill: University of North Carolina Press; 2000. 198 p.

91. Conrad R. The Contraband Slave Trade to Brazil, 1831-1845. Hispanic American Historical Review [Internet]. 1969 Nov 1 [cited 2023 Feb 7];49(4):617–38. Available from: https://read.dukeupress.edu/hahr/article/49/4/617/157301/The-Contraband-Slave-Trade-to-Brazil-18311845

92. Goldberg A, Verdu P, Rosenberg NA. Autosomal Admixture Levels Are Informative About Sex Bias in Admixed Populations. Genetics [Internet]. 2014 Nov 1 [cited 2021 Jun 4];198(3):1209–29. Available from: https://academic.oup.com/genetics/article/198/3/1209/6065659

93. The 1000 Genomes Project Consortium. A global reference for human genetic variation. Nature. 2015 Oct 1;526(7571):68–74.

94. Gurdasani D, Carstensen T, Tekola-Ayele F, Pagani L, Tachmazidou I, Hatzikotoulas K, et al. The African Genome Variation Project shapes medical genetics in Africa. Nature [Internet]. 2015 Jan 15 [cited 2021 Jun 4];517(7534):327–32. Available from: http://www.nature.com/articles/nature13997

95. Malaria Genomic Epidemiology Network, Band G, Le QS, Clarke GM, Kivinen K, Hubbart C, et al. Insights into malaria susceptibility using genome-wide data on 17,000 individuals from Africa, Asia and Oceania. Nat Commun [Internet]. 2019 Dec 16 [cited 2023 Jan 20];10(1):5732. Available from: https://www.nature.com/articles/s41467-019-13480-z

96. Perry GH, Foll M, Grenier JC, Patin E, Nédélec Y, Pacis A, et al. Adaptive, convergent origins of the pygmy phenotype in African rainforest hunter-gatherers. Proc Natl Acad Sci USA [Internet]. 2014 Sep 2 [cited 2023 Jan 20];111(35). Available from: https://pnas.org/doi/full/10.1073/pnas.1402875111

97. Manichaikul A, Mychaleckyj JC, Rich SS, Daly K, Sale M, Chen WM. Robust relationship inference in genome-wide association studies. Bioinformatics [Internet]. 2010 Nov 15 [cited 2021 Jun 4];26(22):2867–73. Available from: https://academic.oup.com/bioinformatics/article-lookup/doi/10.1093/bioinformatics/btq559

98. Chafe WL, editor. The Pear stories: cognitive, cultural, and linguistic aspects of narrative

production. Norwood, N.J: Ablex Pub. Corp; 1980. 327 p. (Advances in discourse processes).

99. Croft W. Linguistic Selection: An Utterance-based Evolutionary Theory of Language Change. Nordic Journal of Linguistic [Internet]. 1996 Dec [cited 2021 Jun 4];19(2):99–139. Available from: https://www.cambridge.org/core/product/identifier/S0332586500003358/type/journal_article

100. R Development Core Team. R: A language and environment for statistical computing. [Internet]. R Foundation for Statistical Computing; 2020. Available from: http://www.R-project.org

101. Paschou P, Ziv E, Burchard EG, Choudhry S, Rodriguez-Cintron W, Mahoney MW, et al. PCA-Correlated SNPs for Structure Identification in Worldwide Human Populations. Allison DB, editor. PLoS Genet [Internet]. 2007 Sep 21 [cited 2023 Jan 20];3(9):e160. Available from: https://dx.plos.org/10.1371/journal.pgen.0030160

102. Purcell S, Neale B, Todd-Brown K, Thomas L, Ferreira MAR, Bender D, et al. PLINK: A Tool Set for Whole-Genome Association and Population-Based Linkage Analyses. The American Journal of Human Genetics [Internet]. 2007 Sep [cited 2021 Jun 4];81(3):559–75. Available from: https://linkinghub.elsevier.com/retrieve/pii/S0002929707613524

103. Jakobsson M, Rosenberg NA. CLUMPP: a cluster matching and permutation program for dealing with label switching and multimodality in analysis of population structure. Bioinformatics [Internet]. 2007 Jul 15 [cited 2021 Jun 4];23(14):1801–6. Available from: https://academic.oup.com/bioinformatics/article-lookup/doi/10.1093/bioinformatics/btm233

104. Rosenberg NA. DISTRUCT: a program for the graphical display of population structure. Molecular Ecology Notes [Internet]. 2003 Dec 10 [cited 2021 Jun 4];4(1):137–8. Available from: http://doi.wiley.com/10.1046/j.1471-8286.2003.00566.x

105. Morrison ML, Alcala N, Rosenberg NA. FSTruct: an FST-based tool for measuring ancestry variation in inference of population structure [Internet]. Evolutionary Biology; 2021 Sep [cited 2022 Feb 2]. Available from: http://biorxiv.org/lookup/doi/10.1101/2021.09.24.461741

106. Maier R, Flegontov P, Flegontova O, Changmai P, Reich D. On the limits of fitting complex models of population history to genetic data [Internet]. Evolutionary Biology; 2022 May [cited 2022 Nov 30]. Available from: http://biorxiv.org/lookup/doi/10.1101/2022.05.08.491072

107. The International HapMap 3 Consortium. Integrating common and rare genetic variation in diverse human populations. Nature. 2010 Sep;467(7311):52–8.

108. Szpiech ZA, Blant A, Pemberton TJ. GARLIC: Genomic Autozygosity Regions Likelihood-based Inference and Classification. Berger B, editor. Bioinformatics [Internet]. 2017 Jul 1 [cited 2021 Jun 4];33(13):2059–62. Available from: https://academic.oup.com/bioinformatics/article/33/13/2059/3000374

109. Maples BK, Gravel S, Kenny EE, Bustamante CD. RFMix: A Discriminative Modeling Approach for Rapid and Robust Local-Ancestry Inference. The American Journal of Human Genetics [Internet]. 2013 Aug [cited 2022 Feb 2];93(2):278–88. Available from: https://linkinghub.elsevier.com/retrieve/pii/S0002929713002899

110. Snyder JP. Map projections--a working manual [Internet]. 1987 [cited 2022 Feb 2]. Available

from: https://purl.fdlp.gov/GPO/gpo93084

111. Fisher RA. Darwinian evolution of mutations. Eugen Rev. 1922 Apr;14(1):31–4.

112. Wright S. Evolution in Mendelian Populations. Genetics. 1931 Mar;16(2):97–159.

113. Buzbas EO, Verdu P. Inference on admixture fractions in a mechanistic model of recurrent admixture. Theoretical Population Biology [Internet]. 2018 Jul [cited 2022 Feb 2];122:149–57. Available from: https://linkinghub.elsevier.com/retrieve/pii/S0040580918300662

114. Pritchard JK, Seielstad MT, Perez-Lezaun A, Feldman MW. Population growth of human Y chromosomes: a study of Y chromosome microsatellites. Molecular Biology and Evolution [Internet]. 1999 Dec 1 [cited 2023 Jan 20];16(12):1791–8. Available from: https://academic.oup.com/mbe/article-lookup/doi/10.1093/oxfordjournals.molbev.a026091

115. Raynal L, Marin JM, Pudlo P, Ribatet M, Robert CP, Estoup A. ABC random forests for Bayesian parameter inference. Stegle O, editor. Bioinformatics [Internet]. 2019 May 15 [cited 2022 Feb 2];35(10):1720–8. Available from: https://academic.oup.com/bioinformatics/article/35/10/1720/5132692

116. Jay F, Boitard S, Austerlitz F. An ABC Method for Whole-Genome Sequence Data: Inferring Paleolithic and Neolithic Human Expansions. Hernandez R, editor. Molecular Biology and Evolution [Internet]. 2019 Jul 1 [cited 2022 Feb 2];36(7):1565–79. Available from: https://academic.oup.com/mbe/article/36/7/1565/5345566

117. Pereira L, Černý V, Cerezo M, Silva NM, Hájek M, Vašíková A, et al. Linking the sub-Saharan and West Eurasian gene pools: maternal and paternal heritage of the Tuareg nomads from the African Sahel. Eur J Hum Genet. 2010 Aug;18(8):915–23.

118. Henn BM, Botigué LR, Gravel S, Wang W, Brisbin A, Byrnes JK, et al. Genomic Ancestry of North Africans Supports Back-to-Africa Migrations. Schierup MH, editor. PLoS Genet [Internet]. 2012 Jan 12 [cited 2022 Feb 2];8(1):e1002397. Available from: https://dx.plos.org/10.1371/journal.pgen.1002397

119. Hakluyt R. The Principal Navigations Voyages Traffiques and Discoveries of the English Nation [Internet]. 1st ed. Cambridge University Press; 2014 [cited 2023 Feb 7]. Available from: https://www.cambridge.org/core/product/identifier/9781107286306/type/book

120. dos Reis Duarte, António, Carvalho Furtado, Amândio J., Gomes Furtado, Ana Angelina F. Cabo Verde, Statistical Yearbook 2015 [Internet]. Praia, Santiago, Cabo Verde: Instituto Nacional de Estatística, Cabo Verde; 2015 p. 227. Available from: https://ine.cv/wp-content/uploads/2017/02/statistical-yearbook-cv-2015_en.pdf

APPENDIX 1

1.a. Quality Control and genomic datasets merging procedures

Appendix 1-figure 1:

Quality-control and datasets merging procedures.

Quality controls at the genotyping call level (Stage 1) were conducted with Illumina's GenomeStudio® software Genotyping Module. Cabo Verde original DNA samples have been collected during six separate field-trips between 2010 and 2018, genotyped in four batches using four different versions of the Illumina Omni2.5Million Beadchip genotyping array. The resulting dataset was merged with 2,504 worldwide samples from the 1000 Genomes Project Phase 3 (1000 Genomes Project Consortium, 2015); with 1,307 continental African samples from the African Genome Variation Project (EGA accession number EGAD00001000959, (94)); and with 1,235 African samples from (7) (EGA accession number EGAS00001002078). We retained only autosomal SNPs common to all datasets, and excluded one individual for each pair of individuals related at the 2nd degree (at least one grand-parent in common) as inferred with KING (97), following previous procedures (23).

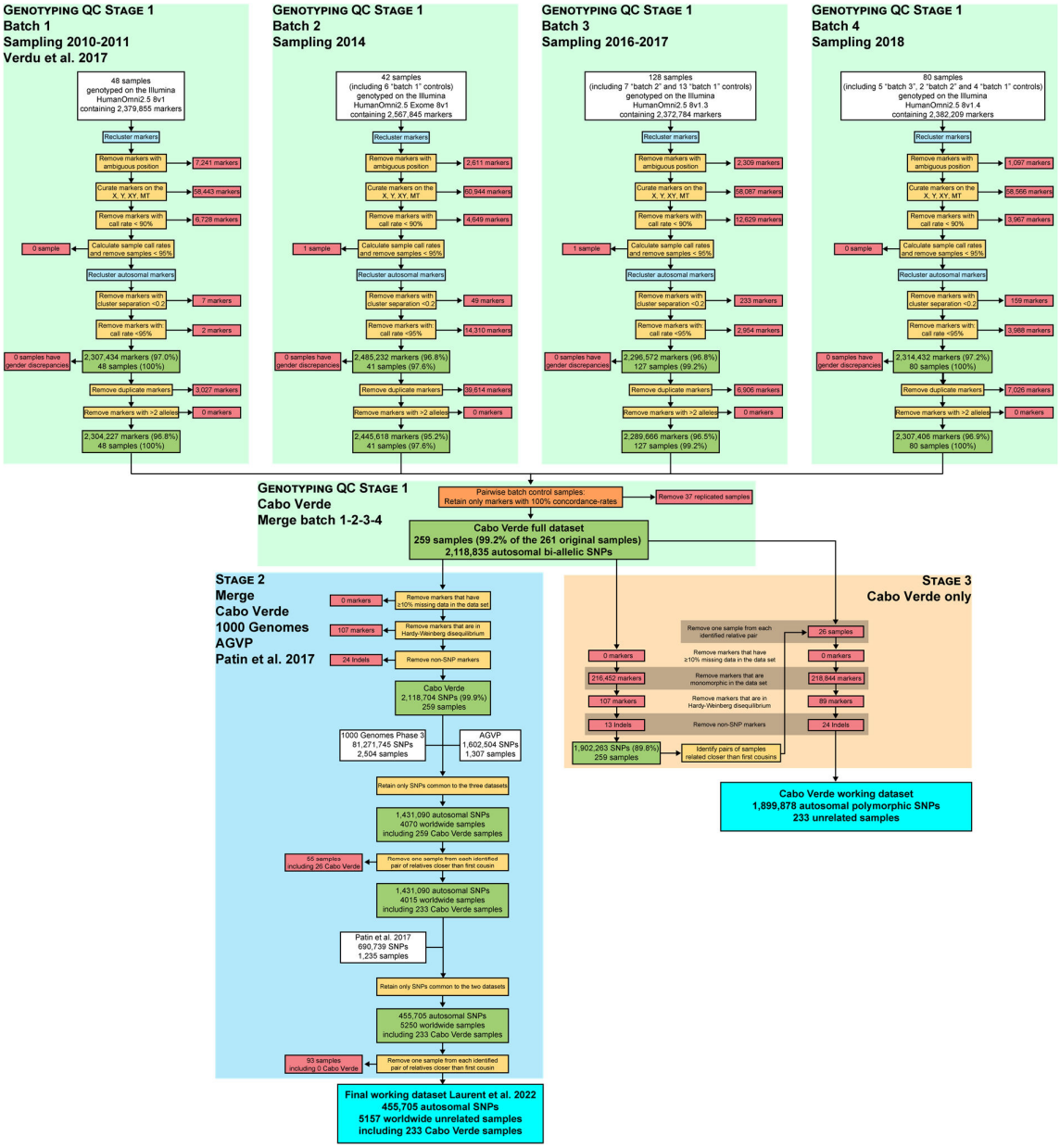

1.b. Summary statistics for ABC inference

We used *MetHis* (45) summary statistics calculation tools to calculate, for each simulated dataset, a vector of 42 summary statistics listed with references in main-text **Table 3**. We computed the same 42 summary-statistics using the real data set for each Cabo Verdean island of birth and for all Cabo Verde-born individuals grouped in a single population, respectively. Henceforth, Population H refers to the admixed population simulated with *MetHis* corresponding, in turn, to each Cabo Verdean island of birth and the 225 Cabo Verde-born individuals grouped in a single population.

Within-population summary statistics

We computed the mean and variance of interindividual ASD (46) within Population H. Furthermore, we computed the mean and variance of average heterozygosities (where the average is taken over independent SNPs for each individual and then over individuals within an island) as in (74). We also calculated the mean and variance of inbreeding coefficient F (75). Intuitively, we *a priori* expected these statistics to be particularly sensitive to genetic-drift and possibly informative specifically about reproductive population size N_e parameters in our scenarios.

Admixture patterns summary statistics

We analytically showed previously that the distribution of admixture fractions across individuals within admixed populations carried identifiable information about the history of admixture (73,113). Furthermore, we showed with *MetHis* (45) that summary statistics describing this distribution could be successfully used in ABC inferences.

Therefore, we considered the 16 admixture-related summary statistics describing the mode, the first four moments (as mean, variance, skewness, and kurtosis), and the minimum, maximum, and all deciles of the ASD-MDS admixture estimates of individual admixture fractions from the African source population (or one minus that from the European source in a two-source admixture scenario). ASD-MDS admixture estimates were obtained as described in **Material and Methods 2.,** represented schematically in **Appendix 1-figure 2**, considering the 2D-MDS centroids, respectively, of the African and European sources, and the projection on the line joining these two points of each Population H individual. Furthermore, to further capture the ASD-MDS admixture patterns, we calculated the distribution of the angles between population H's individuals and the source populations' centroids on the 2D ASD-MDS. We then considered as summary-statistics for ABC inference the mode, the first four moments (as mean, variance, skewness, and kurtosis), the minimum and maximum, and the deciles of this distribution of angles in radian (**Appendix 1-figure 2**).

Among-populations summary statistics

Using *MetHis* summary-statistic calculation tools, we computed F_{ST} values between either Source population (African or European) and Population H following (76). We also computed the mean ASD between the Source Population and Population H. Finally, we computed the f_3 statistic (50) with African and European populations as the two sources and Population H as the targeted admixed population.

2016 **Appendix 1-figure 2:**
2017 **Schematic representation of the ASD-MDS estimates of individual admixture proportions and angles, also used as sum-**
2018 **mary statistics for ABC inference and implemented in *MetHis* summary-statistic calculation tools.**
2019 All the panels of the figure are schematic.
2020
2021

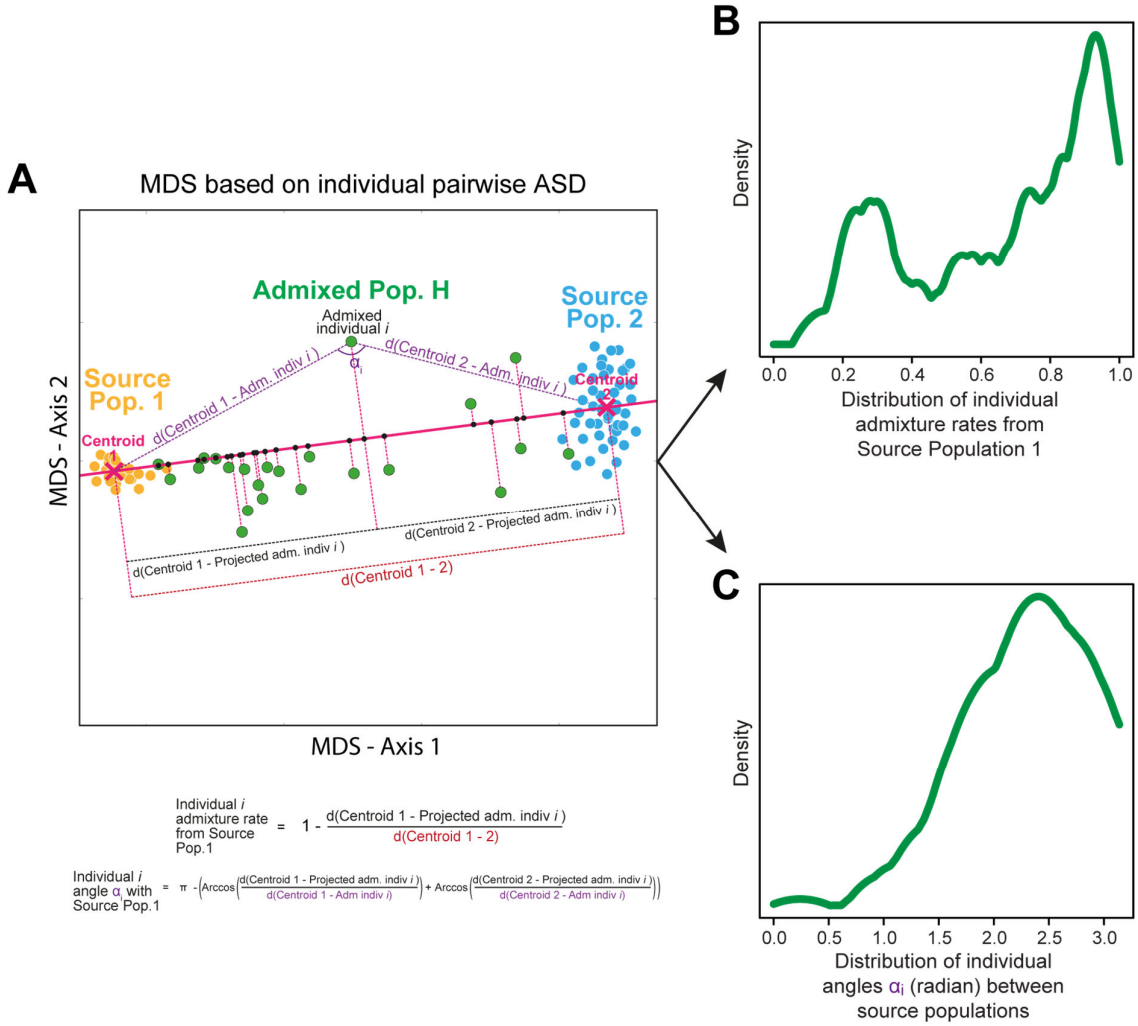

2022
2023

2024 **1.c. Prior-ABC checking**
2025
2026 Before conducting any ABC inference, we needed to statistically evaluate whether the 42 summary-
2027 statistics calculated on the observed datasets were within the range of the sets of summary statistics
2028 computed on the simulated datasets with *MetHis*. To do so, we considered each Cabo Verdean birth-
2029 island and Cabo Verde as a whole, in turn as population H, and conducted the following three-step
2030 procedure whose results are provided in **Appendix 1-figure 3**, **Appendix 1-figure3-figure supplement**
2031 **1-10**.
2032 (i) first, we conducted a goodness-of-fit test between the 40,000 vectors of summary statistics com-
2033 puted for each simulation under the four competing scenarios, and the vector of observed summary
2034 statistics with the *gfit* function of the R package *abc* (72), with 1000 random repetitions and a 1% toler-
2035 ance level (**Appendix 1-figure 3A**).
2036 (ii) second, we computed a Principal Component Analysis considering each simulation as an indi-
2037 vidual and all the summary statistics as observed variables. By projecting the observed summary statis-
2038 tics onto this PCA along the first three PCA axes of variation (with the *princomp* function in R), we
2039 visually evaluated whether the observed data fell into the range of simulated statistics along the major
2040 PCA axes (**Appendix 1-figure 3B**-**C**).
2041 (iii) finally, we present the distribution of each summary statistic obtained for the 40,000 simula-
2042 tions and the observed value, for each summary statistic and each Cabo Verdean birth-island and for
2043 Cabo Verde as a whole, separately (**Appendix 1-figure 3-figure supplement 1-10**).
2044

Appendix 1-figure 3:

ABC Prior-checking for *MetHis* simulations for each island separately.

10,000 simulations are conducted under each four competing scenarios of historical admixture considered in Random-Forest ABC scenario-choice (see **Figure 6**). **A) Goodness-of-Fit tests: w**e use as goodness-of-fit statistic the median of the distance between one target vector of 42 summary-statistics and the vectors of 42 statistics obtained for the 1% simulations in the 40,000 simulations reference table that are closest to the target (as identified by simple rejection (114)). Results obtained with the observed data as target are indicated in the vertical red line. Null-distribution of the goodness-of-fit statistics as histograms are obtained by considering as target in-turn 1000 random simulations as pseudo-observed data, for each island and for the 225 Cabo Verde-born individuals grouped in a single random-mating population, separately. **B)** First two axes of a principal component analysis performed on the 42 summary-statistics obtained for 40,000 simulations per island (10,000 simulations for each of four competing-scenarios). Each point corresponds to a single simulation colored per scenario: simulations under Scenario 1 are in blue; Scenario 2 in green; Scenario 3 in red; and Scenario 4 in yellow (**Figure 6-7**). The pink white-circled dot corresponds to the vector of summary-statistics from the observed dataset. **C)** Axes 1 and 3 of the same PCA projection as in panel **B**.

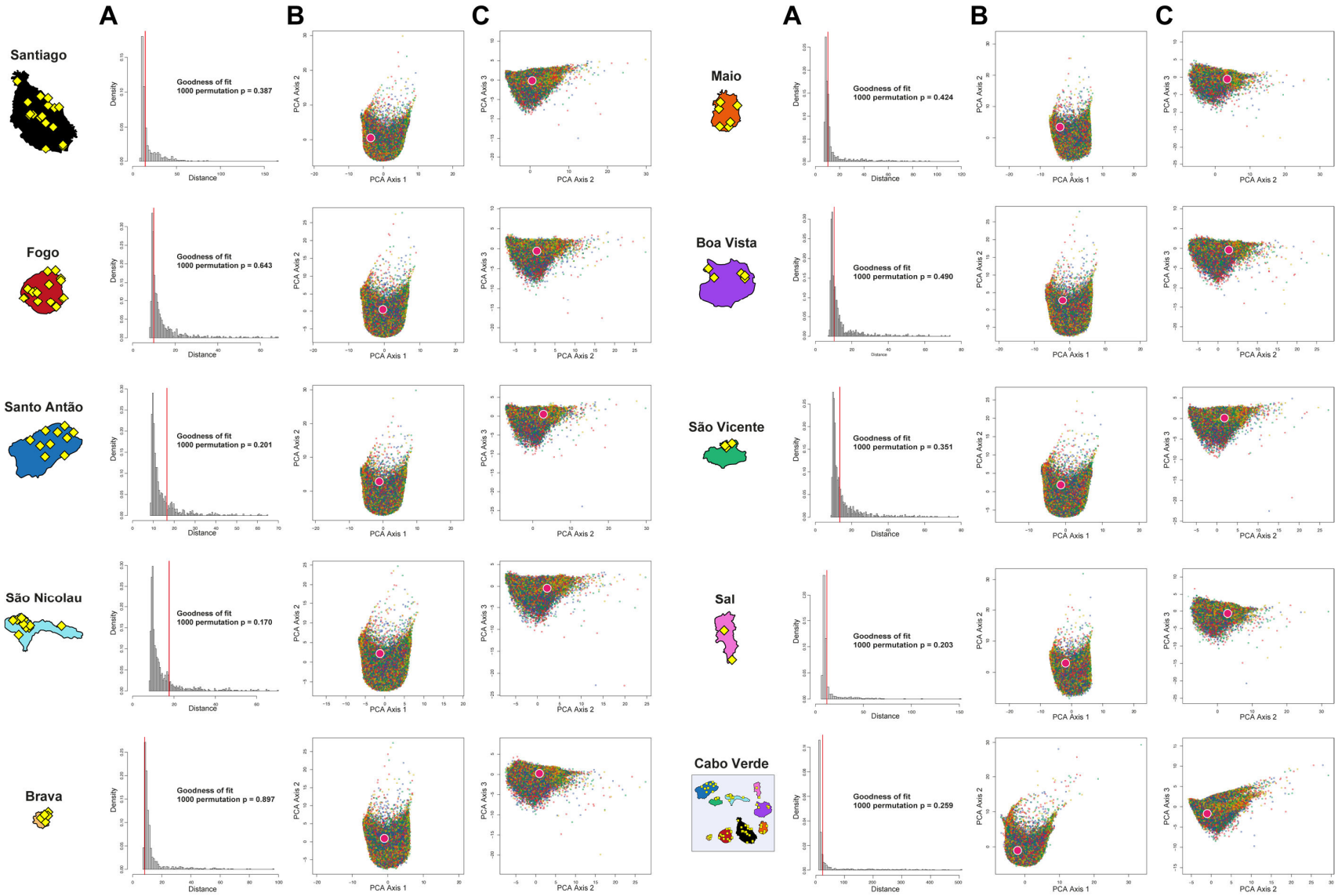
A
B
C
Santiago
Goodness of fit
1000 permutation p = 0.387
Fogo
Goodness of fit
1000 permutation p = 0.643
Santo Antão
Goodness of fit
1000 permutation p = 0.201
São Nicolau
Goodness of fit
1000 permutation p = 0.170
Brava
Goodness of fit
1000 permutation p = 0.897
Maio
Goodness of fit
1000 permutation p = 0.424
Boa Vista
Goodness of fit
1000 permutation p = 0.490
São Vicente
Goodness of fit
1000 permutation p = 0.351
Sal
Goodness of fit
1000 permutation p = 0.203
Cabo Verde
Goodness of fit
1000 permutation p = 0.259
Density
Distance
PCA Axis 1
PCA Axis 2
PCA Axis 3

2061

2062 **Appendix 1-figure 3-figure supplement 1:**
2063 **Density distributions (black line) of each of 42 summary-statistics obtained from 40,000 simulations, 10,000 under each of four**
2064 **competing scenarios for Santiago, compared to the observed statistic obtained in this island (red vertical line).**
2065 The four scenarios are synthetically described in **Figure 6** and the 42 summary-statistics in **Table 3**.
2066

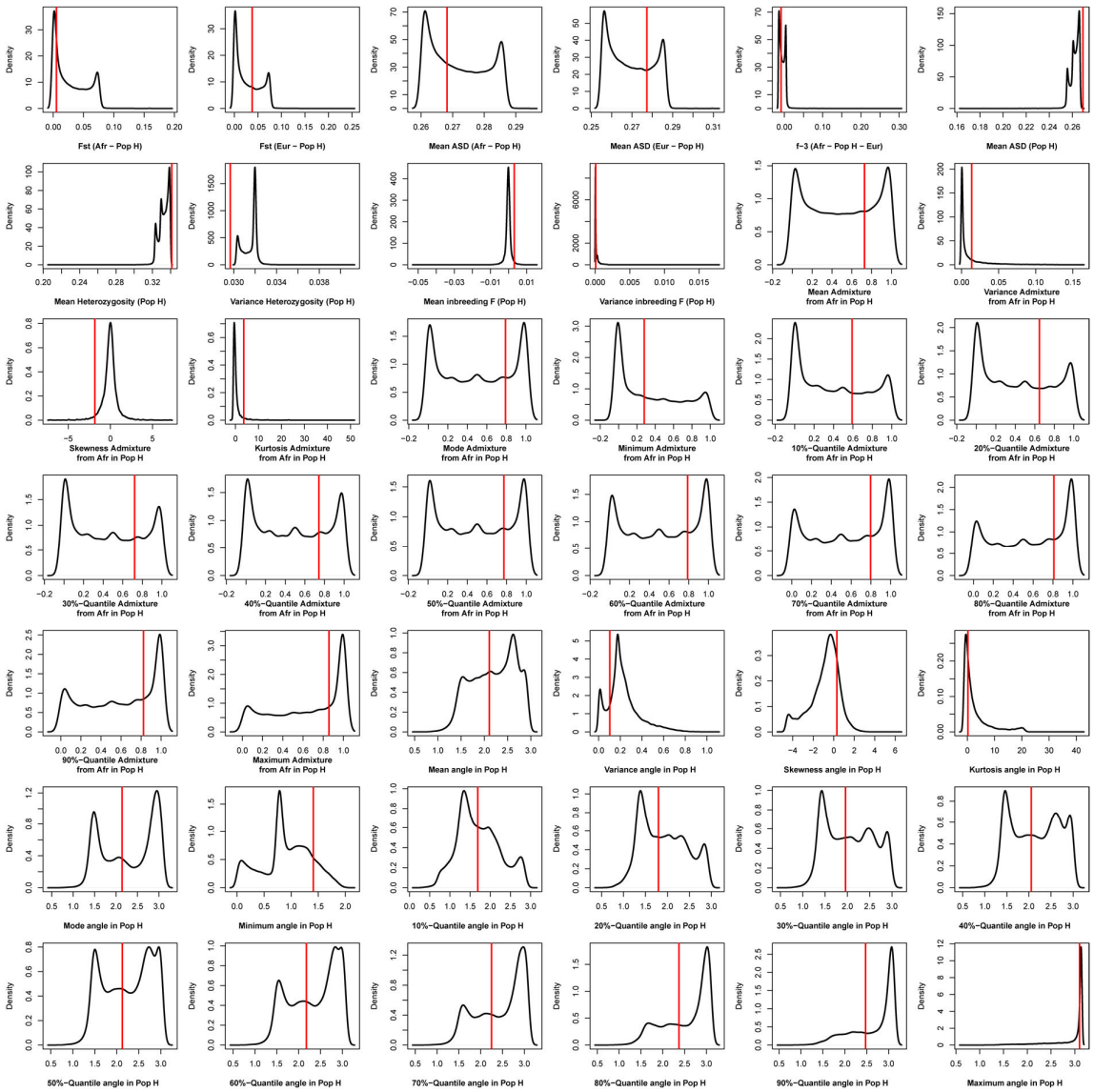

2067
2068
2069

2070 **Appendix 1-figure 3-figure supplement 2:**
2071 **Density distributions (black line) of each of 42 summary-statistics obtained from 40,000 simulations, 10,000 under each of four**
2072 **competing scenarios for Fogo, compared to the observed statistic obtained in this island (red vertical line).**
2073 The four scenarios are synthetically described in **Figure 6** and the 42 summary-statistics in **Table 3**.
2074

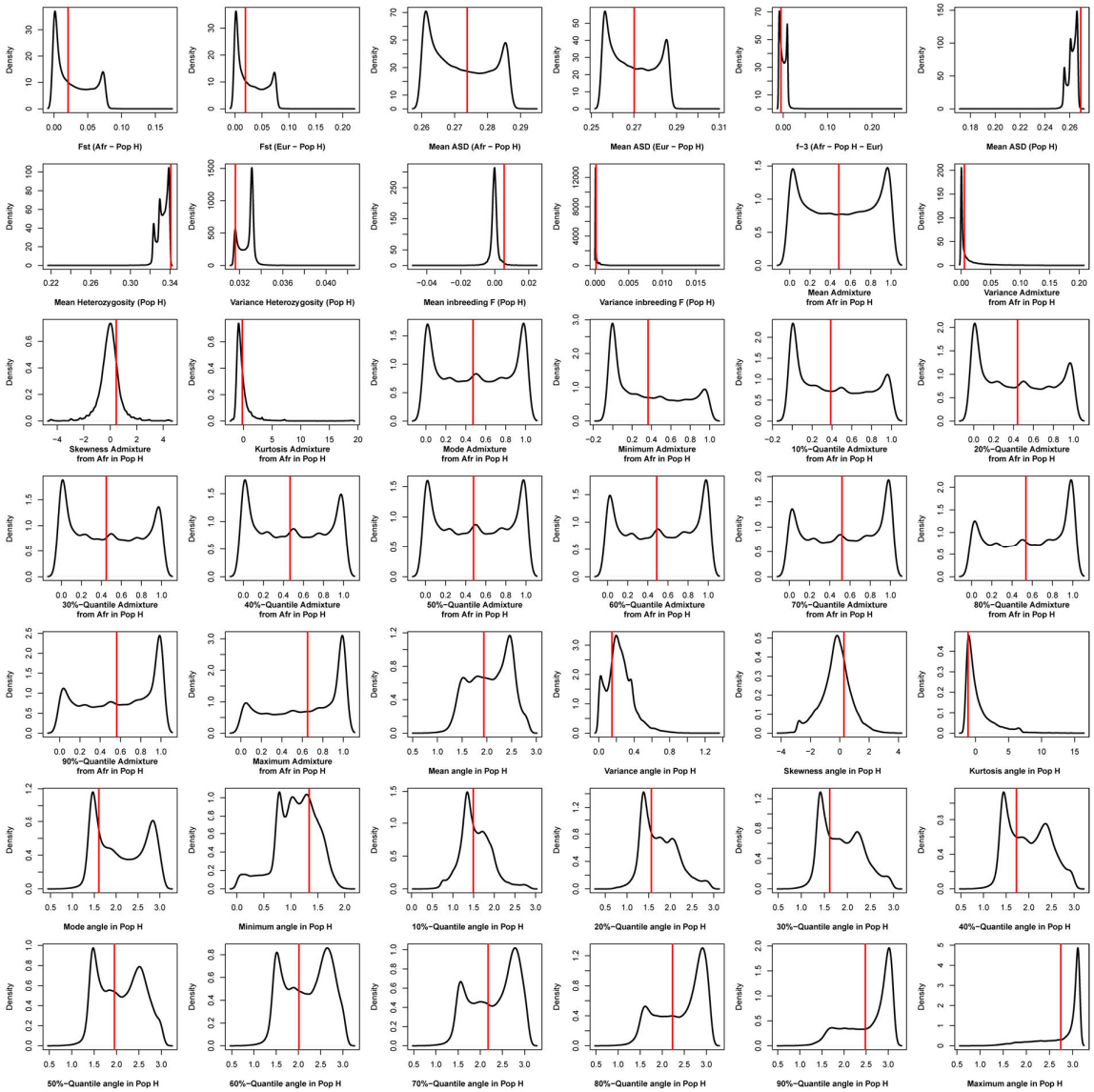

2075
2076
2077

2078 **Appendix 1-figure 3-figure supplement 3:**
2079 **Density distributions (black line) of each of 42 summary-statistics obtained from 40,000 simulations, 10,000 under each of four**
2080 **competing scenarios for Santo Antão, compared to the observed statistic obtained in this island (red vertical line).**
2081 The four scenarios are synthetically described in **Figure 6** and the 42 summary-statistics in **Table 3**.
2082

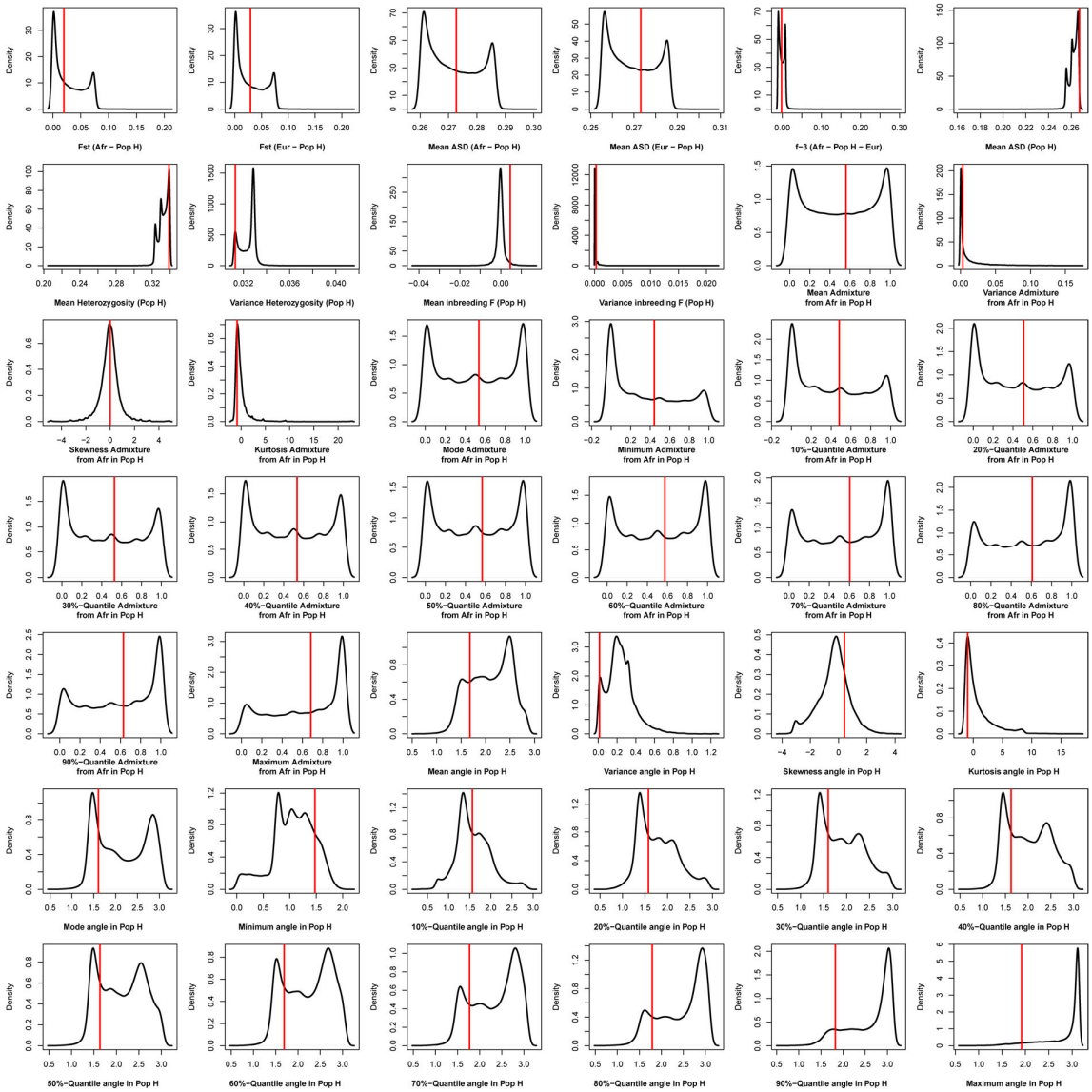

2083
2084
2085

2086 **Appendix 1-figure 3-figure supplement 4:**
2087 **Density distributions (black line) of each of 42 summary-statistics obtained from 40,000 simulations, 10,000 under each of four**
2088 **competing scenarios for São Nicolau, compared to the observed statistic obtained in this island (red vertical line).**
2089 The four scenarios are synthetically described in **Figure 6** and the 42 summary-statistics in **Table 3**.
2090

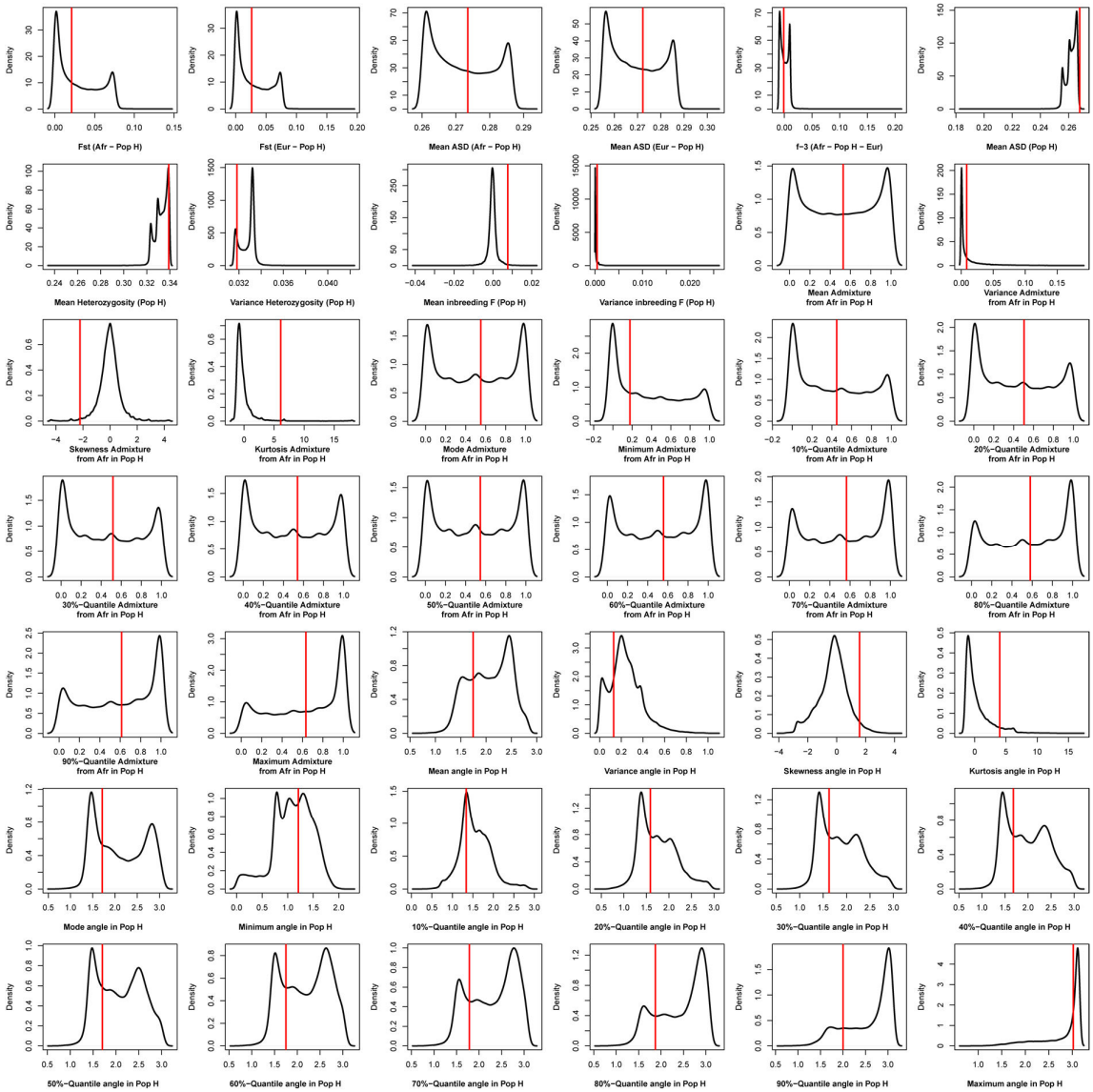

2091
2092

2093 **Appendix 1-figure 3-figure supplement 5:**
2094 **Density distributions (black line) of each of 42 summary-statistics obtained from 40,000 simulations, 10,000 under each of four**
2095 **competing scenarios for Brava, compared to the observed statistic obtained in this island (red vertical line).**
2096 The four scenarios are synthetically described in **Figure 6** and the 42 summary-statistics in **Table 3**.
2097

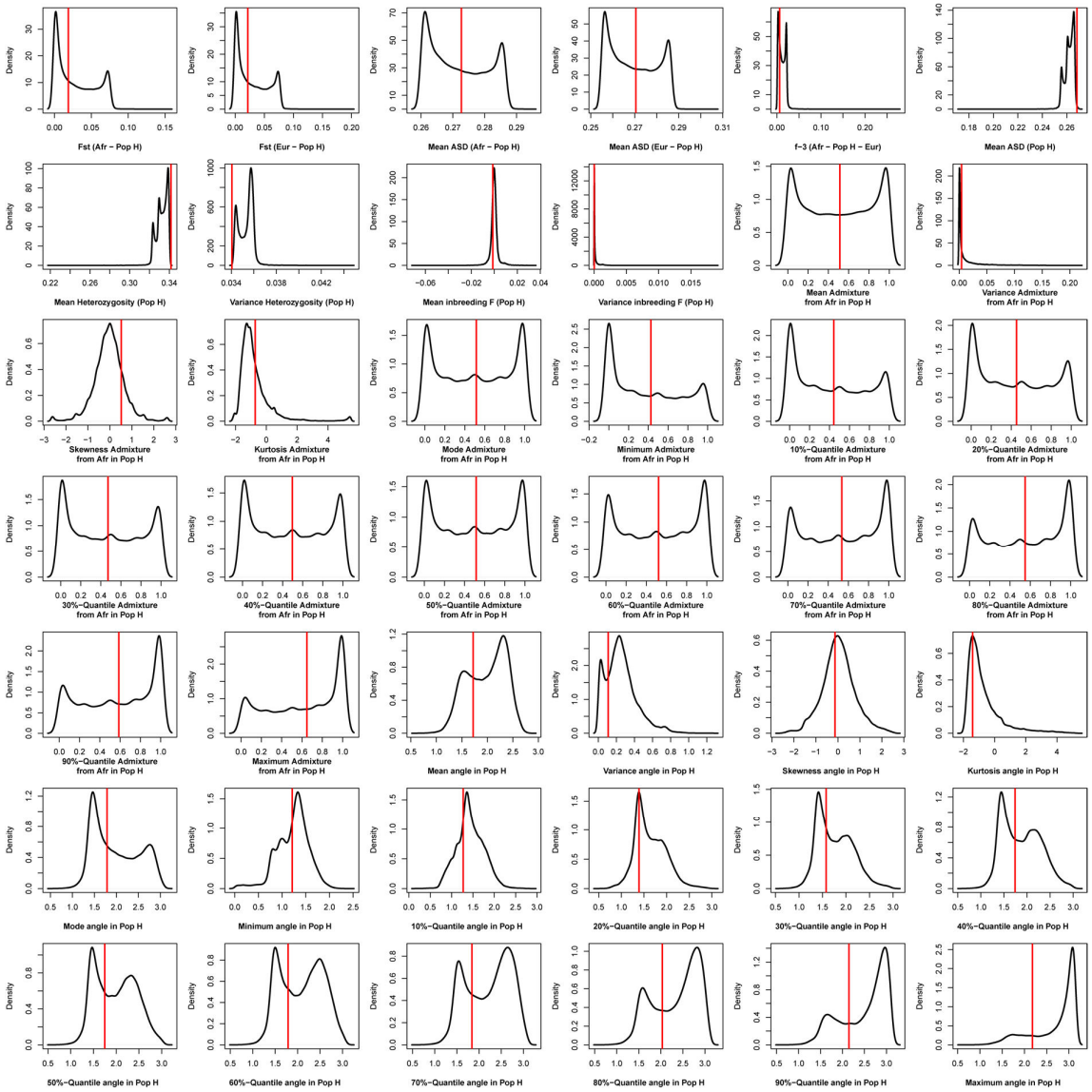

2098
2099
2100

2101 **Appendix 1-figure 3-figure supplement 6:**
2102 **Density distributions (black line) of each of 42 summary-statistics obtained from 40,000 simulations, 10,000 under each of four**
2103 **competing scenarios for Maio, compared to the observed statistic obtained in this island (red vertical line).**
2104 The four scenarios are synthetically described in **Figure 6** and the 42 summary-statistics in **Table 3**.
2105

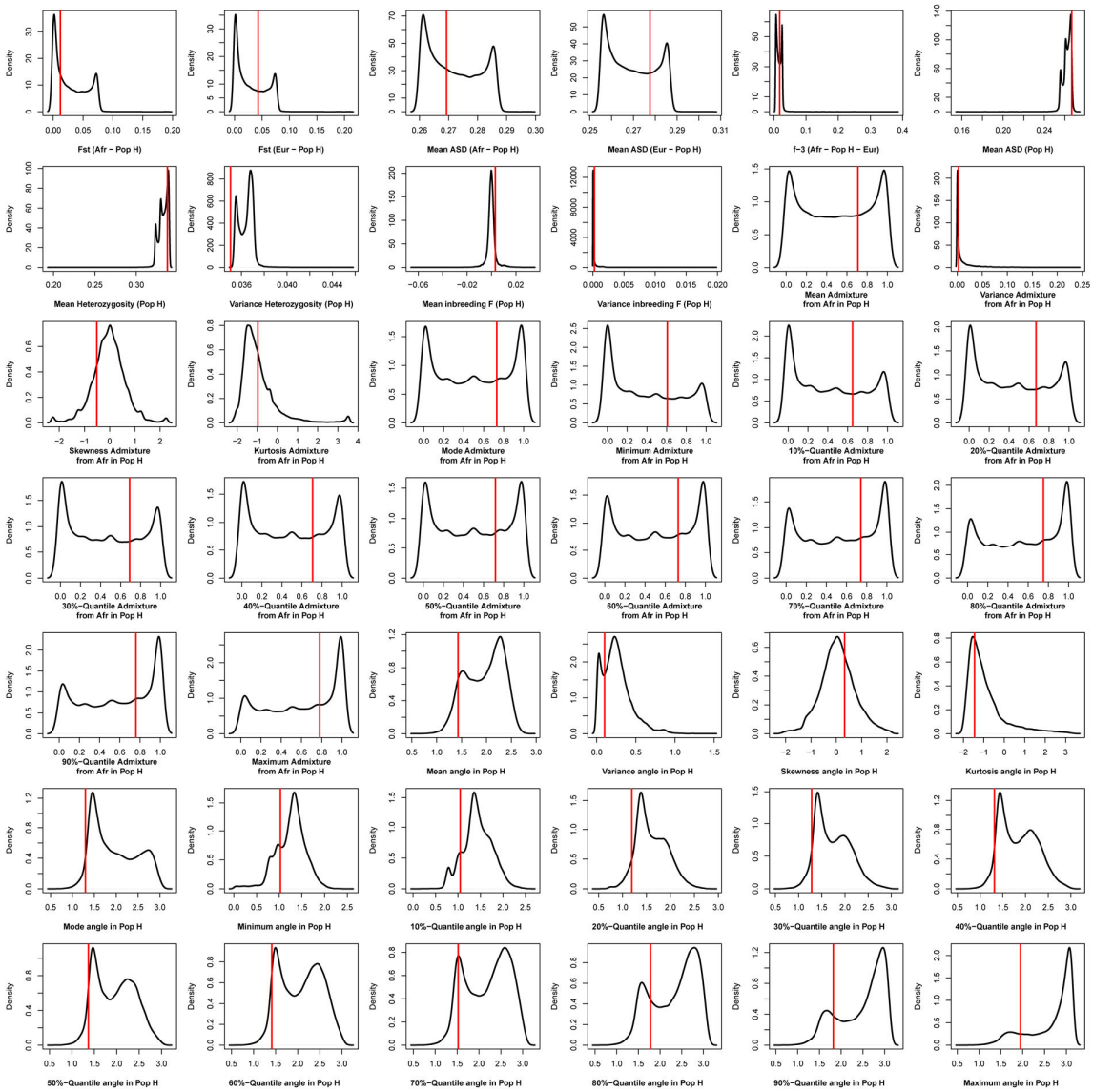

2106
2107

2108 **Appendix 1-figure 3-figure supplement 7:**
2109 **Density distributions (black line) of each of 42 summary-statistics obtained from 40,000 simulations, 10,000 under each of four**
2110 **competing scenarios for Boa Vista, compared to the observed statistic obtained in this island (red vertical line).**
2111 The four scenarios are synthetically described in **Figure 6** and the 42 summary-statistics in **Table 3**.
2112

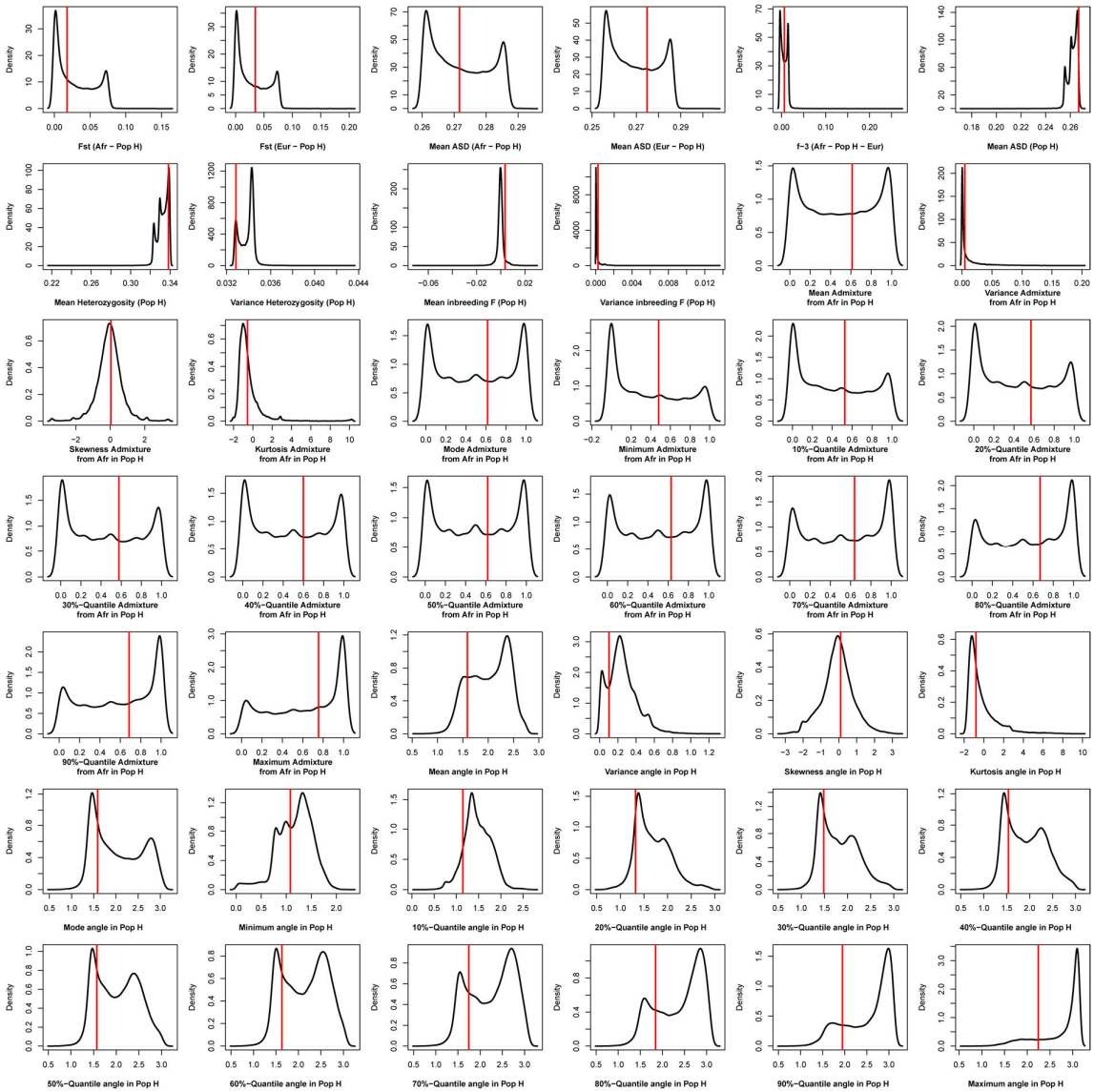

2113
2114

2115 **Appendix 1-figure 3-figure supplement 8:**
2116 **Density distributions (black line) of each of 42 summary-statistics obtained from 40,000 simulations, 10,000 under each of four**
2117 **competing scenarios for São Vicente, compared to the observed statistic obtained in this island (red vertical line).**
2118 The four scenarios are synthetically described in **Figure 6** and the 42 summary-statistics in **Table 3**.
2119

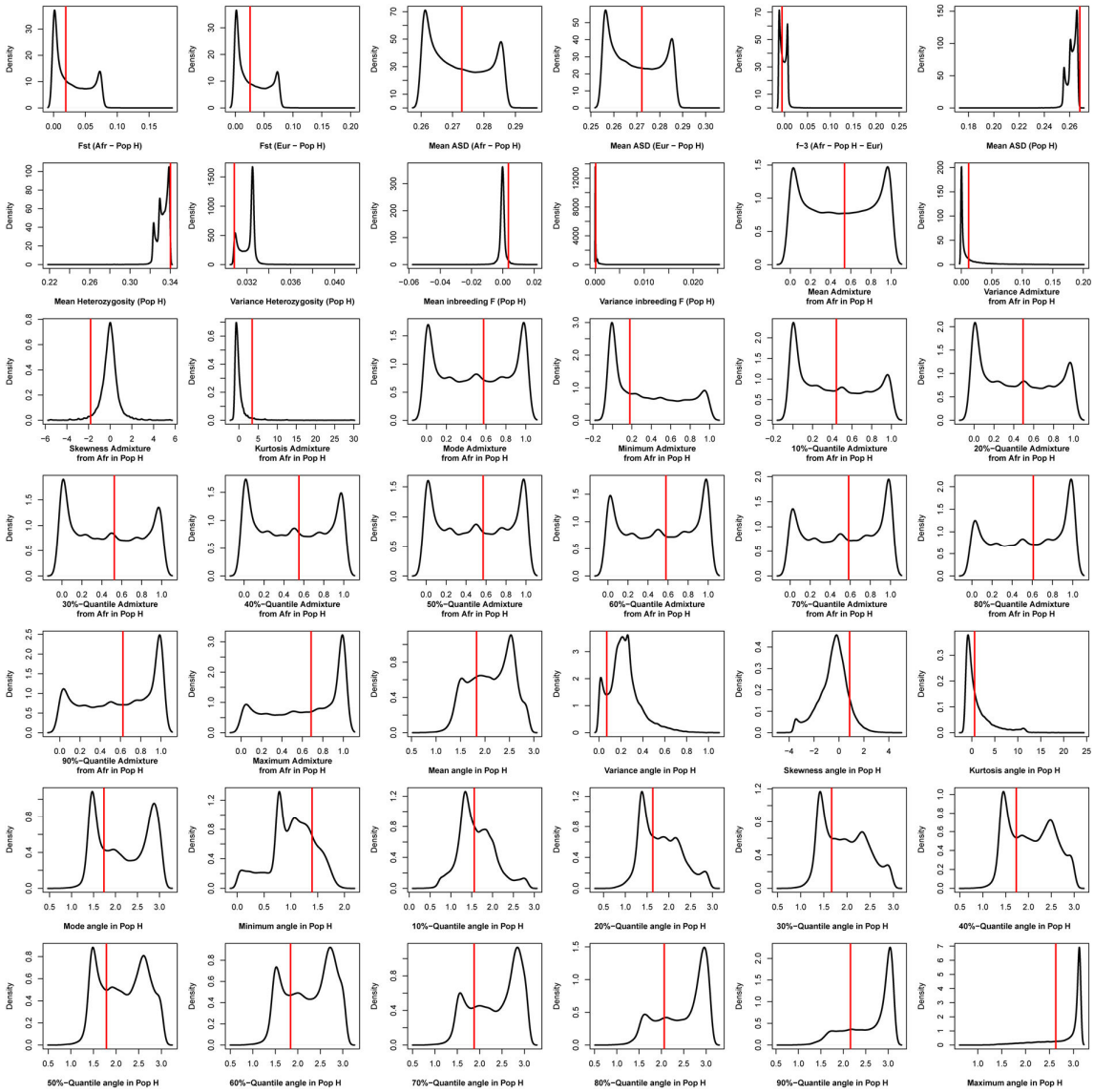

2120
2121

2122 **Appendix 1-figure 3-figure supplement 9:**
2123 **Density distributions (black line) of each of 42 summary-statistics obtained from 40,000 simulations, 10,000 under each of four**
2124 **competing scenarios for Sal, compared to the observed statistic obtained in this island (red vertical line).**
2125 The four scenarios are synthetically described in **Figure 6** and the 42 summary-statistics in **Table 3**.
2126

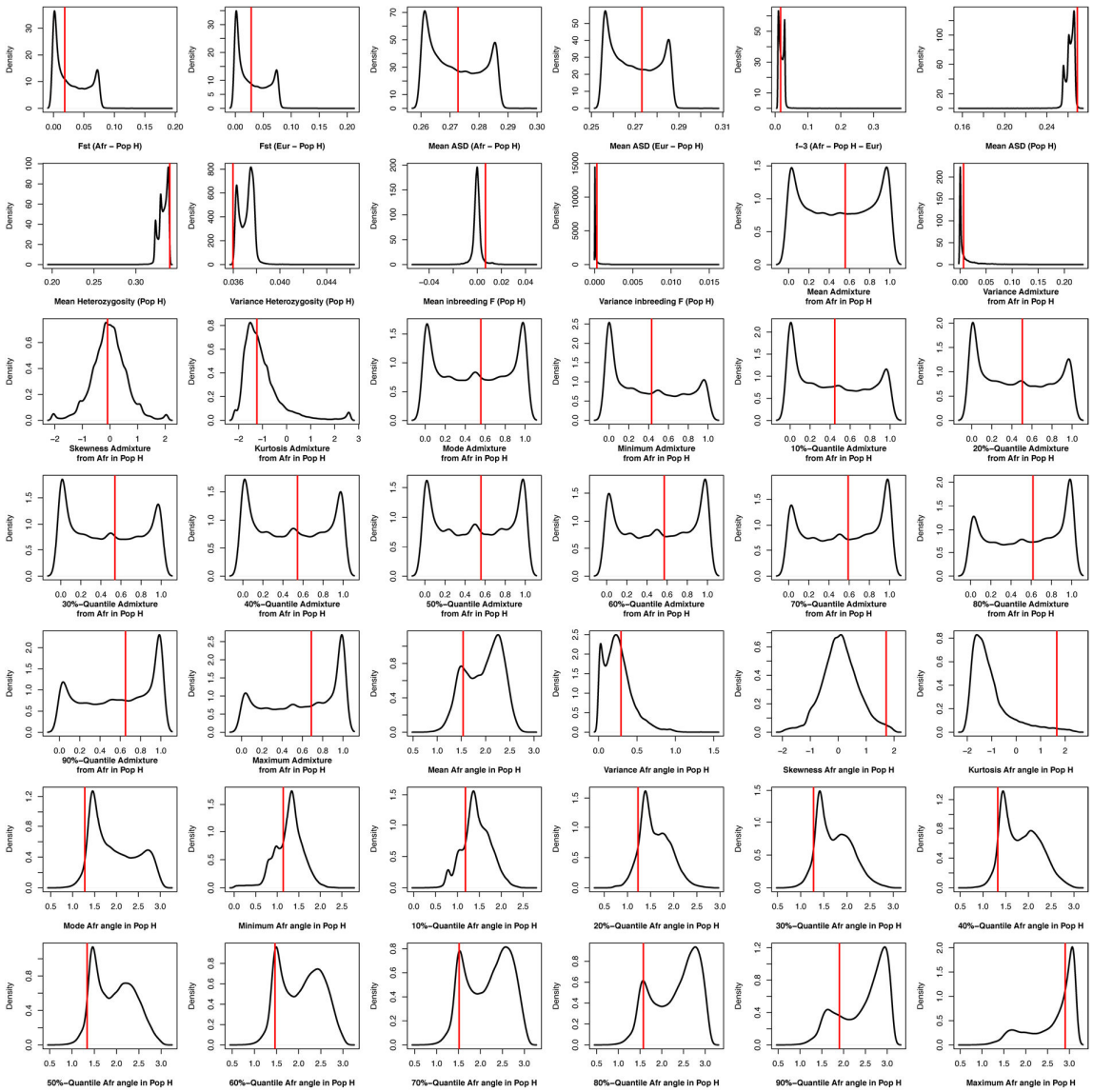

2127
2128

2129 **Appendix 1-figure 3-figure supplement 10:**
2130 **Density distributions (black line) of each of 42 summary-statistics obtained from 40,000 simulations, 10,000 under each of four**
2131 **competing scenarios for the 225 Cabo Verde-born individuals grouped in a single random-mating population, compared to the**
2132 **observed statistic obtained in this dataset (red vertical line).**
2133 The four scenarios are synthetically described in **Figure 6** and the 42 summary-statistics in **Table 3**.
2134

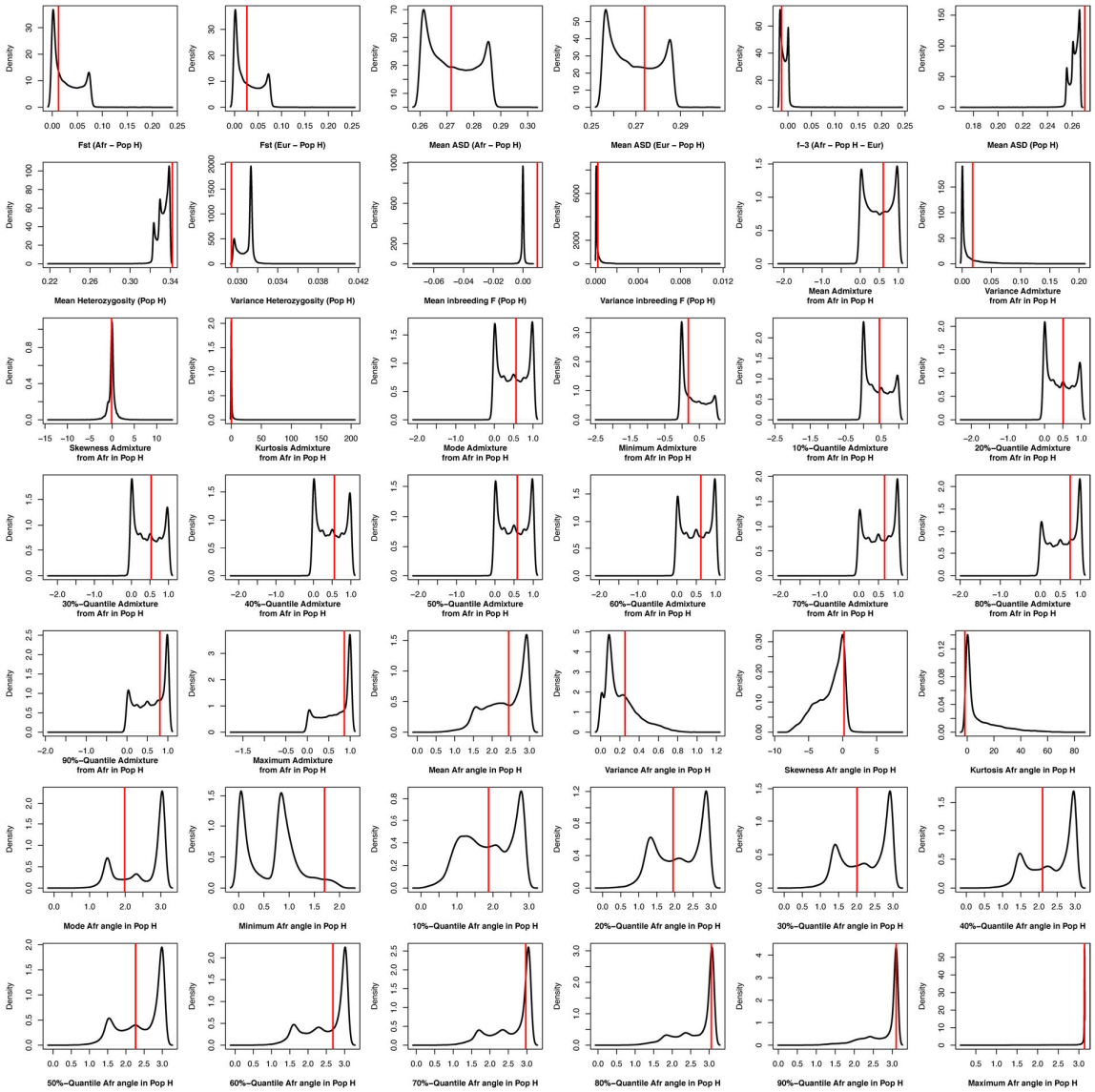

2135
2136

1.d. Random-Forest (RF) ABC scenario-choice cross-validation

We used the Random-Forest ABC algorithm implemented in the *abcrf* package in R (71,115) for scenario-choice, as in the *MetHis*-ABC pipeline previously described (45). Random-Forest classification has been shown to allow for robust ABC scenario-choice with relatively small numbers of simulations and, most importantly, to be unaffected by correlations among summary statistics; thus outperforming local linear regression classically used in ABC scenario-choice (69). Here, we considered the same prior probability (25%) for the four competing scenarios.

First, for each island separately, we used the *abcrf* function in this R package to conduct ABC scenario-choice cross-validation. Each of 40,000 simulations served in-turn as pseudo-observed data and the remaining 39,999 simulations as training (**Appendix 1-figure 4A**), using 1000 decision trees in the Random-Forest. We visually checked that prior error rates (the rates of erroneously assigned scenario in the cross-validation) were minimized for this number of decision trees, using the *err.abcrf* function in the same R package. Each summary-statistic's importance to the cross-validation accurate decision was calculated and plotted using the *abcrf* function (**Appendix 1-figure 4B**).

Second, for each birth-island and for Cabo Verde as a whole, separately, we used the *predict.abcrf* function on the trained Random Forest with all simulations in the reference table, to determine which competing scenario produced simulations whose summary statistics most resembled those from the observed data. We then estimate the posterior probability of accurately finding such winning scenario in our framework (indicated as "Post. prob. Scen." in **Figure 7B**).

Appendix 1-figure 4:

Random-Forest ABC scenario-choice cross validation results and summary-statistics' importance.

We considered four competing scenarios as described in **Material and Methods 7** and in **Figure 6**, with associated prior parameter distributions in **Table 2** and 42 summary-statistics described in **Table 3**, for each Cabo Verdean birth-island and the 225 Cabo Verde-born individuals grouped in a single random mating population, separately. Cross-validation results are obtained by conducting RF scenario-choices using, in-turn, each 40,000 simulations (10,000 per competing scenario) as pseudo-observed data and the remaining 39,999 simulations as the reference table. We considered 1,000 trees in the random-forest for each analysis. Cross-validation results and associated summary-statistics' importance for the RF decisions are obtained from the function *abcrf* in the R package *abcrf*.

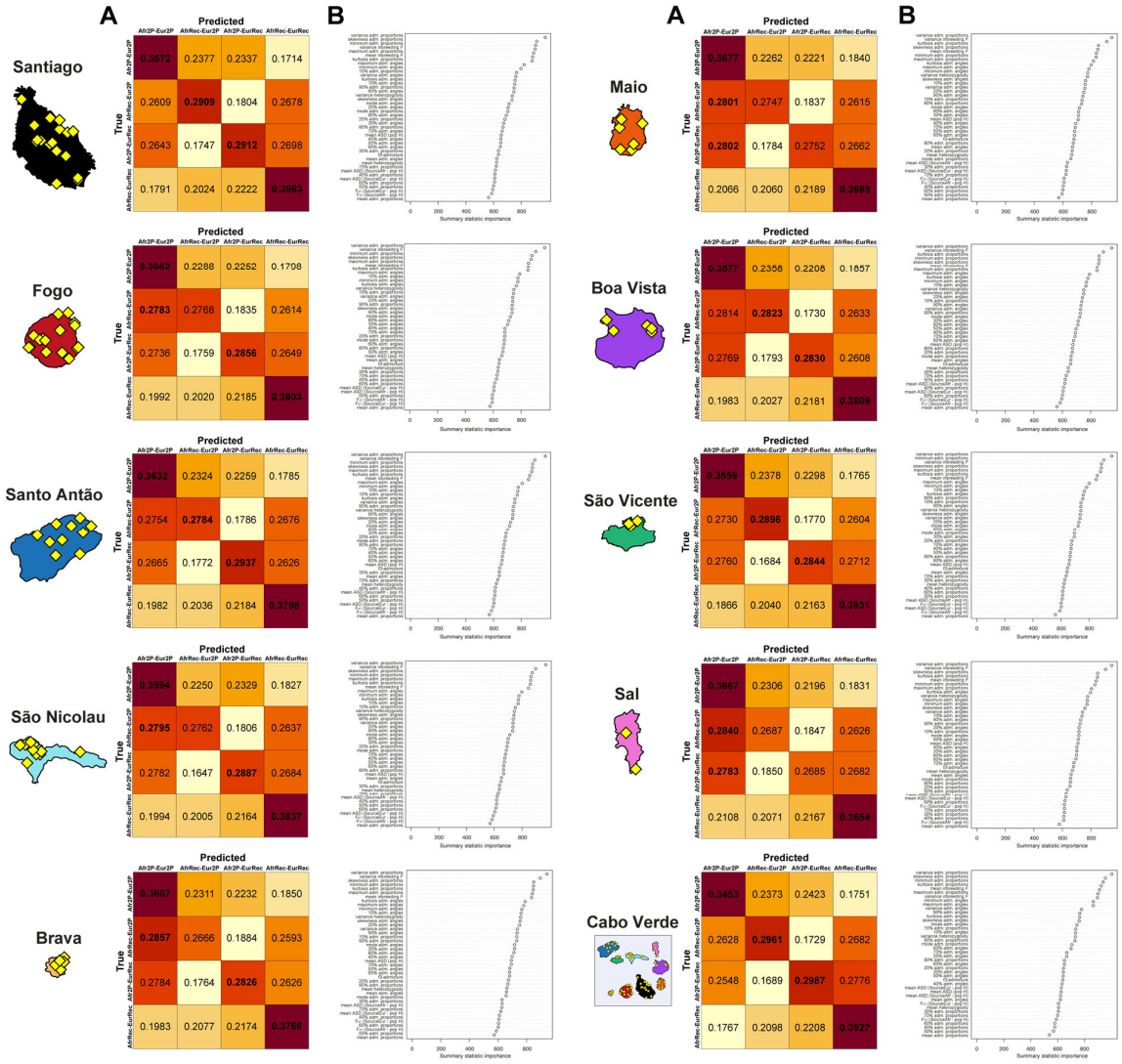

1.e. Neural Network ABC posterior parameter inference procedures

While RF-ABC scenario-choice procedures are specifically designed to accurately work with a relatively small number of simulations compared to classical regression ABC (69,71), posterior joint-estimations of all scenario-parameters under the winning scenario remain difficult in Random-Forest (45,115). In this context, our previous benchmarking of various ABC posterior-parameter estimation under the *MetHis* framework showed that Neural Network ABC joint parameter estimations outperformed other approaches (45). However, Neural Network ABC posterior parameter inferences have been shown in multiple previous investigations, including ours with *MetHis*, to require substantial amounts of information in the reference table to perform satisfactorily (45,72,116). Therefore, we conducted anew 90,000 simulations with *MetHis*, for each birth-island and for Cabo Verde as a whole, separately, under the winning scenario determined with RF-ABC, thus obtaining a total 100,000 simulations under the winning scenario, for each birth-island or for Cabo Verde as a whole, separately, for further Neural Network ABC posterior parameter estimation using the *abc* package in R (72).

NN-ABC parameter inference settings

We followed the same empirical approach as in *MetHis*-ABC (45) to determine the most suitable number of neurons in the hidden layer and associated number of simulations closest to the target data and retained for training the Neural Network (called "tolerance level") for further NN-ABC posterior parameter estimation for this target. Indeed, there is no rule-of-thumb to determine these parameters *a priori* in order to obtain the most informative posterior parameter inference while minimizing overfitting using a Neural-Network approach under a given scenario (72,116).

Therefore, we empirically tested three different tolerance-level values to be used in NN-ABC posterior parameter estimation: 1%, 5%, or 10% of the total 100,000 simulations generated under the winning scenario determined by our RF-ABC procedure for each Cabo Verdean island and for Cabo Verde as a whole, respectively. Furthermore, for each one of the three tolerance-level values, we tested associated numbers of neurons in the hidden layer between 5 and 11, or 12, the number of free parameters minus one in the winning scenario for each Cabo Verdean island and for Cabo Verde as a whole, respectively (**Figure 6-7**).

Then, for each pair of tolerance-level value and number of neurons for each targeted data separately, we performed 1,000 cross-validation NN-ABC posterior parameter inferences using the *cv4abc* function in the *abc* package (72). This procedure draws 1,000 simulations at random and considers them, in turn, as pseudo-observed data for posterior-parameter inference using the remaining 99,999 simulations as the reference table. For the 1,000 pseudo-observed cross-validations and each pair of tolerance level and number of hidden neurons, we calculated the error between the median posterior point-estimate of each parameter $(\hat{\theta}_i)$ and its' known true-value used for simulation (θ_i), as the mean-square error (MSE) scaled by the parameter's variance across the 1,000 cross-validations (72):

$$Scaled\ MSE\ (\hat{\theta}_i) = \sum_1^{1000}(\hat{\theta}_i - \theta_i)^2/(1000 \times Variance(\theta_i)).$$

Therefore, we conducted, in total, 219,000 NN-ABC cross-validation parameter inference procedures to identify the NN-ABC settings most suitable for further posterior parameter estimations using the observed data for each Cabo Verdean birth-island and for Cabo Verde as a whole. For each Cabo Verdean island and for Cabo Verde as a whole, separately under the corresponding winning scenario, we chose the pair of tolerance-level values and number of hidden neurons that minimized the average error across all estimated parameters, as the Neural-Network setting used in further ABC posterior parameter inferences based on the observed data (**Appendix 1-table 1**).

Appendix 1-table 1:

Average parameter posterior random cross-validation error across all model parameters as a function of the number of neurons in the hidden layer and the rejection tolerance level (number of simulations retained for training the Neural-Network) under the winning scenario for each island respectively.

For each island separately, and for the 225 Cabo Verde-born individuals grouped as a single "Cabo Verde" population, we considered, 1,000 random simulations in-turn as pseudo-observed data to estimate posterior parameter distributions and 100,000 total simulations in the reference table. For each cross-validation procedure, we considered between 5 and 11 neurons in the hidden layer ("NN-HL") for the winning scenarios with 12 original parameters, and between 5 and 12 NN-HL for the winning scenarios with 13 original parameters. We considered three different tolerance levels of 0.01, 0.03, and 0.1 ("Tol.") corresponding, respectively, to 1,000, 3,000, and 10,000 simulations, in turn closest to each one of the 1,000 cross-validation pseudo-observed simulation retained for training the NN. The median values of posterior parameter distributions were used as point estimates for the calculation of the error of each parameter (72).

For each birth-island and Cabo Verde as a whole, and corresponding winning scenario, separately, we considered, for further posterior parameter estimation using the observed "real" data, only the pair of tolerance level and number of hidden neurons that minimized the average error on posterior parameter estimations across all parameters (indicated in bold in the table).

	Individual birth-island	SANTIAGO	FOGO	SANTO ANTAO	SAO NICOLAU	BRAVA	MAIO	BOA VISTA	SAO VICENTE	SAL	CABO VERDE
	Winning scenario	Scenario 1: Afr2pulses-Eur2pulses	Scenario 1: Afr2pulses-Eur2pulses	Scenario 1: Afr2pulses-Eur2pulses	Scenario 1: Afr2pulses-Eur2pulses	Scenario 1: Afr2pulses-Eur2pulses	Scenario 1: Afr2pulses-Eur2pulses	Scenario 2: Afr2pulses-Eur-Reccurring	Scenario 3: Afr-Reccurring-Eur2pulses	Scenario 2: Afr2pulses-Eur-Reccurring	Scenario 1: Afr2pulses-Eur2pulses
Number of scenario parameters		12	12	12	12	12	12	13	13	13	12
NN-HL = 5	Tol. = 0.01	0.79264	0.79943	0.80170	0.79380	0.81251	0.83232	0.79972	0.77795	0.82888	**0.79532**
NN-HL = 5	Tol. = 0.03	0.80866	0.81252	0.81257	0.80711	0.81703	0.83470	0.79708	0.80208	0.81783	0.83438
NN-HL = 5	Tol. = 0.1	0.84002	0.84001	0.84662	0.84970	0.84526	0.85366	0.83374	0.82312	0.83264	0.85271
NN-HL = 6	Tol. = 0.01	**0.77139**	0.80186	0.79800	0.80765	0.81085	0.82516	0.78239	0.77743	0.81601	0.82118
NN-HL = 6	Tol. = 0.03	0.78501	0.81397	0.80533	0.80483	0.83318	0.83673	0.80492	0.80127	0.81325	0.82982
NN-HL = 6	Tol. = 0.1	0.84684	0.84072	0.84028	0.84484	0.85753	0.85428	0.82136	0.81617	0.83773	0.84745
NN-HL = 7	Tol. = 0.01	0.78525	0.79836	0.79075	0.81595	0.82657	0.82662	0.79304	0.77898	0.80415	0.80413
NN-HL = 7	Tol. = 0.03	0.80899	0.81151	0.81000	0.81035	0.83069	0.83474	0.80060	0.79491	0.81855	0.83622
NN-HL = 7	Tol. = 0.1	0.85600	0.84844	0.83704	0.84737	0.85071	0.85582	0.81083	0.81619	0.83779	0.85601
NN-HL = 8	Tol. = 0.01	0.78512	0.79805	0.79127	0.80886	0.82241	0.83397	**0.77998**	0.78077	0.80992	0.80783
NN-HL = 8	Tol. = 0.03	0.80595	0.81077	0.81353	0.82455	0.82334	0.83718	0.79490	0.79639	0.80666	0.83396
NN-HL = 8	Tol. = 0.1	0.83938	0.84904	0.83681	0.85231	0.84982	0.84614	0.83499	0.81671	0.82696	0.84774
NN-HL = 9	Tol. = 0.01	0.77910	0.79899	0.81027	0.80103	0.81898	0.82483	0.79744	0.78619	0.81770	0.80542
NN-HL = 9	Tol. = 0.03	0.81192	0.81046	0.81474	0.81642	0.82593	0.82631	0.80830	0.78640	0.82212	0.84165
NN-HL = 9	Tol. = 0.1	0.84379	0.84721	0.83676	0.84813	0.85218	0.85223	0.83254	0.81696	0.81723	0.85381
NN-HL = 10	Tol. = 0.01	0.78593	**0.79615**	0.80275	0.79444	**0.80692**	**0.82095**	0.80121	0.77644	0.81801	0.80485
NN-HL = 10	Tol. = 0.03	0.80159	0.80818	0.81143	0.80949	0.82496	0.82787	0.79994	0.78673	0.81565	0.82157
NN-HL = 10	Tol. = 0.1	0.85245	0.84242	0.84222	0.83444	0.85410	0.85424	0.83049	0.81742	0.84950	0.84183
NN-HL = 11	Tol. = 0.01	0.79994	0.81073	**0.78479**	**0.78709**	0.82527	0.84091	0.79414	**0.77365**	**0.79984**	0.80239
NN-HL = 11	Tol. = 0.03	0.82611	0.80802	0.80825	0.81653	0.82511	0.82334	0.80234	0.80333	0.81750	0.82959
NN-HL = 11	Tol. = 0.1	0.84914	0.83930	0.84011	0.84941	0.85471	0.85756	0.82120	0.81919	0.83044	0.85282
NN-HL = 12	Tol. = 0.01	na	na	na	na	na	na	0.79915	0.78138	0.81418	na
NN-HL = 12	Tol. = 0.03	na	na	na	na	na	na	0.79959	0.79306	0.81551	na
NN-HL = 12	Tol. = 0.1	na	na	na	na	na	na	0.81731	0.82090	0.82284	na

NN-ABC posterior parameter estimation

For each Cabo Verdean island and for all Cabo Verde-born individuals grouped in a single population, separately, under the winning scenario identified with RF-ABC, we jointly estimated the posterior distributions of all parameters using NN-ABC "*neuralnet*" method option in the function *abc* of the R package *abc* (72), with logit-transformed parameters ("*logit*" transformation option) using the tolerance level and number of neurons in the hidden layer identified previously in **Appendix 1-table 1**. For each birth-island and for Cabo Verde as a whole, separately, a synthetic schematic figure of the complex admixture processes identified using median point estimates of the posterior scenario-parameter distribution is provided in **Figure 7**, and full posterior parameter distributions with 95% Credibility-Intervals (CI) are provided in **Figure 7-figure supplement 1-3** and **Appendix 5-table 1-10**.

NN-ABC posterior parameter errors

We evaluated posterior parameter error rates and 95%-CI accuracies in the vicinity of the observed data, for each island and for Cabo Verde as a whole, separately, and for each corresponding NN-ABC posterior parameter joint estimation.

First, we identified the 1,000 simulations closest to the observed "real" data for each target data separately using a 1% tolerance level in the "*neuralnet*" option from the *abc* function. We then used each one of these 1,000 specific simulations, in turn, as pseudo-observed target data for cross-validation NN-ABC posterior parameter estimation using the same NN settings as previously, logit-transformed parameters, and the 99,999 remaining simulations in the reference table. We then compared the median posterior estimate of each scenario parameter $(\hat{\theta}_i)$, with the original parameter value used for the simulation (θ_i), respectively for each 1,000 cross-validation posterior parameter estimation; and calculated the cross-validation mean absolute error (MAE), for each scenario parameter (**Appendix 5-table 1-10**):

$$MAE(\hat{\theta}_i) = \sum_1^{1000} |\hat{\theta}_i - \theta_i| / 1000.$$

Second, for each island and for Cabo Verde as a whole, and for each scenario-parameter separately, we calculated how many times the true parameter values (θ_i), used for simulating the 1,000 simulations closest to the observed data, fell within the 95%-CI [2.5% quantile$(\hat{\theta}_i)$; 97.5% quantile$(\hat{\theta}_i)$] estimated using the observed data. Thus, if the 1,000 cross-validation true parameter values fell more than 95% of the time within the estimated 95%-CI, the length of the estimated 95%-CI was considered over-estimated and thus excessively conservative; and, alternatively, if it was the case less than 95% of the time, the length of the 95%-CI was considered under-estimated thus indicating a less conservative behavior of our CI estimation procedure (**Appendix 5-table 1-10**).

APPENDIX 2

Genetic diversity patterns with ASD-MDS at different geographical scales, complementary to Results 1.

At the worldwide scale (**Appendix 2-figure 1**), the first MDS axis is mainly driven by genetic differentiation between African individuals and non-African individuals, the second MDS axis by differentiation between European and East Asian individuals, and the third axis by differentiation between South Asian and American individuals.

We explored successive subsamples of this worldwide dataset in order to decompose apparent preferred relationships between each admixed population related to the TAST with respect to African and European populations only. We find (**Appendix 2-figure 2**) that the first MDS axis differentiates African and European individuals; the second axis differentiates mainly Senegambian West Western African individuals from Congo Basin hunter-gatherer individuals (namely the Baka, Ba.Bongo, Ba.Koya, Ba.Mbuti, Ba.Twa and Bezan); and the third axis differentiates further these latter populations from Eastern African individuals. In this context, we find Cabo Verdean individuals clustering along an axis going from the European cluster to a cluster formed mainly by West Western African individuals, with the sole exception of two individuals with fathers born on Angola as per our familial anthropology questionnaires and consistently clustering closer to our Angolan samples. Instead, ASW, ACB and PUR individuals are found on a slightly different trajectory going from European individuals towards East Western Africa mainly (**Appendix 2-figure 2**).

Further resampling our ASD matrix (**Appendix 2-figure 3**), we find no signs of particular genetic affinity, along the first three MDS axes, between enslaved-African descendants and Eastern and Southern African individuals.

Notably, we find Cabo Verdean individuals clustering similarly to Senegambian Fulani individuals in between European and other Senegambian populations, the Fulani being known to have historically received gene-flow from Northern African populations (81,94,117,118). In the absence of Northern African populations in our dataset, the South-Western European Iberian-IBS population represented the best such proxy-populations with known historical relationship with Northern Africa, hence resulting, at this geographical scale, in the similar clustering of Cabo Verdean and Fulani individuals. Note that Fulani and Cabo Verdean individuals substantially departed from each other along higher MDS axes, the Cabo Verdeans remaining on a European-African axis while the Fulani departed from this trajectory on the European side (**Appendix 2-figure 3**).

Finally, considering only populations related to the TAST with respect to European and East, Central, and West Western African populations (excluding the Fulani), we find (**Appendix 2-figure 4**) that Cabo Verdeans cluster separately from other TAST populations not only with respect to African populations, but also with respect to their relationships to European populations (**Figure 2**).

Appendix 2-figure 1:

Multidimensional scaling three-dimensional projection of allele sharing pairwise dissimilarities, for all worldwide populations in our dataset.

Each individual in the plot is represented by a single point. See **Figure 1-source data 1** for the population list used and **Figure 1** for sample locations and symbols.

A) Axis 1 and 2; B) Axis 1 and 3. 3D animated plot is provided in *.gif* format.

We evaluate the Spearman correlation between 3D MDS projections and the original ASD pairwise matrix to evaluate the precision of the dimensionality reduction along the first three axes of the MDS. We find significant Spearman ρ of 0.9796 ($p<2.2\times10^{-16}$).

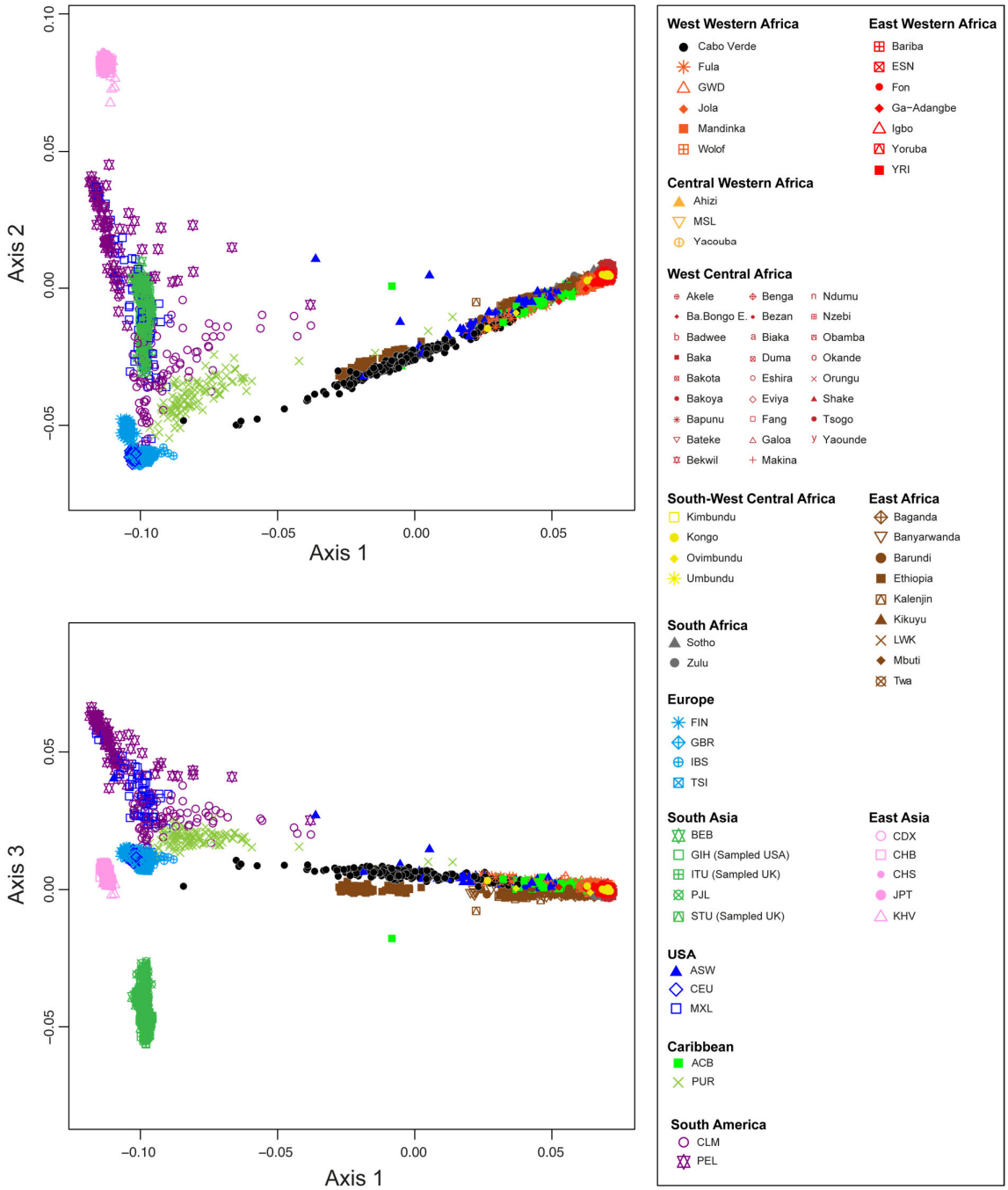

Appendix 2-figure 2:

Multidimensional scaling three-dimensional projection of allele sharing pairwise dissimilarities, for all of the African, European and other admixed populations related to the TAST.

Each individual is represented by a single point. We removed all Asian and South American samples compared to the sample set employed in **Appendix 2-figure 1**, and recomputed the MDS based on this reduced sample set. See **Figure 1-source data 1** for the population list used in these analyses. The sample map used in these analyses is extracted from **Figure 1** and provided in panel **D**.

A) Axis 1 and 2; B) Axis 2 and 3; C) Axis 1 and 3. 3D animated plot is provided in *.gif* format.

We evaluate the Spearman correlation between 3D MDS projections and the original ASD pairwise matrix to evaluate the precision of the dimensionality reduction along the first three axes of the MDS. We find Spearman ρ of 0.9392 ($p<2.2\text{x}10^{-16}$).

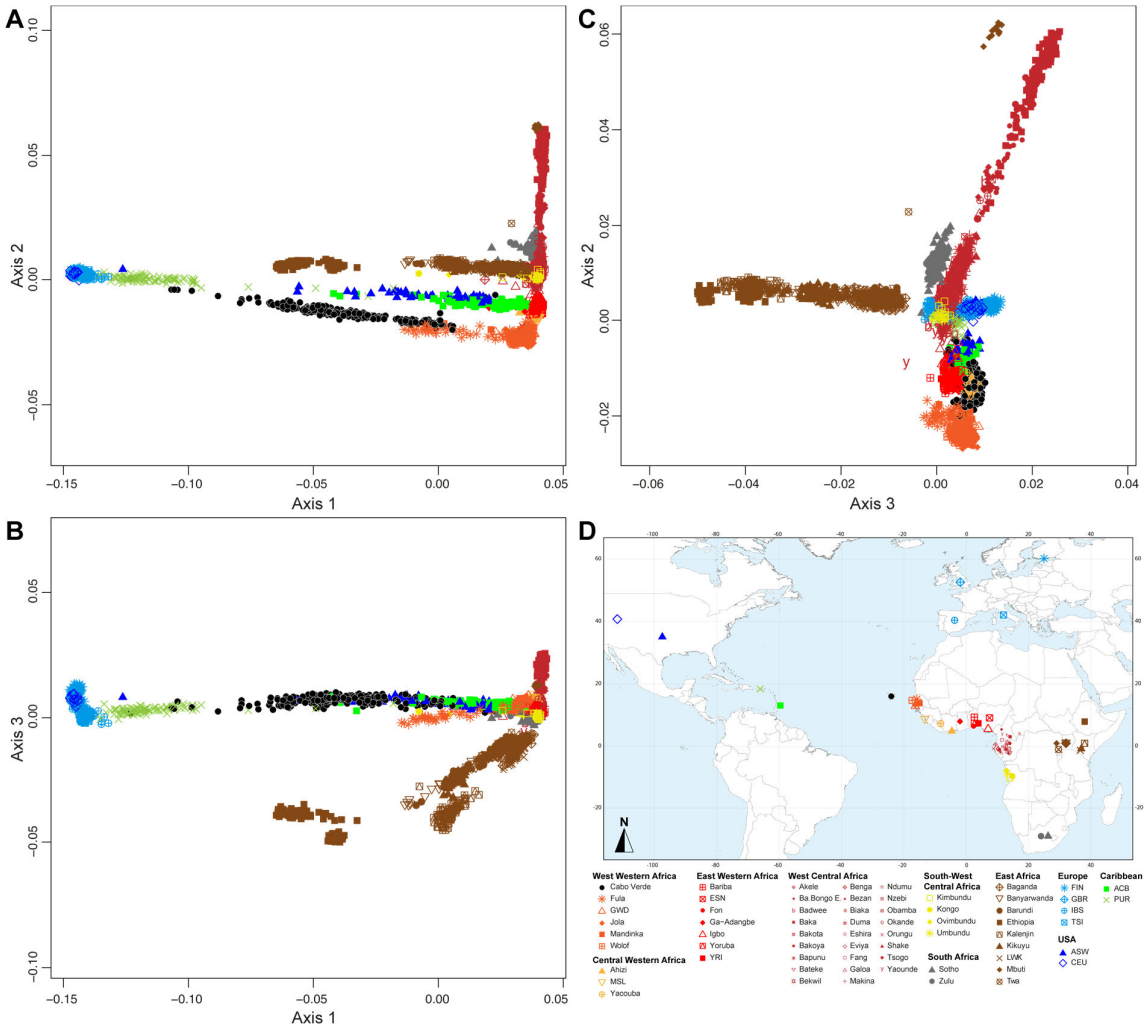

Appendix 2-figure 3:

Multidimensional scaling three-dimensional projection of allele sharing pairwise dissimilarities, for a subset of African, European and other admixed populations related to the TAST.

Each individual is represented by a single point. We removed all East African and Central African hunter-gatherer samples (Baka, Bezan, Ba.Bongo, Ba.Koya, Ba.Twa, Bi.Aka, Mbuti) compared to the sample set employed in **Appendix 2-figure 2**, and recomputed the MDS based on this reduced sample set. See **Figure 1-source data 1** for the population list used in these analyses. Sample map used in these analyses is extracted from **Figure 1** and provided in panel **D**.

A) Axis 1 and 2; B) Axis 2 and 3; C) Axis 1 and 3. 3D animated plot is provided in *.gif* format.

We evaluate the Spearman correlation between 3D MDS projections and the original ASD pairwise matrix to evaluate the precision of the dimensionality reduction along the first three axes of the MDS. We find Spearman ρ of 0.9450 ($p<2.2\text{x}10^{-16}$).

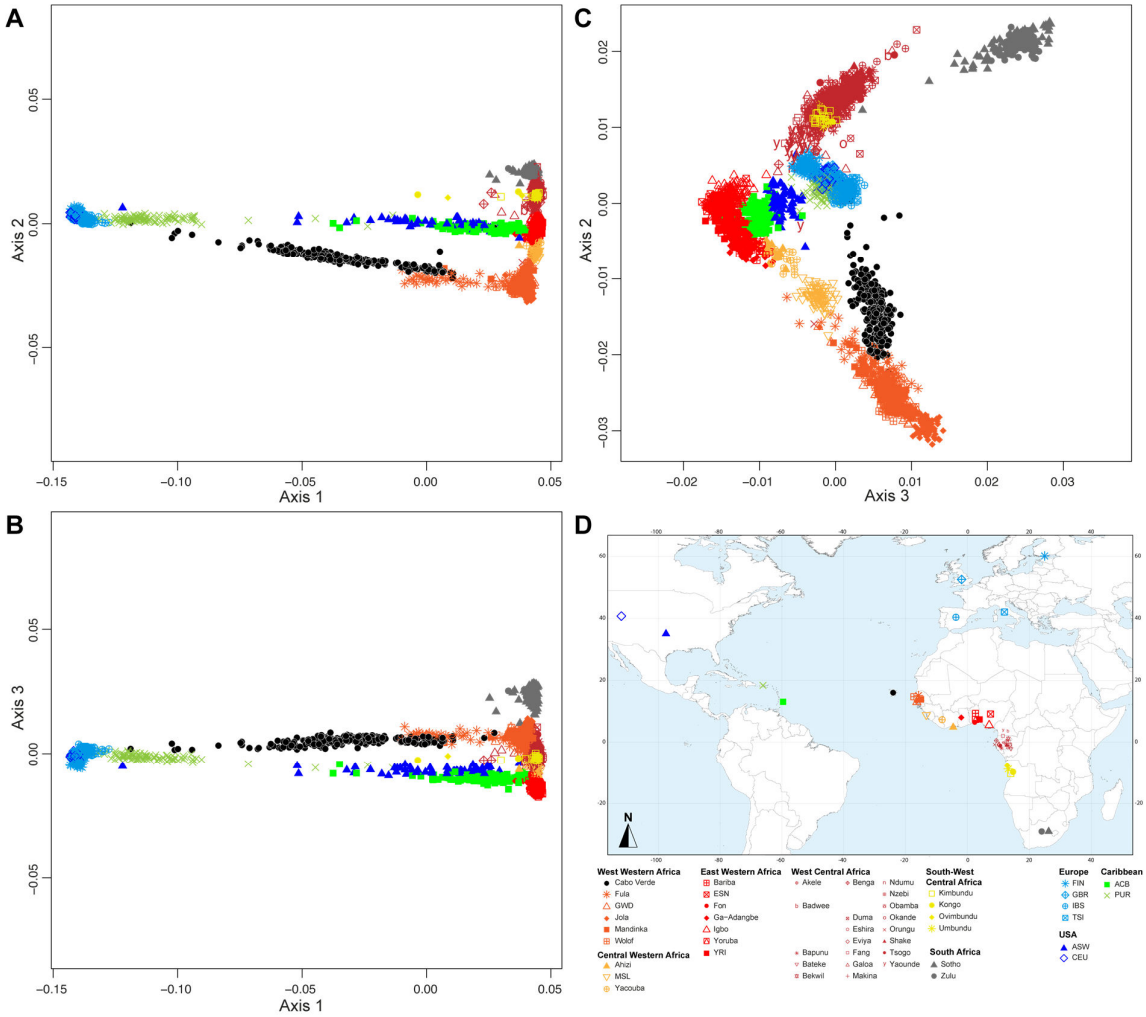

Appendix 2-figure 4:

Multidimensional scaling three-dimensional projection of allele sharing pairwise dissimilarities, for the closest subsets of West African, European and other admixed populations related to the TAST.

Each individual is represented by a single point. We removed all West and South-West Central African samples, as well as South African samples, compared to the sample set employed in **Appendix 2-figure 3**, and recomputed the MDS based on this reduced sample set. See **Figure 1-source data 1** for the population list used in these analyses. Sample map used in these analyses is extracted from **Figure 1** and provided in panel **D**.

A) Axis 1 and 2; B) Axis 2 and 3; C) Axis 1 and 3. 3D animated plot is provided in *.gif* format.

We evaluate the Spearman correlation between 3D MDS projections and the original ASD pairwise matrix to evaluate the precision of the dimensionality reduction along the first three axes of the MDS. We find Spearman ρ of 0.9636 ($p<2.2\text{x}10^{-16}$).

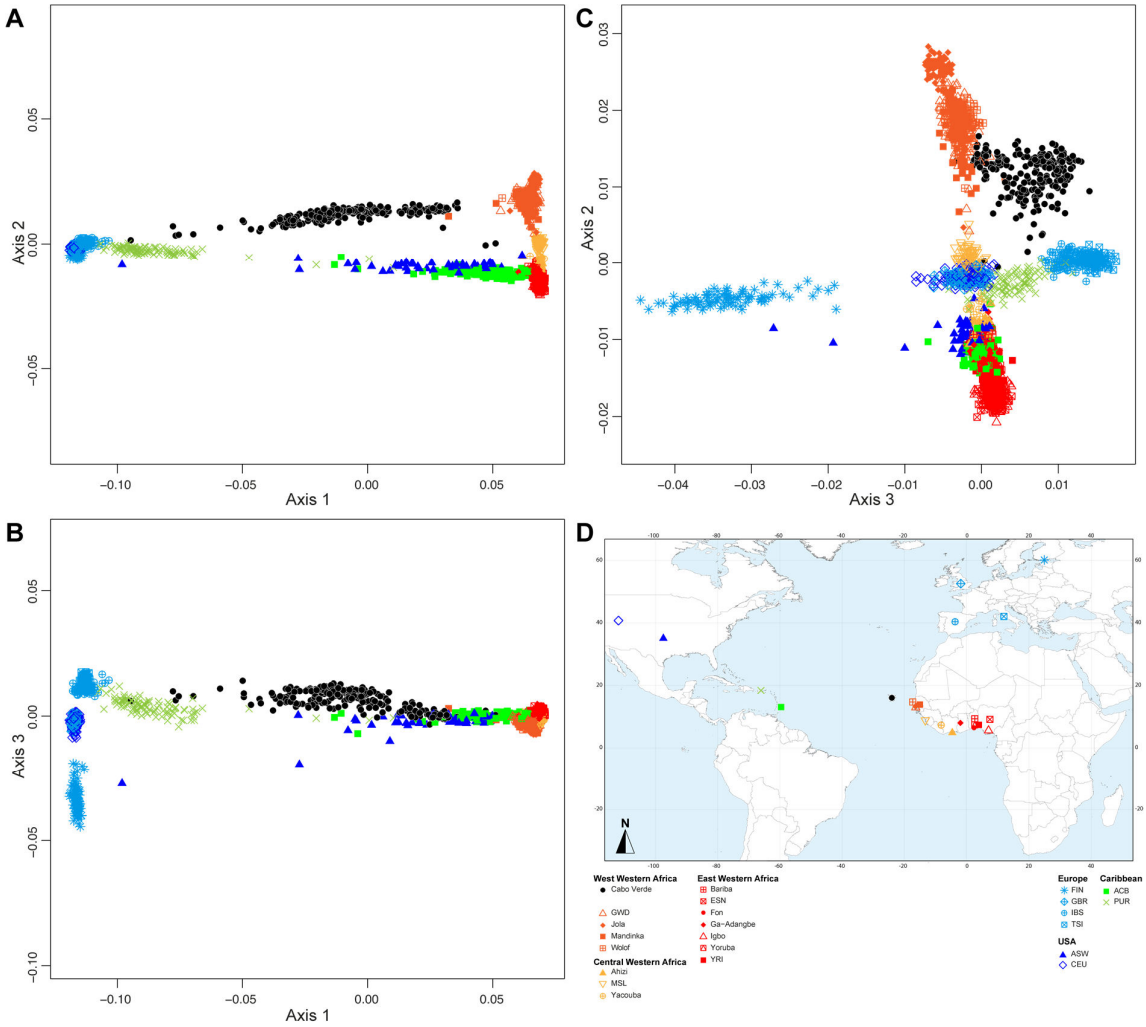

APPENDIX 3

Alternative ADMIXTURE modes, complementary to Results 2.

In **Figure 3A**, ADMIXTURE results at *K*=3 show that the new pink cluster is maximized in East Asian Chinese-CHB individuals, with a few African-American ASW and Barbadian-ACB individuals exhibiting relatively high membership to this cluster as visually identified in the ASD-MDS analysis (**Appendix 2-figure 1**), and previously reported (10). While Finnish-FIN individuals all exhibit low membership to this cluster, such signal probably emerges from unresolved clustering for this population geographically between Western Europe and East Asia. This is further evidenced by the almost complete disappearing of this resemblance of FIN individuals with the pink cluster at higher values of *K*. No other individuals or populations in our analysis show signals of strong resemblance with the East Asian Chinese-CHB for higher values of *K*.

The fourth gray cluster at *K*=4 in **Figure 3A** is maximized in Southern African individuals from the Soto and Zulu populations. At this value of *K*, the original orange cluster is maximized in the West Western African Jola from Senegambia and all other African populations exhibit intermediate membership between the gray and the orange cluster. Interestingly, the average membership to the gray "Southern African" cluster decreases with increasing geographic distance from Southern Africa, along the Atlantic Ocean coast of the continent. This echoes the relatively continuous clustering observed in the ASD-MDS analysis for the Atlantic African populations in our dataset (**Appendix 2-figure supplement 2-4**). Notably, the Cabo Verdean individuals born on Brava, Fogo, Santiago, and Maio, exhibit membership to both the orange and the gray clusters, albeit with a majority of membership to the orange cluster rather than the gray cluster. All other Cabo Verdean individuals show virtually no membership to the gray cluster. While indicating the stronger resemblance between all Cabo Verdean individuals with genetic patterns observed mostly in West Western Africa and Senegambian populations, this provides a first indication of differentiated genetic structure across islands within Cabo Verde. Conversely, the orange cluster previously identified in the ASW and ACB is, at *K*=4 in **Figure 3A**, divided into gray and orange with a slight excess of gray. A similar pattern is found among Central and East Western African populations, such as the Yoruba-YRI, the Nigerian-ESN, the Igbo, and the Ga-Adangbe populations, hence providing a first indication of a closer resemblance of the individuals of these two enslaved-African descendant populations with East Western Africa rather than with West Western Africa.

At *K*=5 in **Figure 3A**, note that West Central and South-West African populations exhibit a distinctive unique pattern with high membership to both the red and gray clusters. However, note that ADMIXTURE clustering is largely unresolved at this value of *K* as no individuals exhibit close (<1%) to 100% membership to the red cluster, and as only 27 out of the 30 ADMIXTURE iterations provide similar results. Indeed, an alternative minor mode is identified at this value of *K* (**Appendix 3-figure 1**).

At *K*=7 in **Figure 3A**, the novel light-blue cluster is maximized only in Finnish-FIN individuals, while the blue cluster is now maximized only in Tuscan-TSI individuals. British-GBR and USA-CEU individuals exhibit intermediate membership between the two clusters while Iberian-IBS individuals strongly resemble TSI individuals. This clustering patterns further echoes the observed ASD-MDS clustering of European populations identified in **Figure 2**. Importantly, the "European" membership of all Cabo Verdean islands resembles, relatively, the patterns exhibited in TSI and IBS individuals (with high proportions of blue and minimal proportion of light-blue), while African-American ASW and Barbadian-ACB individuals show relatively much higher proportions of light-blue, hereby resembling, for this genotype membership, GBR and CEU individuals rather than other Europeans. Nevertheless, variable results across runs at this value of K indicate unresolved clustering and these interpretations should be considered cautiously at this point (see alternative ADMIXTURE modes at *K*=7, **Appendix 3-figure 1**).

At *K*=8 in **Figure 3A**, the novel dark-red cluster is maximized in West Central African Tsogho individuals and at very high proportions in all other individuals from West-Central and South-West Africa, hence resolving the unresolved clustering identified for these populations at *K*=5. Interestingly, substantial traces of this cluster are found in YRI, Igbo and ESN East Western African populations as well as ASW and ACB individuals, but

virtually absent from Cabo Verdeans or any other African population. This further indicates the closer resemblances of ASW and ACB African genetic component to East Western and West Central Africa than to other African populations in our dataset, as echoed in our ASD-MDS analyses (**Figure 2**, **Figure 2-figure supplement 1**).

At *K*=9 in **Figure 3A**, the novel light-yellow cluster is maximized in Sierra Leone-MSL population from Central West Africa, albeit imperfectly. This further illustrates the intermediate clustering of Central Western African populations in between Senegambian and East Western African populations, largely overlapping on both sides, and observed in ASD-MDS analyses (**Appendix 2-figure supplement 1-4**). Nevertheless, patterns should be interpreted with caution at this value of *K*, as clustering is largely unresolved, also indicated by the alternative ADMIXTURE solutions (**Appendix 3-figure 1**).

At *K*=11 in **Appendix 3-figure 1**, we find five alternative ADMIXTURE solutions to **Figure 3**. In one alternative solution, the novel dark blue cluster is maximized either in the Fang from West Central Africa hereby distinguished from the Tsogho from the same geographic region. Other modal results show this novel dark-blue cluster maximized instead in the Wolof from West Western Africa, hence distinguished from the Jola from the same geographic region; or instead in the British GBR, thus distinguishing three different ADMIXTURE patterns among Western European populations and hence resolving minoritarian modes observed previously at *K*=10; or, finally, among individuals from Fogo island, and Brava to a lesser extent, thus indicating further sub-structure among Cabo Verdean islands. Interestingly, note that for all ADMIXTURE solutions at this value of *K*, the light-yellow cluster is majoritarian in Sierra Leone MSL individuals, hence more clearly differentiated from either West Western and East Western African individuals compared to results obtained at previous values of *K*.

At *K*=12 in **Appendix 3-figure 1**, we find three alternative modes to the results presented in **Figure 3**. These results resolve alternative modes obtained at the previous values of *K*, thus further differentiating populations within Africans and Europeans sub-regions, respectively.

At *K*=13 in **Appendix 3-figure 1**, we find five alternative mode results compared to the one presented in **Figure 3**. These further resolve the various modal results obtained at previous values of *K*=10, 11, and 12. Furthermore, note that three minoritarian such modes maximize the novel light-brown cluster in Boa Vista individuals, while memberships to this specific cluster are virtually absent from all other individuals in our data set, except for a substantial proportion in individuals born on Maio.

At *K*=14 in **Appendix 3-figure 1**, we find three alternative solutions compared to **Figure 3**. Note that some such solutions resolve separate modal solutions obtained at previous values of *K*. Furthermore, interestingly, in one modal solution, the novel bright yellow cluster is maximized in Ga-Adangabe individuals, hence fdifferentiating this population from others in the East Western African sub-region.

Finally, at *K*=15 in **Appendix 3-figure 1**, we obtain four alternative solutions compared to **Figure 3** results. Interestingly, in two such solutions, the novel dark-green cluster is maximized in Nzebi West Central Africans thus further differentiating the three populations from Gabon (the Fang, the Tsogho and the Nzebi) in three different cluster. Note that in this cases, geographically close South-West Central African individuals from Angola exhibit membership proportion patterns resembling more the Nzebi than the two other Gabonese populations. An alternative mode interestingly differentiates some individuals within the CHB East Asian population, and is virtually absent from all other individuals in our data set. Finally, the last alternative mode encompasses the smallest number of runs and resolves some of the alternative solutions previously obtained at *K*=14 (**Figure 3A**, **Appendix 3-figure 1**).

Appendix 3-figure 1:

Alternative ADMIXTURE mode results for the individual genetic structure among Cabo Verdean, Barbadian-ACB and African-American ASW populations related to the TAST.

ADMIXTURE (48) analyses using resampled individual sets for the population sets originally containing more than 50 individuals (**Figure 1-source data 1**). 225 unrelated Cabo Verdean-born individuals are grouped by island of birth (**Figure 1-source data 1**). All analyses considered 102,543 independent autosomal SNPs, for values of *K* between 2 and 15. 30 independent ADMIXTURE runs were performed for each value of *K*, and groups of runs (>2) providing similar results (all pairwise SSC > 99.9%) were averaged in a single "mode" result using CLUMPP (103), and plotted with DISTRUCT (104). Number of runs in the presented modes are indicated below the value of *K*. All other modes are presented in **Figure 3**.

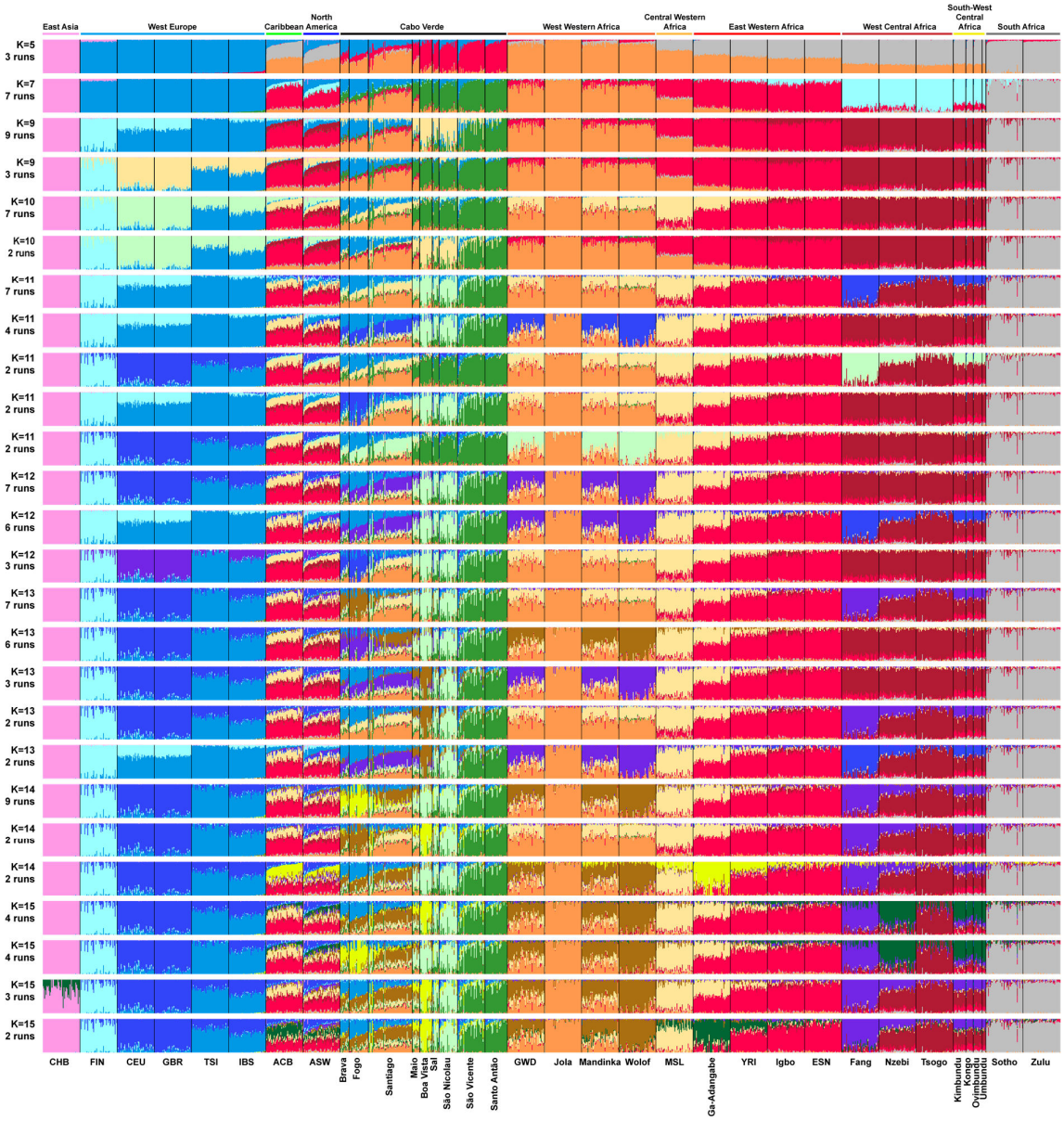

APPENDIX 4

Runs of homozygosity patterns in Cabo Verde and other admixed populations related to the TAST, complementary to Results 4.

Examining patterns of ROH less than 1cM long, we find generally low levels of short and medium ROH in continental Africa (**Appendix 4-figure 1**), with the lowest levels in Southern Africa. Conversely, we found high levels of such short and medium-size ROH among European and East Asian populations, likely reflecting ancient migration bottlenecks during the Out-of-Africa expansion (61). We note that the Cabo Verdean individuals have slightly elevated levels of short and medium ROH compared to continental Africa, similarly to the ACB and ASW populations. This may stem from the known admixture with European populations that occurred recently during the TAST. Admixture can be intuitively expected to decrease ROH levels compared to the source populations in general. However, recent admixture between African and European populations, the latter who exhibit much higher levels of short and medium ROH than the former (**Appendix 4-figure 1**), may inflate levels of such ROHs in the admixed population compared to continental African sources. Consistently with our findings for the African American ASW and Barbadian ACB (**Appendix 4-figure 1**), such phenomenon had been previously reported (60). Finally, overall total ROH levels reflected the generally higher levels of ROH in Cabo Verde compared to continental African and other admixed populations from the Americas (**Appendix 4-figure 1C**), patterns likely related to the relative isolation of populations within the archipelago (**Figure 5**, **Table 1**).

Exploring how local ancestry intersects with ROH less than 1cM long, since short and medium ROH are comprised of old haplotypes that likely predate over 50 generations ago (59), the colonization of the Cabo Verde islands and the subsequent admixture histories of their populations, we expected that the local ancestry content of these ROH classes should be correlated with total non-ROH local ancestry levels. **Appendix 4-figure 2** illustrates the relationship between total ancestry in a given ROH size class versus the total ancestry not in that ROH size class for all Cabo Verdean individuals. We find strong correlations among the short ROH and local ancestry (**Appendix 4-figure 2A**; African local ancestry: Pearson ρ=0.9372, $p < 2.2\text{x}10^{-16}$; European local ancestry: Pearson ρ=0.9496, $p < 2.2\text{x}10^{-16}$; Asian local ancestry: Pearson ρ=0.7516, $p < 2.2\text{x}10^{-16}$), and medium ROH and local ancestry (**Appendix 4-figure 2B**; African local ancestry: Pearson ρ=0.9071, $p < 2.2\text{x}10^{-16}$; European local ancestry: Pearson ρ=0.9379, $p < 2.2\text{x}10^{-16}$; Asian local ancestry: Pearson ρ=0.3905, $p < 1.298\text{x}10^{-9}$).

2496 **Appendix 4-figure 1:**
2497 **The distribution of (A) short, (B) medium, and (C) all ROH per individual, for each Cabo Verdean birth-island and other**
2498 **worldwide populations.**

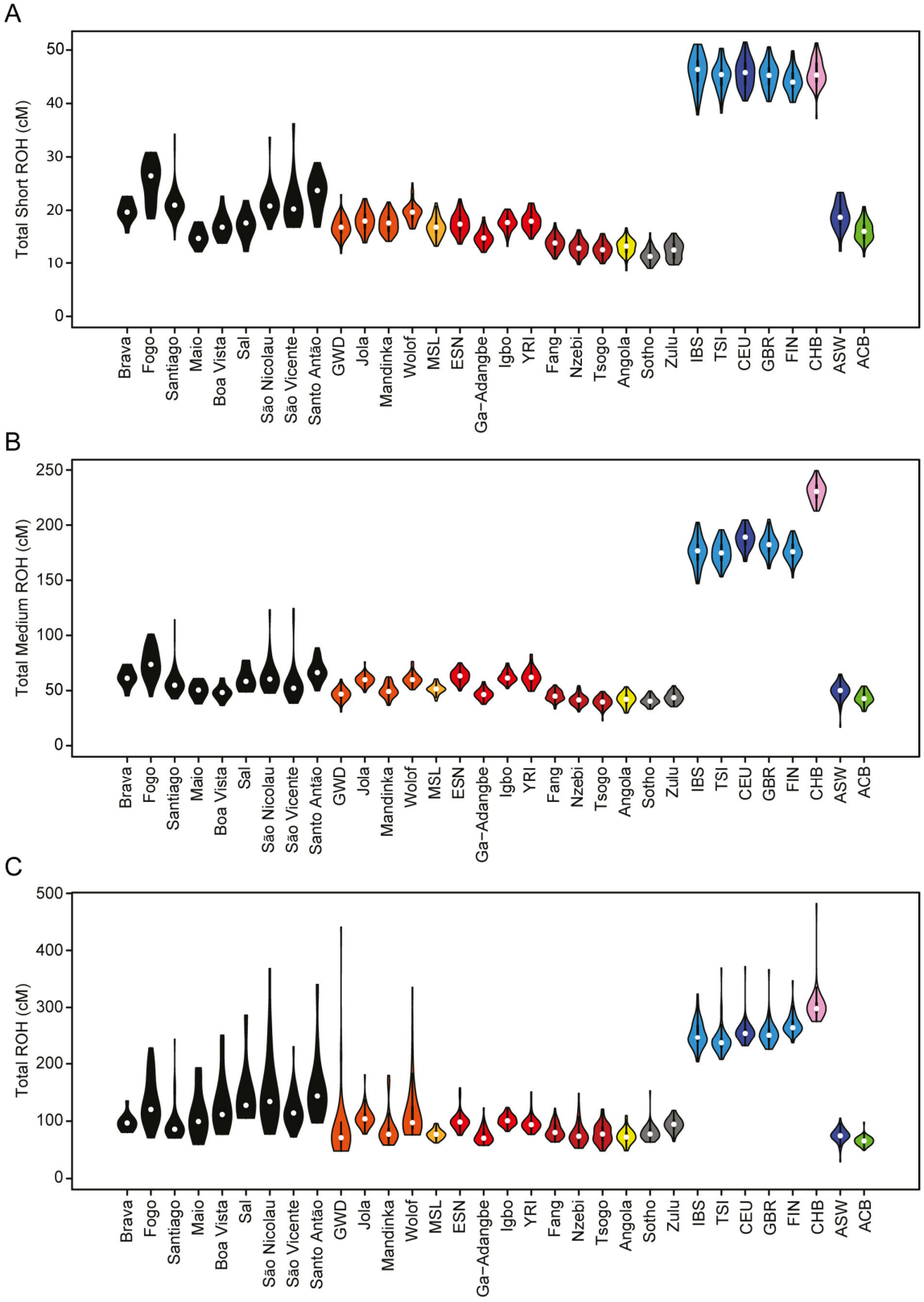

2499
2500

2501 **Appendix 4-figure 2:**
2502 **Individual total ancestry contained in (A) short, (B) medium, and (C) long ROH versus total ancestry not in that class ROH,**
2503 **for each Cabo Verdean birth-island and other worldwide populations.**
2504

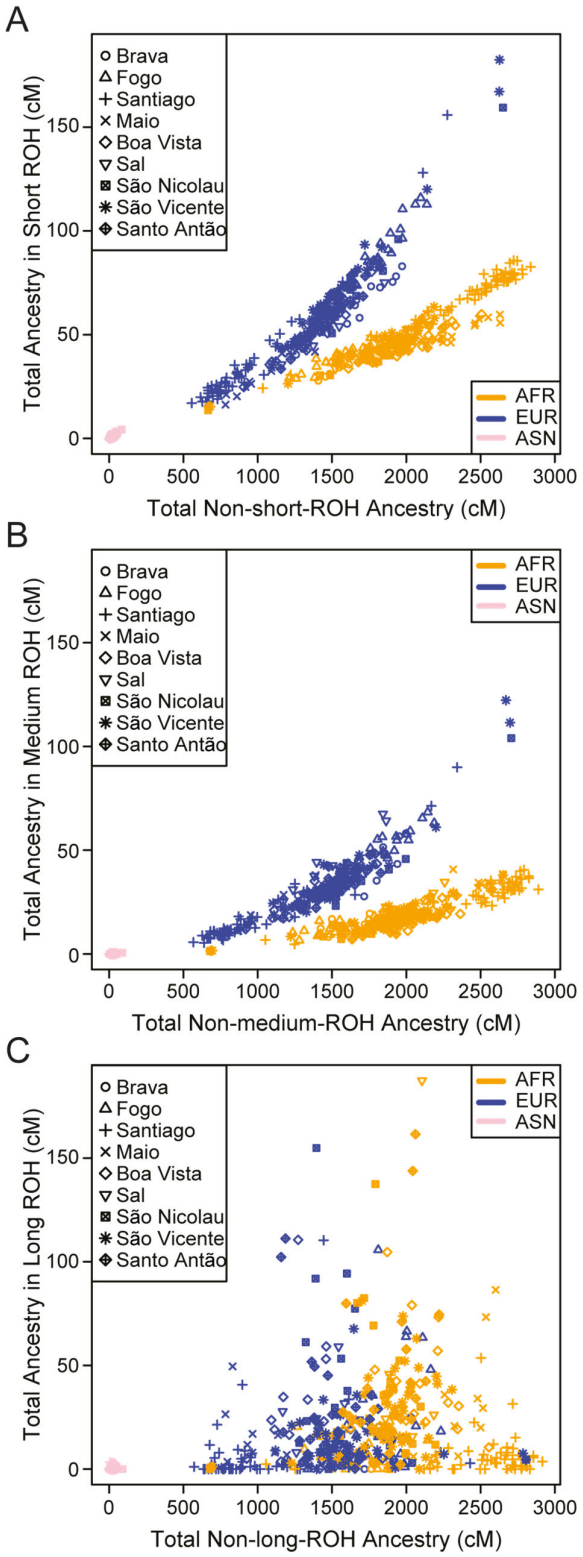

2505
2506

APPENDIX 5

Genetic admixture histories of each Cabo Verdean island of birth inferred with *MetHis*-ABC, complementary to Results 7. and Discussion sections.

Results for the detailed admixture history of each island separately are henceforth presented in the chronological order of the first time in an islands' history when more than 100 individuals are reported in historical census information, and after which further census reports always exceeded this number until today; hereafter called "first perennial peopling" of an island (**Figure 7D**, **Figure 7-source data 1**). As in the main text of the article, note that this historical date can vastly differ from the date for the first official settlement of an island inferred via political, administrative and tax records, and witnessed by parishes foundations, illustrating the complex and versatile peopling history of each Cabo Verdean island after the initial establishment of the Portuguese dominion over the archipelago.

Admixture history of Santiago (First official settlement 1460; Perennial peopling: 1470)

MetHis-ABC inferences detailed results for Santiago

For individuals born on Santiago island, we find that the most recent pulses of admixture from Africa and Europe, respectively, occurred after the official abolition of the TAST in the Portuguese Empire in the 1830's, and after the effective abolition of slavery in the Portuguese empire in the 1860's (**Figure 7**). Both admixture pulses are characterized by posterior distributions with narrow 95%CIs clearly departing from their respective priors, both for the timing of each pulse and their respective intensities, in particular for the European admixture pulse (**Figure 7-figure supplement 1-3**, **Appendix 5-table 1**). For these recent events, observed genetic patterns are consistent with a relatively intense African admixture event (median=0.5913, mode=0.6837, 95%CI=[0.0642–0.9038]), occurring between generation sixteen and seventeen after the founding of Cabo Verde at generation 0 (generation median=16.6, mode=17.2, 95%CI=[10.0–18.9]). Furthermore, we find strong evidence for the most recent European admixture pulse being weak (median=0.0684, mode=0.0258, 95%CI=[0.0028–0.6021]), and having occurred between one and two generations before the sampled generation (generation median=18.7, mode =19.1, 95%CI=[11.7–19.6]).

NN-ABC posterior parameter estimations perform less accurately to infer the dates of the earlier admixture pulses and their associated intensities, both from Africa and Europe respectively, as shown by posterior distribution departing less clearly from their respective priors and overall large 95%CI. Nevertheless, results indicate that both the African and European pulses may have occurred in a more remote past; the African pulse was inferred at generation 9.2 (median) after founding at generation 0 (mode=13.9, 95%CI=[1.7–16.8]); the European pulse at generation 7.5 (median, mode=3.4, 95%CI=[2.3–15.9]), towards the beginning of the plantation economy era in the Americas and during the intensification of the TAST in the second half of the 17th century (1,2) (**Figure 7D**). Conversely, the initial founding admixture pulse, set to occur at generation 0 at the beginning of Cabo Verde settlement history in the 1460's, is more accurately estimated *a posteriori*, as indicated by substantial departure from the prior distribution and relatively narrow CI. Results here indicate a stronger contribution from Africa than Europe (median=0.6365, mode=0.8816, 95%CI=[0.0538–0.9858]), at the root of the genetic make-up of Santiago-born individuals in our sample set.

Finally, effective population sizes in Santiago indicate a strong, relatively linear (u_{Ne} median=0.365, mode=0.440, 95%CI=[0.150–0.494]), increase since the 1460's up to 80,077 effective individuals (median, mode=92,109, 95%CI=[30,408–98,975]), in the sampled generation born on average between the 1960's and the 1980's.

Appendix 5-table 1-Santiago:

NN-ABC posterior parameter estimations for Santiago island, cross-validation posterior parameter errors, and cross-validation 95% Credibility Interval accuracies.

Cross-validation errors and 95% CI accuracies are based on 1,000 NN-ABC posterior parameter inferences using, in turn, each one of the 1,000 simulations closest to the observed data used as pseudo-observed data, and the remaining 99,999 simulations as the reference table.

Error calculations are based on the mode and, separately, the median point estimate for each 1,000 pseudo-observed simulations posterior parameter estimation, compared to the known parameter used for simulation. We considered 6 neurons in the hidden layer and a tolerance level of 0.01 (1000 simulations) for all posterior parameter estimation in this analysis as identified in **Appendix 1-table 1**. Plotted distributions for posterior parameter estimations can be found in **Figure 7-figure supplement 1-3**.

SANTIAGO	Parameter posterior estimation				1,000 cross-validation errors		
Afr2P-Eur2P scenario parameters	**Mode**	**Median**	**50% Credibility Interval**	**95% Credibility Interval**	**Mode mean absolute error**	**Median mean absolute error**	**95% CI length accuracy**
Ne.0	142	431	[194 - 692]	[28 - 974]	305	255	0.059
Ne.20	92109	80077	[63220 - 91349]	[30408 - 98975]	25426	21558	0.045
u.Ne	0.440	0.365	[0.284 - 0.438]	[0.150 - 0.494]	0.113	0.096	0.042
sAfr,0	0.8816	0.6365	[0.3884 - 0.8415]	[0.0538 - 0.9858]	0.3147	0.2507	0.056
tAfr,p1	13.9	9.2	[4.9 - 13.4]	[1.7 - 16.8]	5.3	4.2	0.101
sAfr,tAfr,p1	0.7844	0.5986	[0.3421 - 0.7861]	[0.0420 - 0.9479]	0.2618	0.2204	0.054
tAfr,p2	17.2	16.6	[15.2 - 17.5]	[10.0 - 18.9]	1.8	1.6	0.199
sAfr,tAfr,p2	0.6837	0.5913	[0.3894 - 0.7241]	[0.0642 - 0.9038]	0.1597	0.1458	0.052
tEur,p1	3.4	7.5	[4.3 - 11.1]	[2.3 - 15.9]	4.0	3.1	0.161
sEur,tEur,p1	0.1617	0.3969	[0.1957 - 0.6606]	[0.0185 - 0.9564]	0.3042	0.2439	0.056
tEur,p2	19.1	18.7	[17.7 - 19.2]	[11.7 - 19.6]	3.0	2.9	0.115
sEur,tEur,p2	0.0258	0.0684	[0.0250 - 0.1501]	[0.0028 - 0.6021]	0.2749	0.2254	0.057

Discussion for the admixture history of Santiago

Altogether, our results indicate that admixture in Santiago occurred mainly between Senegambian and South Western European populations (**Figure 2-3**), at the very beginning of the Portuguese colonization of the archipelago in the 15th century. This early admixture history is likely due to an initial peopling of Cabo Verde strongly biased towards solitary males (familial permanent migrations from Portugal being a minority), who reproduced with African enslaved women, and whose admixed offspring constituted the first Cabo Verdean generations, as shown by some recorded instances of legitimizations of the admixed offspring to allow them to legally inherit dating back to the early 16th century (25).

Our results further indicate that two substantial admixture events from Africa and Europe, respectively, occur concomitantly to the early expansion of the TAST during the 17th-century, although we are unable to precisely date both events. Nevertheless, our results support a more tenuous genetic admixture history from Africa experienced by Cabo Verdeans from Santiago during the most intense period of the TAST (18th-century) and the height of plantation economy in European colonial empires (1,2). This apparent reduced influence of the most intense period of the TAST on admixture pattern in Santiago is also echoed in our ASD-MDS, ADMIXTURE, and SOURCEFIND results, where Santiago Cabo Verdeans today share ancestry with Senegambian Mandinka almost exclusively (**Figure 2-3**). However, historical records unquestionably demonstrated that numerous other populations from West Central and South Western Africa were enslaved and forcibly deported to Cabo Verde during this era (25). Thus, our results highlight that the strong and recurrent demographic migrations of enslaved Africans brought to Santiago during the second half of the TAST do not seem to have left a similar genetic admixture signature. This is consistent with several, mutually non-exclusive, historical scenarios, where enslaved African populations brought to Santiago may have been mostly re-deported to the Americas and Europe after the 17th century, without substantially contributing to the genetic landscape of this island, whether due to rapid re-deportation, and/or to slave-owners and colonial society strongly preventing

marriages and reproduction between newly arrived enslaved individuals and pre-existing enslaved or non-enslaved communities in Santiago (see **Discussion** in main text).

Conversely, our results indicate an intense introgression event from Africa in Santiago, occurring shortly after the TAST and the abolition of slavery in the Portuguese empire in the 1860's. This may have been caused by a relaxation of the socio-economic constraints that predominated during most of the TAST against marriages between enslaved and non-enslaved communities as well as the control of marriages among enslaved individuals imposed by slave-owners; concomitant with the strong intensification of the illegal slave-trade which deported numerous enslaved Africans in a short amount of time shortly after the end of the TAST (25–28).

Our results also clearly identify a European introgression event in Santiago having occurred at the beginning of the 20th century, which may be explained by the European migrations towards African colonies triggered by European empires' policies during the first half of this century. Interestingly, we find that this recent admixture event was of very limited intensity, thus indicating that European emigration to Santiago during the 20th century only had a quantitatively limited, albeit precisely detectable, influence on genetic admixture patterns.

Finally, Santiago-born individuals also show the lowest ROH levels and generally some of the shortest ROH in Cabo Verde (**Figure 4** and **Appendix 4-figure 1-2**). When examining ancestry patterns within ROH in Santiago-born individuals, although proportions within ROH are on average consistent with an individuals' overall genetic ancestry, there are some outlier individuals with much higher European ancestry within ROH compared to the remainder of the genome. This could possibly reflect historical marriage prohibitions and other social constraints against intercommunity reproductions (see **Discussion** in main text). These ROH results combined with the evidence for the relatively constantly increasing reproductive population in Santiago over the course of the peopling of Cabo Verde (**Figure 7C**), was consistent with this island being the administrative historical capital, and principal entry to the archipelago throughout its' history (26,27).

Admixture history of Fogo (First official settlement 1460; Perennial settlement: 1570)

MetHis-ABC inferences detailed results for Fogo

For individuals born on Fogo island, we find that both European admixture pulses were precisely inferred with NN-ABC, for the time of their occurrence and for their respective intensities, as posterior parameter distributions and 95%CI substantially depart from their respective priors (**Figure 7**, **Figure 7-figure supplement 1-3**, **Appendix 5-table 2**). The most recent European admixture pulse in Fogo occurred concomitantly to the abolition of the TAST and of slavery in the Portuguese empire in the 1860's (generation median=15.5 after the founding of Cabo Verde at generation 0, mode=16.7, 95%CI=[6.7–18.2]), and was of substantial intensity (median=0.2428, mode=0.2101, 95%CI=[0.0157–0.8485]). The older European pulse occurred much more remotely in the past (generation median=5.3, mode=2.5, 95%CI=[1.9 –13.9]), shortly after the first perennial census above 100 individuals in 1570 for this island, and long before the increase in TAST intensity due to the expansion of Plantation Economy in the Americas in the second half of the 17th century. Furthermore, note that our results indicate that this European pulse is of relatively similar intensity compared to the most recent one (median=0.2234, mode=0.1149, 95%CI=[0.0223–0.8383]).

Interestingly, we find that the African admixture history of individuals from Fogo occurred at very different periods of time than the European ones, the timing for both African admixture pulses being also well estimated with substantial departure from the prior and relatively narrow 95%CI. Indeed, we find strong indications of a very recent pulse of African admixture of overall limited intensity (median=0.2034, mode=0.1174, 95%CI=[0.0120–0.8225]), having occurred around the first part of the 20th century (generation median=19.3 after the founding of Cabo Verde at generation 0, mode=19.5, 95%CI=[15.6–19.8]). Furthermore, we find that the previous African admixture pulse likely occurred between six and eight generations before the sampled one (generation median=12.0 after Cabo Verde founding, mode=13.3, 95%CI=[4.7–16.9]), in the midst of the most intense period of the TAST and plantation economy in the Americas, around the 1760's. However, we cannot recover a precise estimation for the intensity of this older pulse, as its' posterior parameter distribution seldom depart from its' prior. We also find that the founding admixture event set to occur at the beginning of the colonization history of the archipelago in the 1460's is substantially departing from its' prior distribution and very similar to the founding admixture event found for individuals born on Santiago (median=0.6831, mode=0.7407, 95%CI=[0.1679–0.9600]).

Finally, our posterior estimation of the demographic history of Fogo-born individuals substantially differs from that of Santiago. Indeed, while we find similar effective sizes towards the present between the two islands (median=72,023, mode=90,370, 95%CI=[18,011–98,846]), we find that the demographic increase was much more recent and rapid in Fogo (u_{Ne} median=0.150, mode=0.115, 95%CI=[0.055–0.447]) than in Santiago.

Appendix 5-table 2-Fogo:

NN-ABC posterior parameter estimations for Fogo island, cross-validation posterior parameter errors, and cross-validation 95% Credibility Interval accuracies.

Cross-validation errors and 95% CI accuracies are based on 1,000 NN-ABC posterior parameter inferences using, in turn, each one of the 1,000 simulations closest to the observed data used as pseudo-observed data, and the remaining 99,999 simulations as the reference table.

Error calculations are based on the mode and, separately, the median point estimate for each 1,000 pseudo-observed simulations posterior parameter estimation, compared to the known parameter used for simulation. We considered 10 neurons in the hidden layer and a tolerance level of 0.01 (1000 simulations) for all posterior parameter estimation in this analysis as identified in **Appendix 1-table 1**. Plotted distributions for posterior parameter estimations can be found in **Figure 7-figure supplement 1-3**.

FOGO	**Parameter posterior estimation**				**1,000 cross-validation errors**		
Afr2P-Eur2P scenario parameters	**Mode**	**Median**	**50% Credibility Interval**	**95% Credibility Interval**	**Mode mean absolute error**	**Median mean absolute error**	**95% CI length accuracy**
Ne.0	349	511	[274 - 737]	[44 - 969]	295	253	0.063
Ne.20	90370	72023	[50948 - 87248]	[18011 - 98846]	27142	22749	0.057
u.Ne	0.115	0.150	[0.104 - 0.230]	[0.055 - 0.447]	0.085	0.081	0.074
sAfr,0	0.7407	0.6831	[0.5218 - 0.8152]	[0.1679 - 0.9600]	0.2936	0.2432	0.069
tAfr,p1	13.3	12.0	[8.1 - 14.4]	[4.7 - 16.9]	4.2	3.3	0.157
sAfr,tAfr,p1	0.4667	0.4549	[0.2286 - 0.6721]	[0.0251 - 0.9555]	0.2498	0.2315	0.056
tAfr,p2	19.5	19.3	[18.9 - 19.5]	[15.6 - 19.8]	2.6	2.5	0.100
sAfr,tAfr,p2	0.1174	0.2034	[0.1051 - 0.3560]	[0.0120 - 0.8225]	0.2032	0.1891	0.060
tEur,p1	2.5	5.3	[2.7 - 8.8]	[1.9 - 13.9]	3.6	3.0	0.216
sEur,tEur,p1	0.1149	0.2234	[0.1146 - 0.3943]	[0.0223 - 0.8383]	0.2804	0.2371	0.062
tEur,p2	16.7	15.5	[13.1 - 16.8]	[6.7 - 18.2]	3.2	3.0	0.070
sEur,tEur,p2	0.2101	0.2428	[0.1393 - 0.3966]	[0.0157 - 0.8485]	0.1751	0.1686	0.060

Discussion for the admixture history of Fogo

Our results indicate a very similar founding admixture event for Fogo island compared to that of Santiago, strongly suggesting that the admixture event at the root of Fogo peopling occurred early in Cabo Verde history, likely in Santiago island. This scenario is consistent with historical data suggesting an initial peopling of Fogo from Santiago at the end of the 15th century and the beginning of the 16th century, rather than independent founding events between islands (26,27).

Interestingly, we find a European pulse of admixture concomitant with the perennial peopling of the island at the end of the 16th century and the establishment of Fogo as an important center of agricultural and free-range cattle herding in the economic triangle between Europe, Cabo Verde, and continental Africa. Later on, we identify traces of an African admixture pulse having occurred during the most intense period of the TAST in the mid-18th century, thus consistent with increased African enslaved individuals' forced deportations to Fogo as showed by historical records, but we could not infer its intensity, suggesting the difficult identifiability of such admixture event in the genetic landscape of Fogo island today with the methods here deployed.

This history of admixture is likely related to the intense control on the island's economic expansion and regulated immigration imposed after 1532 by the central political, administrative, and commercial power of Santiago, with the notable exception of direct commercial relationships allowed between Fogo and Europe under the rule of the Portuguese crown (26–28). This could thus explain the limited African admixture during Fogo history and more intense European admixture on this island, identified with our ASD-MDS/ADMIXTURE, and SOURCEFIND results (**Figure 2-3**). Furthermore, these socio-political factors likely also explain the maintaining of a relatively low reproductive population size on Fogo until very recently, as opposed to the more continuous population increase on Santiago (**Figure 7C**). In addition, this demographic history may be further explained by the recurrent eruptions of the Fogo volcano, which unquestionably chronically disrupted

the island's development, although historical records showed limited direct mortality due to these events and that communities fleeing the island often migrated back after each cataclysm (26).

We identify a much more recent pulse of European admixture, having occurred in the first half of the 19th century, shortly after the abolition of the TAST in the Portuguese empire, possibly due to the profound socio-cultural changes in marital relationships between enslaved and non-enslaved communities during the abolition of slavery in colonial empires (see **Discussion** in main text). Finally, we identify precisely a weak African admixture pulse having occurred in Fogo during the 20th century possibly consistent with more recent work-related migrations from Africa to Cabo Verde (28).

Finally, ROH patterns in Fogo are similar to Santiago, in that ROH levels are relatively low and individual ROH are relatively short (**Figure 4**, **Appendix 4-figure 1-2**). This is consistent with Fogo's history of economic control and influx of European individuals. Interestingly, when exploring ancestry proportions within ROH relative to the remainder of the genome, we see on average more European ancestry within ROH. This could possibly reflect the historical influx of Europeans onto the island and/or a legacy of preferential marriages between individuals of shared family origin.

Admixture history of Santo Antão (First official settlement 1570; Perennial settlement: 1580)

MetHis-ABC inferences detailed results for Santo Antão

For individuals born on Santo Antão island, we find that both European admixture pulses after the founding admixture event are substantially departing from their respective priors and have relatively narrow 95%CI, both for the timing of their occurrence and their respective intensities (**Figure 7**, **Figure 7-figure supplement 1-3**, **Appendix 5-table 3**). We find that Santo Antão-born individuals have experienced a recent European admixture pulse of weak intensity (median=0.0847, mode=0.0467, 95%CI=[0.0056–0.6382]), that occurred roughly three generations before the sampled generation, at the turn of the 20th century (generation median=17.2 after Cabo Verde founding at generation 0, mode=18.1, 95%CI=[7.6–19.1]). Furthermore, we find a much more ancient European admixture pulse of strong intensity (median=0.3592, mode=0.1542, 95%CI=[0.0216–0.9522]), occurring concomitantly (generation median=5.8, mode=3.2, 95%CI=[2.6–15.6]) with the first perennial census in this island dated in 1580, and before the massive increase of TAST during the 17th century.

Interestingly, we find that the first African admixture pulse after founding at generation 0 occurred at generation 4.9 (median, mode=2.4, 95%CI=[1.9–11.9]), almost synchronically to the oldest European admixture pulse and the first perennial settlement of the island recorded in 1580. Furthermore, this African admixture pulse was intense (median=0.6255, mode=0.7574; 95%CI=[0.0451–0.9749]), which summed close to 100% with the European admixture pulse having occurred at very similar times. This obliterated any older admixture events, consistently with the wide 95%CI obtained for the intensity of the founding admixture event for this island (median $s_{Afr,0}$=0.5681, mode=0.8047, 95%CI=[0.0260–0.9839]). Importantly, our NN-ABC posterior parameter estimation fail to infer the second African admixture pulse identified by our RF-ABC scenario-choice. Indeed, the posterior distributions of both the timing of this most recent pulse and its' intensity depart little from their respective priors.

Finally, despite the relatively poor performances of our inferences of demographic changes in Santo Antão, our results are indicative of a very reduced population in this island over the course of Cabo Verdean peopling history until a very recent increase up to 41,256 individuals (median, mode=12,056, 95%CI=[3570–96,855]).

Appendix 5-table 3-Santo Antão:

NN-ABC posterior parameter estimations for Santo Antão island, cross-validation posterior parameter errors, and cross-validation 95% Credibility Interval accuracies.

Cross-validation errors and 95% CI accuracies are based on 1,000 NN-ABC posterior parameter inferences using, in turn, each one of the 1,000 simulations closest to the observed data used as pseudo-observed data, and the remaining 99,999 simulations as the reference table.

Error calculations are based on the mode and, separately, the median point estimate for each 1,000 pseudo-observed simulations posterior parameter estimation, compared to the known parameter used for simulation. We considered 11 neurons in the hidden layer and a tolerance level of 0.01 (1000 simulations) for all posterior parameter estimation in this analysis as identified in **Appendix 1-table 1**. Plotted distributions for posterior parameter estimations can be found in **Figure 7-figure supplement 1-3**.

SANTO ANTAO	**Parameter posterior estimation**				**1,000 cross-validation errors**		
Afr2P-Eur2P scenario parameters	**Mode**	**Median**	**50% Credibility Interval**	**95% Credibility Interval**	**Mode mean absolute error**	**Median mean absolute error**	**95% CI length accuracy**
Ne.0	411	469	[254 - 706]	[26 - 964]	254	228	0.071
Ne.20	12056	41256	[17145 - 69559]	[3570 - 96855]	32106	25308	0.051
u.Ne	0.035	0.053	[0.033 - 0.093]	[0.015 - 0.334]	0.072	0.067	0.056
sAfr,0	0.8047	0.5681	[0.2995 - 0.7964]	[0.0260 - 0.9839]	0.3029	0.2586	0.068
tAfr,p1	2.4	4.9	[2.9 - 7.4]	[1.9 - 11.9]	3.3	2.6	0.164
sAfr,tAfr,p1	0.7574	0.6255	[0.3644 - 0.7916]	[0.0451 - 0.9749]	0.2512	0.2283	0.055
tAfr,p2	13.6	11.6	[7.7 - 14.9]	[3.0 - 18.5]	2.8	2.7	0.072
sAfr,tAfr,p2	0.6294	0.4716	[0.2596 - 0.6733]	[0.0338 - 0.9233]	0.2435	0.2150	0.049
tEur,p1	3.2	5.8	[3.2 - 10.2]	[2.6 - 15.6]	2.6	2.4	0.265
sEur,tEur,p1	0.1542	0.3592	[0.1709 - 0.6051]	[0.0216 - 0.9522]	0.2767	0.2347	0.059
tEur,p2	18.1	17.2	[14.8 - 18.2]	[7.6 - 19.1]	3.2	3.0	0.074
sEur,tEur,p2	0.0467	0.0847	[0.0416 - 0.1656]	[0.0056 - 0.6382]	0.1868	0.1763	0.059

Discussion for the admixture history of Santo Antão

Our results for the admixture history of Santo Antão indicate that individuals born today on this island experienced an African-European admixture event concomitant with the first perennial settlement of the island in the 1580's, at the root of the genetic makeup of this island.

Most interestingly, we find no identifiable genetic admixture events, from Europe or Africa, throughout the height of the TAST on Santo Antão, albeit this island experienced a strong agricultural expansion during the plantation economy era which triggered recurrent African enslaved individuals' deportations to this island, as shown by historical records (26–28). Thus, even more strikingly than observed in Santiago, our results indicate that the enslaved-African forced deportations to Santo Antão during most of the TAST did not leave a statistically significant genetic contribution to the genetic landscape of the island, for likely the same complex socio-cultural reasons suggested for the rest of Cabo Verde (see **Discussion** in main text).

In this context, our ADMIXTURE and SOURCEFIND results identify two different Senegambian populations, the Mandinka and the Wolof, sharing significant African haplotypic ancestry with Santo Antão-born individuals, as well as a much more limited shared ancestry with the West Central Africa Igbo population (**Figure 3B**). Our ABC results would thus be consistent with a scenario where different enslaved-African populations from Senegambia and West Central Africa where brought together to settle Santo Antão in the early stages of the TAST in the late 16th century, a pattern distinct to our findings for Santiago and Fogo. Alternatively, it is possible that the Igbo shared ancestry identified in our analyses stem from another admixture event that we failed to identify. This is likely due to an overall limited shared ancestry between this population and Santo Antão identified only with haplotypic local ancestry inferences, as our *MetHis*-ABC procedure considered a single Senegambian population at the root of the admixture history of the island and a much more limited number of independent SNPs compared to the haplotypic local ancestry analysis.

Finally, we find that a weak but significant European admixture pulse occurred at the turn between the 19th and the 20th centuries, substantially later than the end of the TAST and the abolition of slavery and before the 20th European colonial migrations, whose putative historical causes remain to be elucidated. Furthermore, we find that the reproductive population of Santo Antão remained overall small during its' entire history until a very recent expansion, although much more limited than the expansions observed in Santiago and Fogo. This is somewhat surprising with the census records showing that Santo Antão was the second most peopled island after Santiago during most of Cabo Verde history (**Figure 7-source data 1**). Nevertheless, our results could be explained by the demographic collapse experienced by Santo Antão since the beginning of the 20th century, due to several intense famine episodes and rural-urban emigration from the island; a demographic history scenario thus much more complex than the relatively simple scenario here explored. Reflecting the historically small population size on the island, Santo Antão show high total ROH and generally quite long individual ROH among the islands (**Figure 4** and **Appendix 4-figure 1-2**).

Admixture history of São Nicolau (First official settlement 1580; Perennial settlement: 1580)

MetHis-ABC inferences detailed results for São Nicolau

For individuals born on São Nicolau island, we find that the two most recent admixture pulses from Europe and Africa, respectively, are precisely estimated with posterior distributions substantially departing from their priors and reduced 95%CI, for the pulses' timing and intensities (**Figure 7**, **Figure 7-figure supplement 1-3**, **Appendix 5-table 4**). We find that the most recent pulse of European admixture is weak in intensity (median=0.0731, mode=0.0297, 95%CI=[0.0038–0.6642]), and occurred very recently at the generation before that of the sampled individuals (generation median=19.0 after the founding at generation 0, mode=19.2, 95%CI=[10.3–19.8]). Furthermore, we find that the most recent African admixture pulse is very intense (median=0.6398, mode=0.7132, 95%CI=[0.0877–0.9380]), and occurred at generation 14.5 after founding (median, mode=14.6, 95%CI=[8.3–16.4]), during the abolition of the TAST in the first half of the 19th century.

Interestingly, for both the more ancient admixture pulses from either Africa or Europe, our NN-ABC posterior parameter estimation provide reasonably informative posterior distributions pointing towards relatively weak African and European admixture intensities (median=0.3133, mode=0.1695, 95%CI=[0.0171–0.9262]; and median=0.3240, mode=0.1193, 95%CI=[0.0145–0.9460], respectively). However, our results only provide indications that both pulses were ancient and occurred synchronically (generation median=5.2 after founding, mode=2.4, 95%CI=[1.3–15.5]; generation median=6.7, mode=2.7, 95%CI=[2.0–16.1], for the African and European older pulses respectively), as posterior distributions for the timing of these events are largely confounded with their respective priors.

Finally, we obtain a posterior distribution of the founding admixture intensity largely confounded with its prior, similarly as for the demographic parameters, thus showing a limit of our ABC inferences procedures.

Appendix 5-table 4-São Nicolau:

NN-ABC posterior parameter estimations for São Nicolau island, cross-validation posterior parameter errors, and cross-validation 95% Credibility Interval accuracies.

Cross-validation errors and 95% CI accuracies are based on 1,000 NN-ABC posterior parameter inferences using, in turn, each one of the 1,000 simulations closest to the observed data used as pseudo-observed data, and the remaining 99,999 simulations as the reference table.

Error calculations are based on the mode and, separately, the median point estimate for each 1,000 pseudo-observed simulations posterior parameter estimation, compared to the known parameter used for simulation. We considered 11 neurons in the hidden layer and a tolerance level of 0.01 (1000 simulations) for all posterior parameter estimation in this analysis as identified in **Appendix 1-table 1**. Plotted distributions for posterior parameter estimations can be found in **Figure 7-figure supplement 1-3**.

SAO NICOLAU	Parameter posterior estimation				1,000 cross-validation errors		
Afr2P-Eur2P scenario parameters	**Mode**	**Median**	**50% Credibility Interval**	**95% Credibility Interval**	**Mode mean absolute error**	**Median mean absolute error**	**95% CI length accuracy**
Ne.0	360	457	[238 - 734]	[34 - 979]	309	255	0.059
Ne.20	28767	48793	[25155 - 70475]	[3686 - 96753]	27502	23452	0.055
u.Ne	0.135	0.238	[0.133 - 0.358]	[0.025 - 0.483]	0.132	0.113	0.057
sAfr,0	0.3249	0.4730	[0.2491 - 0.7393]	[0.0327 - 0.9752]	0.3017	0.2461	0.051
tAfr,p1	2.4	5.2	[2.7 - 9.5]	[1.3 - 15.5]	5.9	4.5	0.145
sAfr,tAfr,p1	0.1695	0.3133	[0.1584 - 0.5404]	[0.0171 - 0.9262]	0.2897	0.2363	0.069
tAfr,p2	14.6	14.5	[13.2 - 14.9]	[8.3 - 16.4]	1.5	1.4	0.522
sAfr,tAfr,p2	0.7132	0.6398	[0.4900 - 0.7736]	[0.0877 - 0.9380]	0.1044	0.0981	0.055
tEur,p1	2.7	6.7	[3.5 - 10.8]	[2.0 - 16.1]	4.6	3.5	0.139
sEur,tEur,p1	0.1193	0.3240	[0.1547 - 0.5711]	[0.0145 - 0.9460]	0.2806	0.2394	0.048
tEur,p2	19.2	19.0	[17.7 - 19.4]	[10.3 - 19.8]	3.3	2.9	0.199
sEur,tEur,p2	0.0297	0.0731	[0.0295 - 0.1465]	[0.0038 - 0.6642]	0.2419	0.2067	0.065

Discussion for the admixture history of São Nicolau

Our results for the admixture history of São Nicolau indicate that two moderate admixture pulses from Africa and Europe occurred synchronically between the date for the first perennial settlement of this island in the 1580s and the onset of the intensification of the TAST at the beginning of the 17th century. Much later in the course of Cabo Verde peopling history at the beginning of the 19th century, we find an intense introgression event from Africa, probably occurring for the same reasons as in Santiago (see above) and other Cabo Verde islands (see below and **Discussion** in main text).

Interestingly, our haplotypic local ancestry inferences identify three African populations with shared ancestries with São Nicolau-born individuals (**Figure 3**); Senegambian Wolof and Mandinka shared-ancestry representing the majority similarly to the rest of Cabo Verde and as expected historically (see **Discussion** in the main text, (25–28)), and South West Central African Angolan Ovimbundu a small minority. Analogous to the Santo Antão inferences' limitations, our analyses cannot disentangle whether either or both African pulses in São Nicolau involved the limited South West Central African populations shared ancestry here identified.

Finally, we identify, much later during the 20th century, a weak event of European introgression for the genetic admixture history of São Nicolau (**Figure 7D**), similarly likely due to labor-induced migrations in the former Lusophone empire as for other islands, and in particular possibly due to the expansion of fishing and cannery industry in São Nicolau at this time (28).

Altogether, our genetic data contain little identifiable information for the demographic history of this island (**Figure 7C, Figure 7-figure supplement 1**). This may be due to the recurrent demographic collapses of the permanent settlement in this island due to intense starvation events, epidemic outbreaks, and destructive pirate raids that affected the peopling of this island throughout history (**Figure 7-source data 1**). Nevertheless, one genetic pattern that was consistent with these recurrent demographic collapses is the high total levels of ROH observed in the data (**Figure 4** and **Appendix 4-figure 1-2**).

Admixture history of Brava (First official settlement 1580; Perennial settlement: 1580)

MetHis-ABC inferences detailed results for Brava

For individuals born on Brava island, we find that the most recent pulse of European admixture is relatively weak (median=0.1697, mode=0.1281, 95%CI=[0.0188–0.6504]), and occurred towards the abolition of slavery in the Portuguese empire in the second half of the 19th century (generation median=16.3 after the founding of Cabo Verde at generation 0, mode=17.9, 95%CI=[4.2–19.3]), as indicated by posterior distributions of parameters for this event largely differing from their priors (**Figure 7**, **Figure 7-figure supplement 1-3**, **Appendix 5-table 5**). We identify a similarly intense pulse of admixture from Africa (median=0.2473, mode=0.1261, 95%CI=[0.0191–0.8266]), for which our inferences only bore indications that it occurred during the second half of the 18th century during the TAST, as the 95%CI for the timing of this event is wide (generation median=13.6 after founding at generation 0, mode=15.7, 95%CI=[2.4–19.2]).

More remotely in the past, we identify strong indications that a very weak European admixture pulse (median=0.0352, mode=0.0157, 95%CI=[0.0007–0.7239]) may have occurred at the beginning of the 17th century (generation median=7.3 after founding, mode=3.6, 95%CI=[2.8–16.1]). Furthermore, we identify a strong signal for an intense African admixture pulse (median=0.6688, mode=0.7403, 95%CI=[0.1358–0.9685]), occurring at the beginning of Cabo Verdean peopling history, during the early 16th century, at generation 2.8 after the founding of the archipelago at generation 0 (median, mode=1.6, 95%CI=[1.1–12.2]), and thus largely before the first perennial settlement of this island.

Finally, our results strongly support a very limited effective size linear increase (u_{Ne} median=0.420, mode=0.435, 95%CI=[0.243–0.494]) throughout the entire history of the island reaching 7337 effective individuals (median, mode=3278, 95%CI=[647–73,114]) in the present.

Appendix 5-table 5-Brava:

NN-ABC posterior parameter estimations for Brava island, cross-validation posterior parameter errors, and cross-validation 95% Credibility Interval accuracies.

Cross-validation errors and 95% CI accuracies are based on 1,000 NN-ABC posterior parameter inferences using, in turn, each one of the 1,000 simulations closest to the observed data used as pseudo-observed data, and the remaining 99,999 simulations as the reference table.

Error calculations are based on the mode and, separately, the median point estimate for each 1,000 pseudo-observed simulations posterior parameter estimation, compared to the known parameter used for simulation. We considered 10 neurons in the hidden layer and a tolerance level of 0.01 (1000 simulations) for all posterior parameter estimation in this analysis as identified in **Appendix 1-table 1**. Plotted distributions for posterior parameter estimations can be found in **Figure 7-figure supplement 1-3**.

BRAVA	Parameter posterior estimation				1,000 cross-validation errors		
Afr2P-Eur2P scenario parameters	**Mode**	**Median**	**50% Credibility Interval**	**95% Credibility Interval**	**Mode mean absolute error**	**Median mean absolute error**	**95% CI length accuracy**
Ne.0	495	501	[309 - 696]	[63 - 919]	308	254	0.068
Ne.20	3278	7337	[2908 - 17935]	[647 - 73114]	31523	24989	0.056
u.Ne	0.435	0.420	[0.374 - 0.455]	[0.243 - 0.494]	0.077	0.073	0.050
sAfr,0	0.7337	0.5666	[0.3452 - 0.7698]	[0.0497 - 0.9737]	0.2836	0.2405	0.059
tAfr,p1	1.6	2.8	[1.5 - 5.3]	[1.1 - 12.2]	3.9	3.1	0.159
sAfr,tAfr,p1	0.7403	0.6688	[0.4987 - 0.7995]	[0.1353 - 0.9685]	0.2418	0.2232	0.060
tAfr,p2	15.7	13.6	[8.4 - 16.3]	[2.4 - 19.2]	2.8	2.7	0.069
sAfr,tAfr,p2	0.1261	0.2473	[0.1272 - 0.3647]	[0.0191 - 0.8266]	0.2118	0.1905	0.058
tEur,p1	3.6	7.3	[4.1 - 11.1]	[2.8 - 16.1]	3.4	2.9	0.204
sEur,tEur,p1	0.0157	0.0352	[0.0116 - 0.1161]	[0.0007 - 0.7239]	0.2658	0.2338	0.064
tEur,p2	17.9	16.3	[12.5 - 18.0]	[4.2 - 19.3]	3.3	3.1	0.054
sEur,tEur,p2	0.1281	0.1697	[0.1054 - 0.2554]	[0.0188 - 0.6504]	0.1844	0.1716	0.057

2878 *Discussion for the admixture history of Brava*
2879 We find an intense first African admixture pulse roughly three generations prior the first official and perennial
2880 peopling of the island in the 1580's (**Figure 7-source data 1, Figure 7**), thus strongly suggesting that Brava
2881 was initially peopled by individuals already admixed and originating from another Cabo Verdean island, sim-
2882 ilarly to what was suggested for Fogo (see above). We hypothesize that Fogo admixed individuals were orig-
2883 inally at the root of this peopling, as the patterns of shared haplotypic ancestry in Brava-born individuals
2884 strongly resemble that of Fogo, rather than Santiago, with shared ancestry exclusively with Senegambian Man-
2885 dinka and in similar proportion, as well as a significant (albeit very reduced) signal for a shared ancestry with
2886 Tuscan TSI otherwise only found in Fogo (**Figure 3**). We find a limited introgression event from Europe
2887 during the late 17th century, possibly consistent with a known immigration event from Madeira and the Açores,
2888 and from Fogo after a volcano eruption, around this time (27). We also find a relatively weak African admix-
2889 ture pulse at some point during the height of the TAST for which the timing remains poorly inferred, and which
2890 will require further investigations.
2891 Finally, we identify a more intense pulse of European admixture shortly after the abolition of slavery in
2892 the Portuguese empire in the second half of the 19th century. This later event may be due to the expansion of
2893 the whaling industry at this time, particularly in Brava due to favorable maritime currents and routes for this
2894 industry, which brought European and European-North American sailors to the island and increased locally
2895 contacts with Europe, and North America. Most interestingly, this historical scenario is also consistent with
2896 the signal, virtually unique across Cabo Verde, of a significant albeit reduced shared haplotypic ancestry be-
2897 tween Brava-born individuals and the British GBR.
2898 Notably, our results indicate that the effective population of Brava remained low during the entire peo-
2899 pling history of Cabo Verde and until today (**Figure 7C**), consistent with this island being the smallest inhab-
2900 ited and the most south-west ward in the archipelago (**Figure 7-source data 1**). Surprisingly, in spite of the
2901 historically low effective population size, Brava shows low total ROH levels and relatively short ROH lengths
2902 (**Figure 4** and **Appendix 4-figure 1-2**), which remains to be elucidated in the future by considering larger
2903 sample sizes from the island.
2904
2905

Admixture history of Maio (First official settlement 1529; Perennial settlement: 1650)

MetHis-ABC inferences detailed results for Maio

For individuals born on Maio island, we find evidence that the most recent pulse of European admixture was of relatively modest intensity (median=0.1472, mode=0.1134, 95%CI=[0.0233–0.5957]), and likely occurred during the 18th century, in the midst of the TAST (generation median=12.7 after founding at generation 0, mode=14.1, 95%CI=[3.7–17.9]), as both posterior distributions substantially departe from their respective priors (**Figure 7**, **Figure 7-figure supplement 1-3**, **Appendix 5-table 6**). Although our RF-ABC scenario-choice favors several pulses of admixture from both sources, our NN-ABC posterior parameter estimation fails to capture sufficient information to infer satisfactorily the most recent pulse of admixture from Africa, as both the posterior distribution of the timing of this event and its intensity seldom depart from their respective priors and have wide 95%CI.

However, we capture substantial information strongly suggesting two, much older, admixture pulses from Europe and Africa, respectively, occurring virtually synchronically in the middle 16th century (generation median=4.1 after founding for the European pulse, mode=2.3, 95%CI=[1.7–14.2]; generation median=4.2 after founding for the African pulse, mode=2.4, 95%CI=[1.5–12.8]), thus much earlier than the first perennial settlement of this island dated in 1650 by historians (**Figure 7-source data 1**). Furthermore, we find that the respective intensities of the two pulses (median=0.3260 for the European pulse, mode=0.1075, 95%CI=[0.0117–0.9497]; median=0.5589 for the African pulse, mode=0.7703, 95%CI=[0.0346–0.9769]), sum close to 100%. This suggests a large replacement of the Maio population at that time, with indications that these synchronic admixture events occur on the basis of a founding admixed population largely of African origin (median $s_{Afr,0=}$0.6757, mode=0.9135, 95%CI=[0.017–0.421]).

Finally, the demographic inference of reproductive size changes in Maio indicates, similarly as for Brava, that the reproductive size of the island remained relatively small during its entire history, and only very recently increased up to a median 21,454 effective individuals (mode=7159), albeit with a large 95%CI ([914–93,656]).

Appendix 5-table 6-Maio:

NN-ABC posterior parameter estimations for Maio island, cross-validation posterior parameter errors, and cross-validation 95% Credibility Interval accuracies.

Cross-validation errors and 95% CI accuracies are based on 1,000 NN-ABC posterior parameter inferences using, in turn, each one of the 1,000 simulations closest to the observed data used as pseudo-observed data, and the remaining 99,999 simulations as the reference table.

Error calculations are based on the mode and, separately, the median point estimate for each 1,000 pseudo-observed simulations posterior parameter estimation, compared to the known parameter used for simulation. We considered 10 neurons in the hidden layer and a tolerance level of 0.01 (1000 simulations) for all posterior parameter estimation in this analysis as identified in **Appendix 1-table 1**. Plotted distributions for posterior parameter estimations can be found in **Figure 7-figure supplement 1-3**.

MAIO	Parameter posterior estimation				1,000 cross-validation errors		
Afr2P-Eur2P scenario parameters	**Mode**	**Median**	**50% Credibility Interval**	**95% Credibility Interval**	**Mode mean absolute error**	**Median mean absolute error**	**95% CI length accuracy**
Ne.0	122	500	[241 - 746]	[29 - 980]	276	240	0.059
Ne.20	7159	21454	[7388 - 49176]	[914 - 93656]	30301	25378	0.072
u.Ne	0.080	0.121	[0.071 - 0.210]	[0.017 - 0.421]	0.082	0.078	0.064
sAfr,0	0.9135	0.6757	[0.3486 - 0.8841]	[0.0177 - 0.9941]	0.3150	0.2509	0.061
tAfr,p1	2.4	4.2	[2.5 - 6.8]	[1.5 - 12.8]	4.1	3.2	0.126
sAfr,tAfr,p1	0.7703	0.5589	[0.2768 - 0.7758]	[0.0346 - 0.9769]	0.2630	0.2350	0.051
tAfr,p2	14.4	11.1	[6.6 - 15.1]	[2.4 - 18.8]	2.5	2.4	0.112
sAfr,tAfr,p2	0.6543	0.5276	[0.2918 - 0.7126]	[0.0452 - 0.9393]	0.2168	0.1937	0.052
tEur,p1	2.3	4.1	[2.2 - 7.4]	[1.7 - 14.2]	3.2	2.8	0.219
sEur,tEur,p1	0.1075	0.3260	[0.1376 - 0.5818]	[0.0117 - 0.9497]	0.3014	0.2415	0.068
tEur,p2	14.1	12.7	[8.7 - 14.9]	[3.7 - 17.9]	3.3	3.1	0.048
sEur,tEur,p2	0.1134	0.1472	[0.0957 - 0.2301]	[0.0233 - 0.5957]	0.2145	0.1899	0.057

Discussion for the admixture history of Maio

Our results for the admixture history of Maio indicate a relatively simple scenario with a single pulse of European and African synchronic admixture having occurred in the mid-16th century in another Cabo Verdean island, long before the first perennial settlement of the island in 1650, similarly to Fogo or Brava. We hypothesize that this event occurred on Santiago, as shared local haplotypic ancestry patterns are highly resembling between islands (**Figure 3**), and also consistently with Maio being located very close to Santiago and historical records showing unequivocally the strong relationships between islands throughout history (25–28).

After the descendants of this initial admixture event settled Maio, they experienced only a single identifiable admixture pulse of weak intensity from Europe, which likely occurred at the turn between the 18th and the 19th century during the TAST, and no clearly identifiable further signal of African admixture in the island. As for some other Cabo Verde islands, we cannot conclude about the timing of the African admixture event that brought the reduced signal of West Central and South West Central Africa shared haplotypic ancestry with Maio, observed in our ADMIXTURE and SOURCEFIND analyses (**Figure 3**).

Finally, the reduced population size throughout the history of Maio is consistent with the island being located close to Santiago and with much less water resources, having made it difficult to maintain and expand the settlement on this island, despite its first peopling having occurred early in the history of Cabo Verde almost exclusively dedicated to free-range cattle herding (25–27).

ROH patterns are also consistent with this history, with high total ROH indicating long term isolation and population bottlenecks. Similar to Santiago there were some outlier individuals with much higher European ancestry within ROH compared to the remainder of the genome (**Figure 4** and **Appendix 4-figure 1-2**). This could possibly reflect historical marriage prohibitions and other social constraints against intercommunity reproductions (see **Discussion** in main text).

Admixture history of Boa Vista (First official settlement 1566; Perennial settlement: 1650)

MetHis-ABC inferences detailed results for Boa Vista

For the admixture history of individuals born on Boa Vista, we find an intense admixture pulse from Africa (median=0.6553, mode=0.7516, 95%CI=[0.1262–0.8949]), that occurred in the mid-19th century (generation median=15.0 after Cabo Verde founding at generation 0, mode=14.8, 95%CI=[11.0–17.4]), during the abolition of the TAST, with posterior distributions for both these parameters substantially departing from their respective priors and relatively reduced 95%CI (**Figure 7**, **Figure 7-figure supplement 1-3**, **Appendix 5-table 7**). Prior to that event, we fail to estimate the timing and intensity of the older African admixture pulse into Boa Vista, as posterior parameter distributions seldom depart from their respective priors for this event.

However, our results strongly support a scenario with an intense period of recurring monotonically decreasing admixture from Europe (median admixture intensity at the period's start=0.8057, mode=0.9219, 95%CI=[0.2736–0.9907]; median admixture intensity at the period's end=0.340, mode=0.120, 95%CI=[0.021–0.880]), between the first official settlement of the island in 1566 (generation median at the start of the European period of admixture=3.9 after founding, mode=2.2, 95%CI=[1.7–11.8]), until shortly after its first perennial peopling dated in 1650 (generation median at the end of the European period of admixture=8.2, mode=8.6, 95%CI=[3.1–14.9]). Interestingly, the initial founding admixture event at the root of the genetic patterns of Boa Vista-born individuals supports a substantially lower amount of African admixture (median=0.3917, mode=0.1706, 95%CI=[0.1814–0.6678]), compared to the rest of Cabo Verde where this parameter could be reliably identified.

Finally, our results show that the demography of Boa Vista remained relatively constant throughout the history of Cabo Verde, and indicate a possible very recent increase in effective size, albeit posterior parameter estimation of the most recent effective size was ambiguous due to large 95%CI (median Ne_{20}=47,744, mode=13,128, 95%CI=[2657–98,587]).

Appendix 5-table 7-Boa Vista:

NN-ABC posterior parameter estimations for Boa Vista island, cross-validation posterior parameter errors, and cross-validation 95% Credibility Interval accuracies.

Cross-validation errors and 95% CI accuracies are based on 1,000 NN-ABC posterior parameter inferences using, in turn, each one of the 1,000 simulations closest to the observed data used as pseudo-observed data, and the remaining 99,999 simulations as the reference table.

Error calculations are based on the mode and, separately, the median point estimate for each 1,000 pseudo-observed simulations posterior parameter estimation, compared to the known parameter used for simulation. We considered 8 neurons in the hidden layer and a tolerance level of 0.01 (1000 simulations) for all posterior parameter estimation in this analysis as identified in **Appendix 1-table 1**. Plotted distributions for posterior parameter estimations can be found in **Figure 7-figure supplement 1-3**.

BOA VISTA	**Parameter posterior estimation**				**1,000 cross-validation errors**		
Afr2P-Eur Rec. scenario parameters	**Mode**	**Median**	**50% Credibility Interval**	**95% Credibility Interval**	**Mode mean absolute error**	**Median mean absolute error**	**95% CI length accuracy**
Ne.0	731	627	[357 - 793]	[57 - 977]	263	230	0.049
Ne.20	13128	47744	[20486 - 76777]	[2657 - 98587]	30386	25219	0.074
u.Ne	0.056	0.079	[0.051 - 0.125]	[0.014 - 0.346]	0.067	0.066	0.059
sAfr,0	0.1706	0.3917	[0.1814 - 0.6678]	[0.0188 - 0.9677]	0.3186	0.2517	0.061
tAfr,p1	14.6	10.4	[5.8 - 14.2]	[2.4 - 16.8]	4.6	3.7	0.137
sAfr,tAfr,p1	0.2027	0.3760	[0.1998 - 0.5640]	[0.0261 - 0.8771]	0.2494	0.2213	0.056
tAfr,p2	14.8	15.0	[14.2 - 16.0]	[11.0 - 17.4]	1.7	1.7	0.113
sAfr,tAfr,p2	0.7516	0.6553	[0.4758 - 0.7671]	[0.1262 - 0.8949]	0.1962	0.1801	0.048
tEur,p1	2.2	3.9	[2.3 - 6.6]	[1.7 - 11.8]	3.7	3.1	0.192
tEur,p2	8.6	8.2	[6.0 - 10.2]	[3.1 - 14.9]	3.3	3.2	0.090
sEur,tEur,p1	0.9219	0.8057	[0.6300 - 0.9141]	[0.2736 - 0.9907]	0.2723	0.2319	0.076
sEur,tEur,p2	0.120	0.340	[0.1643 - 0.5832]	[0.021 - 0.880]	0.1721	0.1579	0.071
u.sEur	0.4444	0.2783	[0.151 - 0.398]	[0.0160 - 0.4907]	0.151	0.128	0.065

Discussion for the admixture history of Boa Vista

Altogether, our results for the admixture history of Boa Vista born-individuals indicate a largely differing admixture history compared to all other islands of the archipelago. First, we find that the admixture event at the root of the genetic peopling of the island, although occurring long before the first perennial peopling of the island similarly to other islands such as Fogo, Brava, and Maio, is largely biased towards European admixture, as opposed to all other islands in the archipelago (**Figure 7D**). Second, we find the beginning of a period of recurring admixture from Europe before the mid-16th century, concomitantly with the first official settlement of the island, and until its first perennial settlement in the 1650s (119)$^{pp.529}$. Interestingly, this corresponds to a period when Boa Vista has been used by Cabo Verde as a penitentiary island for non-enslaved individuals which may explain the recurring admixture process here identified (25–27).

Later-on towards the end of the TAST in the 19th century, Boa Vista experienced an intense pulse of African admixture, similarly to Santiago and Saõ Nicolau and probably for similar complex socio-cultural reasons (see **Discussion** in the main text). However, overall limited historical records specific to this island render speculative the interpretation of our results based on genetics only (**Figure 7-source data 1**).

Finally, the effective size of Boa Vista remained constant and low throughout the history of this island (**Figure 7C**), which echoes its' small historical census sizes, mainly due to limited water resources on the island, up until today (**Figure 7-source data 1**). ROH patterns are also consistent with this history, with the highest total ROH among the Cabo Verdean islands indicating long term isolation and population bottlenecks (**Figures F4** and **Appendix 4-figure 1-2**).

Admixture history of São Vicente (First official settlement 1570; Perennial settlement: 1780)

MetHis-ABC inferences detailed results for São Vicente

For the admixture history of individuals born on São Vicente, we find a recent European admixture pulse of substantial intensity (median=0.2840, mode=0.2596, 95%CI=[0.0397–0.8044]), having likely occurred towards the end of the 19th century (generation median=17.4 after founding of Cabo Verde at generation 0, mode=17.7, 95%CI=[10.6–18.9]); both posterior distributions have relatively narrow 95%CI and clearly depart from their respective priors (**Figure 7**, **Figure 7-figure supplement 1-3**, **Appendix 5-table 8**).

This most recent admixture event is preceded by a period of recurrent decreasing African admixture likely spanning the second half of the most intense period of the TAST starting in the early 18th century (generation median at the start of the African period of admixture=9.7, mode=12.6, 95%CI=[2.5–16.9]), and ending during the end of the TAST and the abolition of slavery in the Portuguese Empire in the mid-19th century (generation median at the end of the African period of admixture=15.8, mode=17.5, 95%CI=[7.4–19.1]), albeit our results are ambiguous for the estimate of the start of this admixture period as indicated by the large 95%CI. Furthermore, our results are also ambiguous to estimate the intensity of the African introgression during the period of recurring admixture, as the posterior distributions for the onset and offset intensities, as well as the shape of the monotonic recurring admixture do not clearly depart from their respective priors and had large 95%CIs.

We find traces of an older European admixture pulse of substantial intensity (median=0.3403, mode=0.1772, 95%CI=[0.0149–0.9133]), which likely occurred at the beginning of the 17th century (generation median =6.4 after founding, mode=2.8, 95%CI=[1.9–15.1]). Our results indicate that this first admixture event occurred on a root-population that exhibited a large African admixture proportion (median $s_{Afr,0}$=0.5983, mode=0.8596, 95%CI=[0.0529–0.9835]), albeit this result should be considered with cautious as CI is overall wide.

Finally, our results clearly indicate a strong effective population expansion since the perennial peopling of the island in the late 18th century, up to 66,715 effective individuals today (median, mode=85,838, 95%CI=[12,159–98,375]).

Appendix 5-table 8-São Vicente:

NN-ABC posterior parameter estimations for São Vicente island, cross-validation posterior parameter errors, and cross-validation 95% Credibility Interval accuracies.

Cross-validation errors and 95% CI accuracies are based on 1,000 NN-ABC posterior parameter inferences using, in turn, each one of the 1,000 simulations closest to the observed data used as pseudo-observed data, and the remaining 99,999 simulations as the reference table.

Error calculations are based on the mode and, separately, the median point estimate for each 1,000 pseudo-observed simulations posterior parameter estimation, compared to the known parameter used for simulation. We considered 11 neurons in the hidden layer and a tolerance level of 0.01 (1000 simulations) for all posterior parameter estimation in this analysis as identified in **Appendix 1-table 1**. Plotted distributions for posterior parameter estimations can be found in **Figure 7-figure supplement 1-3**.

SAO VICENTE	Parameter posterior estimation				1,000 cross-validation errors		
Afr Rec.-Eur2P scenario parameters	**Mode**	**Median**	**50% Credibility Interval**	**95% Credibility Interval**	**Mode mean absolute error**	**Median mean absolute error**	**95% CI length accuracy**
Ne.0	109	262	[115 - 486]	[19 - 918]	288	243	0.061
Ne.20	85838	66715	[42741 - 84818]	[12159 - 98375]	29947	23721	0.048
u.Ne	0.215	0.244	[0.174 - 0.338]	[0.072 - 0.469]	0.094	0.084	0.049
sAfr,0	0.8596	0.5983	[0.3334 - 0.8142]	[0.0529 - 0.9835]	0.3231	0.2499	0.063
tAfr,p1	12.6	9.7	[5.7 - 13.1]	[2.5 - 16.9]	3.9	3.4	0.153
tAfr,p2	17.5	15.8	[13.8 - 17.6]	[7.4 - 19.1]	2.8	2.7	0.235
sAfr,tAfr,p1	0.6796	0.7168	[0.5698 - 0.8525]	[0.2806 - 0.9795]	0.2031	0.1774	0.079
sAfr,tAfr,p2	0.2149	0.2786	[0.1561 - 0.4266]	[0.0256 - 0.7820]	0.1538	0.1457	0.063
u.sAfr	0.072	0.228	[0.111 - 0.360]	[0.015 - 0.484]	0.161	0.126	0.056
tEur,p1	2.8	6.4	[3.1 - 10.0]	[1.9 - 15.1]	4.1	3.3	0.214
sEur,tEur,p1	0.1772	0.3403	[0.1733 - 0.5442]	[0.0149 - 0.9133]	0.2448	0.2126	0.055
tEur,p2	17.7	17.4	[16.3 - 18.0]	[10.6 - 18.9]	2.0	2.1	0.143
sEur,tEur,p2	0.2596	0.2840	[0.1732 - 0.4177]	[0.0397 - 0.8044]	0.1585	0.1498	0.059

Discussion for the admixture history of São Vicente

Our results for the admixture history of individuals born on São Vicente indicate a strong European admixture event concomitant with the first official peopling of the island occurring at the same time as the nearby island of Santo Antão, consistently with historical records (**Figure 7-source data 1**). However, the perennial peopling of this island was difficult due to the very limited water resources, in particular compared to the much more hospitable, larger, and nearby Santo Antão. Thus, São Vicente essentially served as a coal and salt harbor depot during most of its history with a minimal settlement (28), which may explain the initial European admixture pulse we identify (**Figure 7**), and our local haplotypic shared ancestry results (**Figure 3**).

Later-on and unique in Cabo Verde, our results support a long period of recurring African admixture occurring during the entire second half of the TAST and ending with the abolition of slavery in the Portuguese empire. However, only the final admixture event of this period could be precisely inferred to have occurred during the mid-19th century during the abolition of the TAST and of slavery in the Portuguese empire (**Figure 7D**). The small haplotypic ancestry shared between São Vicente-born individuals and West Central and/or South West Central African population may stem from illegal slave-trade known to have surged during this period. Nevertheless, the poor performances of our parameter inference for the other parameters of this recurring admixture period may indicate that more complex admixture scenarios than the ones considered occurred in this island, thus begging for future work further complexifying admixture histories to be reconstructed with ABC.

Interestingly, historical data show that São Vicente census only very recently started to increase, with newly available water sources and a protected deep-water harbor in the bay of Mindelo, unique in Cabo Verde, which favored the massive economic expansion of the island in the late 19th century and throughout the 20th

3088 century (**Figure 7-source data 1**, (120)[p.36]). Furthermore, the end of the agro-slavery system and end of plan-
3089 tation economy in Cabo Verde at the end of the 18th century and beginning of the 19th century are known
3090 historically to have triggered emigration from Santo Antão and rural-urban migrations during the 19th and 20th
3091 century, essential for São Vicente perennial peopling (28,78). This is further consistent with extensive familial
3092 grand-parental birth-places in Santo Antão and extensive familial relationships reported by São Vicente-born
3093 individuals in our familial anthropology interviews.
3094 Altogether, these historical, economic, and demographic processes may well explain the onset of the large
3095 reproductive population increase identified in our analyses (**Figure 7C**), as well as haplotypic local ancestry
3096 patterns largely resembling those obtained for Santo Antão (**Figure 3**). Furthermore, they are consistent with
3097 the substantial European admixture pulse identified at the turn of the 19th and 20th century with our analyses.
3098 Reflecting the historical small population size, São Vicente had high total levels of ROH (**Figure 4**). Interest-
3099 ingly, individuals from this island, on average, show more African ancestry in ROH compared to the remainder
3100 of the genome. This could possibly reflect historical marriage prohibitions or the historically high levels of
3101 recurrent African admixture, or both.
3102
3103

Admixture history of Sal (First official settlement 1529; Perennial settlement: 1841)

MetHis-ABC inferences detailed results for Sal

Finally, the admixture history of individuals born on Sal inferred with NN-ABC is overall ambiguous *a posteriori* (**Figure 7**, **Figure 7-figure supplement 1-3**, **Appendix 5-table 9**). Indeed, while our RF-ABC scenario-choice leaned towards a complex admixture history with a period of recurring admixture from Europe and two African admixture pulses after the initial founding admixture event for the population of Sal, the duration and intensity of the European admixture period, as well as the first African admixture pulse, all showed posterior parameter distributions seldom departing from their priors. Nevertheless, we clearly identify a recent African admixture pulse of moderate intensity (median=0.2401, mode=0.1780, 95%CI=[0.0197–0.6590]), which likely occurred at the end of the 19th century (generation median=17.6 after the founding of Cabo Verde at generation 0, mode=17.9, 95%CI=[12.5–19.0]). Furthermore, our results indicate a strong and very recent effective size expansion in Sal, up to 63,289 individuals (median, mode =88,248, 95%CI=[5689–98,181]).

Appendix 5-table 9-Sal:

NN-ABC posterior parameter estimations for Sal island, cross-validation posterior parameter errors, and cross-validation 95% Credibility Interval accuracies.

Cross-validation errors and 95% CI accuracies are based on 1,000 NN-ABC posterior parameter inferences using, in turn, each one of the 1,000 simulations closest to the observed data used as pseudo-observed data, and the remaining 99,999 simulations as the reference table.

Error calculations are based on the mode and, separately, the median point estimate for each 1,000 pseudo-observed simulations posterior parameter estimation, compared to the known parameter used for simulation. We considered 11 neurons in the hidden layer and a tolerance level of 0.01 (1000 simulations) for all posterior parameter estimation in this analysis as identified in **Appendix 1-table 1**. Plotted distributions for posterior parameter estimations can be found in **Figure 7-figure supplement 1-3**.

SAL	Parameter posterior estimation				1,000 cross-validation errors		
Afr2P-EurRec. scenario parameters	**Mode**	**Median**	**50% Credibility Interval**	**95% Credibility Interval**	**Mode mean absolute error**	**Median mean absolute error**	**95% CI length accuracy**
Ne.0	525	518	[285 - 745]	[41 - 966]	306	250	0.061
Ne.20	88248	63289	[36457 - 82778]	[5689 - 98181]	30007	24554	0.058
u.Ne	0.038	0.076	[0.035 - 0.155]	[0.005 - 0.399]	0.112	0.102	0.056
sAfr,0	0.8853	0.5820	[0.3164 - 0.8077]	[0.0247 - 0.9820]	0.3039	0.2508	0.060
tAfr,p1	3.2	9.0	[4.8 - 13.1]	[1.8 - 16.8]	4.9	4.1	0.122
sAfr,tAfr,p1	0.7261	0.5166	[0.2893 - 0.7374]	[0.0302 - 0.9626]	0.2667	0.2275	0.063
tAfr,p2	17.9	17.6	[16.3 - 18.0]	[12.5 - 19.0]	1.3	1.2	0.212
sAfr,tAfr,p2	0.1780	0.2401	[0.1374 - 0.3655]	[0.0197 - 0.6590]	0.1588	0.1462	0.071
tEur,p1	3.9	9.3	[5.3 - 12.6]	[3.3 - 16.8]	4.2	3.4	0.180
tEur,p2	17.8	16.2	[13.9 - 17.8]	[6.8 - 19.4]	3.7	3.5	0.102
sEur,tEur,p1	0.4931	0.5657	[0.3810 - 0.7810]	[0.1100 - 0.9754]	0.2585	0.2183	0.072
sEur,tEur,p2	0.0730	0.2061	[0.0842 - 0.4034]	[0.0113 - 0.7804]	0.1926	0.1734	0.076
u.sEur	0.137	0.207	[0.102 - 0.346]	[0.011 - 0.486]	0.156	0.128	0.061

Discussion for the admixture history of Sal

Sal was among the early Cabo Verdean islands to be officially settled and exploited, in 1529 (**Figure 7-source data 1**), as a source of sea-salt both exported and employed locally in the free-range herding meat-production and tannery industry at the historical root of Cabo Verde economy with Europe and Africa (26,78). However, its perennial peopling dated only from 1841, the last perennially peopled island of Cabo Verde, as water sources and agricultural surfaces are scarce on this island. This slow demographic expansion is well captured by our inference showing a reduced population size during most Cabo Verde history on Sal, followed very recently by a strong reproductive size increase (**Figure 7C**). Furthermore, in this context, our results clearly

3140 identifying only a recent admixture pulse of African origin at the beginning of the 20th century could reflect
3141 the recent economic migrations of Western African populations to this island, during the development of its
3142 salt mining activities and its travel and tourism activities since then. Nevertheless, our scenario-choice results
3143 suggested the occurrence of a period of recurrent European admixture in Sal, which our posterior parameter
3144 inference largely failed to identify. This is possibly due to the complex recent peopling history of Sal that we
3145 fail to capture with genetic data, which will need to be clarified in the future in particular with additional
3146 samples from this island. Nevertheless, reflecting the historical small population size, Sal has high total levels
3147 of ROH (**Figure 4**).
3148

3149 **Appendix 5-table 10-Cabo Verde:**
3150 **NN-ABC posterior parameter estimations for 225 Cabo Verde-born individuals considered as a single random-mating popu-**
3151 **lation, cross-validation posterior parameter errors, and cross-validation 95% Credibility Interval accuracies.**
3152 Cross-validation errors and 95% CI accuracies are based on 1,000 NN-ABC posterior parameter inferences using, in turn, each one of
3153 the 1,000 simulations closest to the observed data used as pseudo-observed data, and the remaining 99,999 simulations as the reference
3154 table.
3155 Error calculations are based on the mode and, separately, the median point estimate for each 1,000 pseudo-observed simulations pos-
3156 terior parameter estimation, compared to the known parameter used for simulation. We considered 5 neurons in the hidden layer and a
3157 tolerance level of 0.01 (1000 simulations) for all posterior parameter estimation in this analysis as identified in **Appendix 1-table 1**.
3158 Plotted distributions for posterior parameter estimations can be found in **Figure 7-figure supplement 1-3**.
3159

CABO VERDE	**Parameter posterior estimation**				**1,000 cross-validation errors**		
Afr2P-Eur2P scenario parameters	**Mode**	**Median**	**50% Credibility Interval**	**95% Credibility Interval**	**Mode mean absolute error**	**Median mean absolute error**	**95% CI length accuracy**
Ne.0	343	490	[267 - 726]	[34 - 968]	296	238	0.058
Ne.20	86901	61995	[36958 - 82637]	[8050 - 98176]	26496	23321	0.047
u.Ne	0.469	0.400	[0.310 - 0.463]	[0.172 - 0.497]	0.118	0.107	0.041
sAfr,0	0.5801	0.5015	[0.2560 - 0.7308]	[0.0271 - 0.9794]	0.3000	0.2464	0.057
tAfr,p1	3.1	9.0	[5.0 - 13.0]	[2.0 - 18.0]	5.7	4.2	0.090
sAfr,tAfr,p1	0.4597	0.4831	[0.2575 - 0.7249]	[0.0263 - 0.9644]	0.2556	0.2310	0.049
tAfr,p2	19.2	18.6	[17.2 - 19.3]	[11.9 - 19.3]	1.3	1.2	0.153
sAfr,tAfr,p2	0.7056	0.6224	[0.4317 - 0.7576]	[0.1164 - 0.9303]	0.1483	0.1379	0.037
tEur,p1	2.4	6.1	[3.0 - 9.3]	[2.0 - 16.1]	4.4	3.4	0.146
sEur,tEur,p1	0.1193	0.4300	[0.2038 - 0.7022]	[0.0216 - 0.9718]	0.3006	0.2487	0.056
tEur,p2	18.2	15.1	[11.2 - 17.9]	[4.1 - 19.0]	3.1	2.7	0.086
sEur,tEur,p2	0.1882	0.4150	[0.2029 - 0.6780]	[0.0313 - 0.9647]	0.2471	0.2115	0.051

3160
3161